The Dissertation Committee for Prapasri Sinswat Certifies that this is the approved version of the following dissertation:

Enhancing the Delivery of Poorly Water Soluble Drugs Using Particle Engineering Technologies

Committee:

Robert O. Williams III, Supervisor

Keith P. Johnston, Co-Supervisor

James W. McGinity

Robert L. Talbert

Lisa Brannon-Peppas

Enhancing the Delivery of Poorly Water Soluble Drugs Using Particle Engineering Technologies

by

Prapasri Sinswat, B.S. ; M.S. (Pharm.)

Dissertation

Presented to the Faculty of the Graduate School of

The University of Texas at Austin

in Partial Fulfillment

of the Requirements

for the Degree of

Doctor of Philosophy

The University of Texas at Austin

December, 2006

Dedication

To my Father and Mother, Mr. Saiya Sinswat and Mrs. Boonsom Sinswat

To my Family

For their love and support

Acknowledgements

I would like to express my sincere gratitude to my advisor Dr. Robert O. Williams III for giving me the opportunity to pursue my doctoral studies under his supervision. His guidance, understanding, and encouragement through my graduate studies inspired me to persevere. His constructive comments and suggestions have also contributed greatly to my dissertation research. It is really my pleasure and great rewarding to work in this research group. I would also like to thank my co-supervisor, Dr. Keith P. Johnston, for his guidance and invaluable suggestions concerning all aspects of this research project. His unmatched enthusiasm and unwavering optimism will have an everlasting influence on my research career. I feel very indebted to Dr. James W. McGinity for his generous support, encouragement and guidance during my graduate studies at The University of Texas at Austin. His dedication and enthusiasm for being a pharmaceutical scientist set up a great example for me. In addition, I would also like to thank the other members of my dissertation committee, Dr. Robert L. Talbert and Dr. Lisa Brannon-Peppas, for their invaluable advice and time. It was a privilege to have them on my Ph.D. committee.

I would like to extend my appreciation to all of the faculty and staff of the College of Pharmacy and Department of Chemical Engineering at the University of Texas at Austin and at the University of Texas Health Science Center at San Antonio. I especially wish to acknowledge thanks to Dr. James McGinity, Dr. Bill Williams, Dr. Lane Brunner, Dr. Maria Croyle, Dr. Saloman Stavchansky, Dr. Robert Pearlman, for providing an excellent education experience during my studies. My sincere thanks to Ms.

Mickie Sheppard, our graduate coordinator, for her constant support with the bureaucratic hassles including registration and scholarship. Great thanks to Ms. Yolanda Abasta-Ruiz and Ms. Claudia McClelland for their exceptional and continuous help during my studies. A special thanks to our staffs from the Learning Resource Center at the College of Pharmacy for providing hardware/software and technical support, especially Ms. Joyce McClendon, Mr. David Fudell, Mr. Jay Hammon , Ms. Nicole Toomy and Ms. Belinda Gonzalez-Lehmkuhle for providing continuous assistance and encouragement throughout my graduate studies. I am very grateful to having worked with such a lovely and inspiring group of people.

I would most especially like to acknowledge Dr. Jason McConville for his support and collaboration on animal studies. I benefited greatly from discussions with him and was inspired by his insights. I would also like to express my appreciation to Dr. Michael Schmerling for sharing his expertise in scanning electron microscopy, Dr. Miguel Jose-Yacaman, Ms. Xiaoxia Gao and Mr. John M. Mendenhall for their help with scanning electron microscopy TEM, Dr. Stephen Webber for allowing me to use the Goniometer facility and Dr. Steve Swinnea for his assistance in x-ray diffraction analysis. In addition, I am grateful to The Dow Chemical Company for financial support through out this research.

I wish to express my gratitude to all of the past and present graduated colleagues, fellow graduate students and friends for their friendship and cooperation throughout this journey, especially Dr. Vorapann Mahaguna, Dr. Jason Vaughn, Dr. True Rogers, Dr. Tom Leach, Dr. Xiaoxia Chen, Dr. Jiahui Hu, Dr. Zhongshui Yu, Dr.. Weijia Zheng, Dr. Christopher Young, Dr. Michael Crowley, Mr. Troy Purvis, Mr. Kirk Overhoff, Mr.

Justin Tolman, Mr. David Miller, Mr. Shawn Kucera, , Mr. Alan, Ms. Dorothea Sauer, Ms. Caroline Dietzsch, Ms. Lonique Coots , Ms. Sandra Schilling, Ms. Britta Schroeder, Mrs. Michal Mateucci, Mr. Matthew Todd Crisp, Mr. Joshua Engstrom, Ms. Jasmine Tam and Mr. Alejandro Castillo.

I would like to express my grateful thanks to Dr. Jochen Schacht for his invaluable guidance as my mentor and continued to be supportive through my graduate studies. And most of all, I would like to thank my parents, Mr. Saiya and Mrs. Boonsom Sinswat, for guiding me throughout my life with their endless love and unconditional support. I extend thanks to my dear grandparents, aunts and their family.

Enhancing the Delivery of Poorly Water Soluble Drugs Using Particle Engineering Technologies

Publication No._____

Prapasri Sinswat, Ph.D

The University of Texas at Austin, 2006

Supervisor: Robert O. Williams III

Co-Supervisor: Keith P. Johnston

A growing number of potential drug candidates display poor bioavailability related to poor water solubility of the drug molecules in biological fluids. Poorly water soluble drugs require an appropriate technology to engineer particles with enhanced physicochemical properties and deliver it to desired targets in the body. Particle engineering technologies such as evaporative precipitation into aqueous solution (EPAS), controlled precipitation (CP) and ultra-rapid Freezing (URF) were developed to enhance drug dissolution and bioavailablity through the production of stabilized drug nanoparticles and microparticles. The physicochemical properties of nanoparticles and their behavior on exposure to physiological media are greatly dominated by their primary particle size, morphology and surface characteristics.

Both EPAS and CP are nucleation technologies which involve the precipitation of drug from an organic solution into aqueous solution, resulting in rapid nucleation rates and the formation of small stabilized particles. These technologies are different from one another in the type of solvent system and in the specific nozzle mixing (or dispersing) design. The challenge of these technologies is that during the precipitation procedure the growing of the nucleating drug particles must be limited by use of a stabilizer in order to control the particle size.

In contrast to the precipitation technologies, URF utilizes rapid freezing of a drug solution to engineer porous amorphous drug/excipient particles with high dissolution rates. The flexibility of URF provides the potential for the production of particles with a wide array of drug and various dosage forms such as oral, injection, and inhalation. For lung transplant, administering high surface area compositions via pulmonary administration that have been manufactured using nanoparticle technologies represents new potential opportunities to achieve high bioavailability at the target organ. The effect of the differences in the properties of these two types of particles on supersaturation (amorphous vs crystalline) and how it impact on drug absorption were evaluated. Mice were dosed with the inhaled nebulizer dispersions and the lung and whole blood concentrations were studied. Nanostructured aggregates containing amorphous or crystalline nanoparticles of tacrolimus produced by URF showed to be effectively aerosolized in an aqueous dispersion by nebulization.

Table of Contents

List of Tables

List of Figures

CHAPTER 1: Nanoparticle-Based Drug Delivery Technologies and Their Applications for Particulate Drug Delivery Systems

1.1 INTRODUCTION

Recent advances in nanotechnology and nanoscience have the potential to bring benefits in areas of research as diverse as engineering, materials science, physics, chemistry and molecular biology [1-3]. This potential has attracted worldwide investment from governments and private organizations. Overall, worldwide investment in nanotechnology research and development has increased approximately 9-fold in the past nine years, from $432 million in 1997 to about $4 billion in 2005 [4]. The annual federal funding level in the United States for nanotechnology research and development has increased from an initial budget of $270 million in fiscal year 2000 to $1054 million requested for fiscal year 2006 [4]. In 2000, the United States established a multidisciplinary strategy for nanoscale science and engineering research and development through the National Nanotechnology Initiative (NNI) [5,6]. The vision of the NNI for nanotechnology research and development provides an understanding of the full potential of nanoscale science, and will facilitate the transfer of new technologies into products. Potential research and development targets for 2015 suggested by

NNI are shown in Table 1.1 [7]. About half of these potential targets are relevant to drug development and delivery systems. These relevant targets include no suffering and death from cancer when treated with chemotherapeutic agents, advanced materials and manufacturing processes, pharmaceutical synthesis and delivery, converging technologies from the nanoscale, and life-cycle biocompatible/sustainable development.

The field of nanotechnology is currently gaining attention from researchers and government funding agencies and undergoing explosive development for applications in the pharmaceutical industry [8-10]. Examples of current research include nanoparticle technologies that enable enhanced drug delivery leads and superior performance characteristics of the product, either by increasing efficacy or improving safety and patient compliance. These technologies also permit delivery of drugs that are poorly soluble in water or unstable in biological fluids. As a matter of fact, nanoparticles have long been prepared and employed in parenteral therapies since the 1980s [11-13]. However, technologies that enable one to control and engineer the drug itself in nanoparticulate form have only recently become integrated into the drug development process. This chapter provides a comprehensive review of the nanoparticle technologies that are being developed for drug delivery as reported in the literature, with a brief discussion of the background, technological advantages and disadvantages, and recent progress cited for each technology.

These nanoparticle processes include the use of mechanical technologies, emulsification, supercritical fluid technologies, precipitation technologies and cryogenic spray technologies. The challenges and major findings regarding drug delivery systems over the past decade are discussed. Finally, the chapter highlights therapeutic applications including bioavailability enhancements and site-specific delivery, especially the potential for drug targeting for treatment of infection are discussed.

1.2 SIGNIFICANT IMPACT OF NANOPARTICLE TECHNOLOGIES TO DRUG DELIVERY SYSTEMS

Current drug development and delivery systems are increasingly challenging, inefficient and costly. [14-16]. Successful delivery of drugs often requires processing in order to create more desirable physicochemical properties for effective drug delivery. Due to rapid advancements in nanotechnology, significant effort has been devoted to developing nanoparticle processes in order to address issues associated with the current pharmaceutical challenges. These challenges include delivering drugs with poor water solubility, target-specific drug therapy, cost-reduction and product lifecycle extension. In addition, these technologies offer a suitable means of delivering a wide range of drugs including small molecular weight drugs, as well as macromolecules such as proteins, peptides or genes by either localized or targeted delivery to the tissue of interest.

Nanoparticle technologies have already had a significant impact on drug delivery systems in terms of improving the performance of existing drugs and enabling the use of new drug candidates. It will be discussed, later in this chapter, that nanoparticle technologies can enable the use of certain chemical entities or biologics that were previously impractical because of their low systemic bioavailability and/or high toxicity. Schematics of different nanotechnology-based drug delivery systems discussed in this review are shown in Figure 1.1 [8].

1.2.1 Solubility Enhancement

Aqueous solubility of drugs continues to be a significant challenge and major obstacle to overcome for pharmaceutical scientists [17] in their quest to optimize delivery of drugs. The poor wetting and slow dissolution rate of poorly soluble drugs in the biological environment affect their absorption and subsequent distribution, resulting in limiting the drug's clinical drug application [18]. Poorly water soluble drugs often show low systemic bioavailability and erratic absorption. Indeed, a great number of newly developed drugs are poorly soluble in water and in other solvents. As a result, the bioavailability of such drugs is insufficient to achieve the required therapeutic level. Many approaches have been used in an effort to increase the solubility, wetting and dissolution rate of poorly water soluble drugs including chemical modification (salt formation and prodrug) [19], complexation with cyclodextrins [20], formation of solid dispersions [21]

and solubilization in surfactant systems [22]. However, there are several disadvantages associated with these approaches. For example, the alteration of chemical structure by forming water-soluble derivatives often requires long processing times at a very expensive cost to derive the new chemical entities (NCEs) [23]. The use of solubilizing excipients is often limited by their toxicity. For example, the nonionic surfactant polyoxyethylated castor oil (Cremophor EL) has been shown to cause nephrotoxicity, hypersensitivity reactions and lowering of the white blood cell count (neutropenia) [24]. These are considered the severe side effects associated with administration of Taxol® which contains paclitaxel dissolved in a 50:50 v/v mixture of Cremophor EL and dehydrated ethanol. Furthermore, excipients often limit drug potency in the final product to well below 50% (drug wt./tot. wt.). The large quantities of required solubilizing excipients may also limit the choice of route of administration. Oral delivery, for example, may be impractical because the size of tablet or capsule would be too large and difficult to administer.

In addition to the general solubility enhancement approaches described above, the most direct approach for enhancing solubility is to reduce the particle size and size distribution range, thereby increasing surface area and dissolution rate. According to the Noyes-Whitney equation, the dissolution rate correlates directly to the available surface area of the drug as follows,

$$\frac{dm}{dt} = \frac{DS}{h}(C_s - C) \qquad \text{Eq. (1)}$$

Where dm/dt is the rate of dissolution, S is the surface area, D is the diffusion coefficient, C_s is the apparent solubility of the drug in the dissolution medium, C is the solubility of the drug at time t, and h is the boundary layer thickness. The surface area can primarily be increased by reducing the particle size or increasing the porosity of the particles or a combination of both factors.

Nanoparticle technologies have increased dissolution and bioavailability of poorly water soluble drugs after oral administration [25-27]. For example, Liversidge et al was able to enhance the bioavailability of danazol through the production of nanocrystalline particles of drug using wet milling [28]. In this study, danazol particles were milled to the mean size of 169 nm. The absolute bioavailability of danazol nanosuspension (82.3 ± 10.1%) was much higher than the conventional suspension consisting of microparticles (5.1 ± 1.9%). However, the bioavailability was similar to that of a complex of danazol and 2-hydroxypropyl-β-cyclodextrin (106.7 ± 12.3%). Therefore particle size reduction is a rational way to increase the dissolution rate of poorly water soluble drugs and is encouraged as a primary strategy to consider.

Another important factor that influences the dissolution rate according to Noyes–Whitney is the saturation solubility, C_s. The value of C_s may be enhanced through formation of amorphous states with higher free energies than the crystalline state. Amorphous drug particles can reach much higher concentrations

in aqueous solution compared to the crystalline form of the drug. Supersaturation is defined as follows [29],

$$S_d = \frac{C(t)}{C_{eq}}, \qquad \text{Eq. (2)}$$

where C(t) is the measured concentration at time t and C_{eq} is the equilibrium solubility of crystalline drug in the dissolution media at a given temperature. The amorphous form of drugs has been used to form supersaturated solutions that exhibit large increases in membrane flux when compared to saturated solutions [30,31]. The ability of the nanoparticulate and amorphous particles to supersaturate in the biological fluids may have a profound impact on increasing the bioavailability of poorly water soluble drugs, as has been suggested in several recent studies [32-34]. These studies indicate that forming amorphous solid solutions with the drug and excipients can provide superior dissolution properties of the formulation and subsequently enhance drug systemic bioavailability, which is defined as the rate and extent of drug that reaches systemic circulation.

1.2.2 Site Specific Drug Targeting

Another focus of research is the development of nanoparticle technologies to improve and enable drug targeting. Most drugs currently on the market are delivered in a non-specific manner throughout the whole body, rather than directly to the site of action where they are needed. This may result in

unintentional side effects or toxicity in other tissues. Drugs used in cancer therapy represent an excellent example of this problem. These drugs can kill not only target cancer cells, but also normal cells in the body. Site specific targeting (both passive and active targeting) can reduce systemic toxicity by enabling drugs to accumulate selectively in the target tissue. As a result, the local concentration of the drug at the site of action will be high, while its concentration in non-target tissue will be below a certain minimum level to prevent side effects. In addition, targeting ability may allow for lower dosing requirements which also potentially decrease side effects of the drug while maintaining the same therapeutic results. The need to achieve selective delivery of drugs to specific areas of the body has been recognized for many years.

Utilization of nanoparticle technologies represents a potential opportunity in the field of drug targeting [10,35]. Engineered drug particles in the nanometer size range are generally taken up by cells of the reticular endothelium system (RES), also called the mononuclear phagocytotic system (MPS). This allows efficient delivery of drug to target tissue or organ through passive targeting process [36]. A schematic diagram of intracellular targeted drug delivery using colloidal carriers is shown in Figure 1.2. This schematic gives an overview of the uptake mechanisms involved in the opsonization, adhesion and internalization of nanoparticles by the cells of the MPS.

Additionally, nanoparticles can be delivered to remote target sites or non-MPS sites by attaching a ligand onto the surface of the particle which could direct them to the intended organ in the body [37]. The surface-bound ligand, such as monoclonal antibodies or polymer conjugate, can be recognized and bound specifically to target cells. This approach, called active targeting, provides a means of drug delivery to the sites of action with a high degree of specificity. The development of "stealth" technology has provided opportunities for active targeting of nanoparticles. The stealth strategy also avoids major uptake by the MPS cells resulting in an increased systemic circulation time of the nanoparticles [38]. Recently, several groups have reported stealth coatings for nanoparticles consisting of the linkage to the nanoparticles of poly(ethylene glycol) derivatives [39-41]. The linkages resulted in a lower uptake of nanoparticles by the MPS cells and therefore longer circulation times.

On the other hand, the surface of nanoparticle alternatively can be coated which phagocytes will recognize as “self ” to improve biological uptake [41]. By way of example, American Bioscience, Inc. (ABI) has developed a unique nanoparticle-based technology known as nanoparticle albumin-bound (nab™) technology. It involves binding of water-insoluble drug in a nanoparticle state with albumin while retains the full biological properties of albumin. The coating mimics a natural protein in the body and may potentially exploit an

inherent pathway for albumin receptor-mediated transport of drugs across endothelium that becomes permeable due to the presence of tumors.

Albumin is common protein found in the human body thereby the resulting product is readily biocompatible for patients use. It has been shown to accumulate in areas of inflammation and in tumour cells [42]. Furthermore, in vivo studies have confirmed an accumulation of nanoparticles in tumor sites. Abraxane® is the first marketed product to incorporate this technology and use for treatment of metastatic breast cancer. It was initially developed to avoid the toxicities associated with Cremophor EL used in the conventional formulation Taxol® for drug solubilization. It is significant that Abraxane® can be safely administered to both young and elderly patients. This formulation showed a superior efficacy with high reconciled target lesion response rate in the patients with metastatic breast cancer when compared with the conventional formulation Taxol®. The development of drug nanoparticulate for targeted drug delivery systems has been reviewed extensively by Moghimi et al [40].

1.2.3 Extending Product and Patent Lifecycles

In the pharmaceutical industry, advancements in nanoparticle technology represent a powerful, strategic tool not only to improve drug performance but also to expand the original compound's product lifecycle [9]. The technology is a cost effective resource enabling one to expand the success rate for promising

compounds in the pipeline, and to expedite their commercialization to market. Also, they can improve the likelihood of success for compounds that were previously thought to be undeliverable or unstable, or compounds that displayed sub-optimum absorption. Further, applications of nanoparticle technologies are increasing the range of possibilities for biologics because many first-generation biologics are under the threat of generic competition. Reformulation of existing drugs has become valuable near the end of a drug's patent life. It is the best way to maximize a drug's viable time on the market and contributes to creating a new market in the field of drug delivery. In recent years, many pharmaceutical products have been increasingly focused on patented formulation technologies rather than on developing new chemical entities. For example, Roche, Wyeth-Ayerst and Bristol Meyers Squibb have reportedly entered into collaborative research agreements with Élan to develop micron or submicron based drug preparations for the sole purpose of enhancing dissolution and bioavailability of poorly water soluble drugs. Furthermore, nanoparticle technology involves lower cost research relative to that expended for the discovery of new drug substances. The use of nanoparticles may reduce the required dose of drug to be administered and thereby lowering the overall requirement for an expensive drug. This should reduce the cost of the product and undesirable effects in the human body resulting from higher dosing.

1.3 NANOPARTICLE TECHNOLOGIES

In the pharmaceutical field, the term "nanoparticle" is generally used to describe submicron sized particles. The drug of interest is dissolved, entrapped or encapsulated within the particles as depicted in Figure 1.1. Nanoparticle technologies have been used as important strategies to deliver drugs, including peptides and proteins, vaccines and more recently nucleotides [14,35,43,44]. Nanoparticles can be produced by either mechanical or chemical approaches. Mechanical forces during comminution (crushing, grinding, and milling) often cause thermal stress resulting in degradation of heat-sensitive drugs [45]. In contrast, nucleating and growing particles from a solution in a controlled manner requires less particle handling and harsh conditions. These solution-based technologies involve the use of conventional liquids or supercritical fluids (either as solvents or antisolvents) or cryogenic media for ultra-rapid freezing. Such technologies typically result in formation of nanoparticles in amorphous form leading to increasing solubility and dissolution rate. The selection of the appropriate process for production of nanoparticles depends on the physicochemical properties of the drug and excipient(s). The following is an overview of the currently available methods used for production of drug nanoparticles and their noteworthy features.

1.3.1. Mechanical Technologies

The mechanical technologies are conventional approaches used for many years in pharmaceutical industry for producing fine powders. These technologies include mechanical milling and high pressure homogenization. Effective size reduction generally requires high-energy input, resulting in enormous impact forces. High energy shear forces mechanically break down large particles. Conventional dry milling technologies such as ball and jet milling have the disadvantage of being inefficient for producing drug particles in the nanometer range. The typical particle size of powders milled with these technologies ranges from 0.1 μm to 25 μm [46,47]. The proportion of particles in the nanometer range is low due to the absence of stabilizing excipients, such as surfactants and hydrophilic polymers, during processing to prevent particle growth and aggregation. In addition, particle handling of nanoparticles in the dry state are difficult because of the presence of electrostatic forces on the surface of particles. Later, the wet milling (NanoCrystal® technology) was developed by NanoSystems™ (part of Elan Corporation) to overcome these problems by milling particle in presence of hydrophilic stabilizer(s) to prevent particle agglomeration [47, 48].

1.3.1.1 Wet Milling Technology

Wet milling is a particle size reduction technology whereby drug crystals are comminuted using high-shear media mills in the presence of surface stabilizer(s) and grinding media [25, 49]. The grinding media consist of rigid media with an average size ranging from 0.4 to 3 mm. The grinding materials may be composed of glass, zirconium oxide, ceramics and plastics (e.g., cross-linked polystyrene resin). The typical process temperature during is less than 40^{o}C to prevent thermal degradation. In general, the technology involves pre-dispersing drug in aqueous solution containing hydrophilic stabilizers and then the slurry is wet milled with a grinding media over a specified time period. High energy shear forces and the forces generated during impaction mechanically break down drug crystals into nanometer-sized particles which are suspended in a polymer solution. Wet milling often requires grinding for hours to days in order to achieve a desired size range of nanocrystalline particles. The level and type of stabilizer are important parameters to achieve nanoparticle size using this technology and should be investigated for each situation. It was found that higher molecular weight polymeric stabilizers were optimal for effective particle size reduction and shelf stability. Additionally, the size of the grinding media, flow rate and speed of the mill rotor can also be adjusted to achieve optimum results.

NanoSystems™ has commercialized its technology resulting in two products. The first product approved by the United States Food and Drug

Administration (FDA) is the reformulation of Rapamune®, a lipophilic macrolide immunosuppressant (marketed by Wyeth Pharmaceuticals). Previously, Rapamune® (sirolimus) was only available as an oral solution which contains solubilizing agents such as polysorbate 80, phosphatidylcholine, mono- or di-glycerides and propylene glycol. The current oral formulation requires storage under refrigerated conditions and additional preparation steps prior to use. A new formulation is now available as a tablet dosage in which the of the particle size of the drug substance is reduced to less than 200nm in order to improve drug's water solubility. The new tablet formulation also enables more convenient administration and storage than the Rapamune oral solution. The second product is Emend® (aprepitant) developed as a new drug in a NanoCrystal® formulation. It is an antiemetic therapeutic agent used to prevent and control nausea and vomiting caused by chemotherapy treatment.

1.3.1.2 High Pressure Homogenization Technology

High pressure homogenization is another mechanical technology that involves the use of high shear forces to break up particles or droplets into the nanometer range [50, 51]. Traditionally, homogenizers have been used in the pharmaceutical industry for emulsification. More recently, high-pressure homogenization was successfully employed to prepare liposomes, nanosuspensions and solid-lipid nanoparticles [50]. Mechanical forces during homogenization cause droplet or particle size reduction by shear, turbulence,

cavitation and collision of the particles against each other at high velocity. Shear is caused by elongation and subsequent breakup of droplets, due to acceleration of a liquid. During homogenization, fracture of drug particles is caused by cavitation, high shear forces and by the collision of particles with each other. As the dispersion is forced through a narrow homogenization gap, the pressure suddenly rises to ambient pressure leading to implosion of vapor bubbles (cavitation). These cavitation forces are sufficiently high enough to cause disintegration of the suspended microparticles into nanoparticles. The particle size of the starting material for production of nanoparticulate suspensions is normally less than 100 μm in order to prevent the blockade of homogenization gap [52]. This technology has been used in the commercialization of drug nanoparticles such as Disso Cubes® owned by SkyePharma [53]. The Disso Cubes® are produced by using piston-gap type high-pressure homogenizers operating at pressures varying from 100 to 2000 bars. Characteristics of the particles (particle size distribution) are influenced by homogenizer type, applied pressure, number of homogenization cycles and hardness of the drug particles. Changes in drug crystallinity have been reported for high pressure homogenization technology [54]. The use of high pressures can cause changes in the crystal structure and may also produce uncontrollable variations of amorphous structure.

1.3.2 Emulsion Technology

The production of nanoparticles employing emulsions and microemulsions as templates has been reported in the literature [55-57]. Emulsions are heterogeneous systems consisting of two immiscible liquids (i.e. organic and aqueous) in which one liquid is dispersed in the form of small droplets throughout the second liquid. Emulsions are generally classified as oil-in-water (o/w) or water-in-oil (w/o) systems, where the first component represents the dispersed phase, although more complex systems (i.e. w/o/o, w/o/o/o) are feasible. Conventionally, the dispersion of nanoparticles can be prepared through mechanical emulsification which consists of two steps. The first step involves the application of high mechanical energy to break up the dispersed phase. In many cases, the nanoparticle dispersion is produced using a colloid mill, sonication or high pressure homogenization. The second step involves stabilization of the newly formed interfaces by the surfactant. In addition to the method mentioned previously, nanoparticles can also be prepared by the emulsification–solvent evaporation technology [58]. Briefly, the drug of interest is dissolved in the organic solvent, which is subsequently emulsified by adding water and a surfactant to form an oil-in-water (o/w) emulsion. The organic solvent is then evaporated leading to the formation of nanoparticles. These particles are usually collected by centrifugation and lyophilization. Similar processes using both emulsification and diffusion has been developed by Quintanar-Guerrero et al.

[59]. Drug or polymer was added to a water miscible solvent as the oil phase. After the addition of water, the water miscible solvent diffuses to the water phase resulting in the precipitation of nanoparticles. This emulsification procedure is followed by the removal of the solvent by vacuum steam distillation, producing a dispersion of nanoparticles with an average sizes ranging from 0.1–0.3 μm.

In contrast to emulsions, microemulsions are bicontinuous systems of oil-in-water (or water-in-oil) stabilized by an interfacial film of surfactant and co-surfactant. The particle size can be varied depending on the amount of surfactant and co-surfactant used during stabilization of the microemulsion. The application of a microemulsion as a template to produce nanoparticulate drug is usually limited due to limitations on the use of high surfactant concentrations. Trotta et al. were able to obtain griseofulvin nanoparticles from o/w microemulsions [60]. These particles were formed in the average particle size range of 80 – 300 nm. Moreover, microemulsions have been shown to increase solubility or bioavailability of a drug. For example, the microemulsion-based formulation of cyclosporin A (Neoral®) was developed to provide more consistent absorption of the drug from the gastrointestinal tract. Drug absorption of this formulation was improved and more reproducible than the conventional oil-based emulsion (Sandimmune®) due to significant decrease in particle size [61].

1.3.3 Supercritical Fluid Technologies

Particle formation processes that use supercritical fluids (SCFs), especially carbon dioxide, have been applied in a variety of fields including superconductors, catalysts, inorganic compounds, polymers and pharmaceutical compounds [62]. Carbon dioxide (CO_2) is the most commonly used SCFs for pharmaceutical applications due to its unique properties, such as low toxicity, non-flammable, inexpensive and high solubilizing power compared to regular gases. It has a relatively low critical temperature (31.1°C) and pressure (73.8 bar). The solubilizing power of SCFs can be controlled by changing in pressure or temperature. The attractive features of supercritical fluid-based technologies include ease of scale-up, enhanced solubility power, ability to control and vary the nanoparticle size and shape whenever required, use of inert carrier gases like CO_2 and obviously due to advantageous properties of supercritical fluids like high diffusivity, low viscosity, low surface tension and higher solubilizing power. The commonly used technologies based on supercritical fluids include rapid expansion from supercritical solutions (RESS), rapid expansion from supercritical to aqueous solutions (RESAS) and supercritical anti-solvent technologies (SAS) [63]. Within these technologies, the supercritical fluid is used either as the solvent or anti-solvent during particle formation. The choice of method depends on the solubility of the drug of interest in the appropriate SCF. The following section is

brief explanation of the principles of the methods discussing the technological advantages and disadvantages.

1.3.3.1 Rapid Expansion from Supercritical Solutions (RESS), Rapid Expansion from Supercritical to Aqueous Solutions (RESAS)

In the RESS technology, the supercritical fluid acts as the solvent. The solute is first dissolved into the supercritical carbon dioxide. This mixture is then expanded through a nozzle and sprayed into a collection chamber at atmospheric conditions. Upon expansion, the atomization and evaporation of CO_2 causes rapid nucleation and precipitation of dissolved solute in the form of small particles. A schematic representation of the RESS technology is shown in Figure 1.3a [63]. The technology has been applied to engineer the nanoparticles of griseofulvin and β-sitosterol [63]. Türk was able to produce particles of less than 500 nm in diameter by RESS-technology [64]. More recently, rapid expansion from supercritical to aqueous solution (RESAS) has been developed to reduce particle growth and aggregation in the expansion of RESS [65]. In RESAS, the surfactant diffuses rapidly to the particle surface to impede particle agglomeration and growth. The RESAS technology has successfully incorporated aqueous stabilizing solutions into the RESS technology to produce nanoparticles of poorly water soluble drugs. For example, cyclosporine (CsA) nanoparticles produced by RESAS using Tween 80 to prevent particle agglomeration [65]. The particle sizes of 500-700 nm were achieved with drug concentrations as high as 37.5 mg/ml.

The wide size distributions of drug particles were found at a high drug/surfactant ratio (above 0.6-0.7) due to insufficient stabilizer by surfactant. RESAS typically produces smaller particle sizes of water-insoluble drug than does RESS into air. Micron-sized particles were found when cyclosporine A was sprayed directly into air without the aqueous surfactant solution. In these technologies, the characteristics of the particle are dependent on nozzle design, temperature of the mixture before and in the nozzle and pressure in the spray chamber. The major disadvantage of these technologies is the low solubility of many drugs and excipients (e.g. polymers) in SCFs. Therefore, this technology can only be used when the drug of interest has a significant solubility in the SCFs. In addition, low drug loading into SCFs may result in low production rates of powders. This makes RESS not attractive for industrial-scale productions of such low-soluble materials.

1.3.3.2 Supercritical Anti-solvent and Related Processes (GAS, PCA, SAS, ASES, SEDS)

The fact that many compounds have very low solubility in SCFs has given rise to the use of the SCFs as antisolvents to precipitate particles from conventional solvents. The principle is similar to that of conventional liquid antisolvent recrystallization tech. Supercritical antisolvent technologies have been performed using different process arrangements and apparatuses. The technologies relevant to this group include gas anti-solvent precipitation (GAS),

supercritical antisolvent (SAS), precipitation with a compressed fluid anti-solvent (PCA), aerosol solvent extraction system (ASES) and solution enhanced dispersion by supercritical fluids (SEDS). These technologies are different from one another in the contact mode between solution and anti-solvent, in the specific nozzle mixing (or dispersing) design, in the flow direction and in the process mode (batch or semi-continuous). However, different acronyms are often used to indicate the same technology depending on the author's use of the terms. For example, Jung and Perrut have used the acronym GAS to refer to both GAS and SAS technology [66]. In other papers, the SAS or SEDS technology has also been referred to as PCA [67, 68]. In this chapter, we have further classified the supercritical antisolvent into two main distinct groups according to the process mode and the physical state antisolvent of used. The first group includes GAS technology which uses high-pressure gas as an anti-solvent (gaseous antisolvent). This technology is typically operated as a batch process which involves the addition of CO_2 to lower the solvent power of a polar liquid solvent in which the solute(s) is dissolved, thus causing the solute to precipitate or re-crystallize. This technology allows the unidirectional mass transfer of the CO_2 diffusion into the organic phase. A schematic representation of the GAS technology is shown in Figure 1.3b [63]. In this technology, the rate of addition of anti-solvent to the organic solution is an important parameter which affects the particle size and the particle size distribution of the precipitated particles. The second group includes

the semi-continuous processes such as PCA, SAS, ASES and SEDS. These technologies employ either liquid or supercritical carbon dioxide as the antisolvent. Figure 1.3c illustrates a schematic representation of PCA, SAS and ASES [63]. The liquid solution containing the dissolved drug and the anti-solvent are injected separately into the precipitation chamber, resulting in intense atomization and rapid two-direction mass transfer. In this way, high mass transfer rates are achieved and thereby creating nanoparticles [69].

Based on currently published manuscripts, there are no distinctions between the well known SCF antisolvent technologies such as PCA, SAS and ASES [66, 67]. SEDS is the only process that is differentiated due to the use of a nozzle with two coaxial passages with a mixing chamber to improve atomization and mass transfer rates. Figure 1.4 illustrates the SEDS apparatus and the coaxial nozzle [70]. This nozzle design yielded better mixing which enables one to produce nanoparticles with narrow size distributions. Briefly, the drug in organic solvent and the pre-pressurized liquid or supercritical CO_2 are co-introduced using a coaxial nozzle. The two streams are thoroughly mixed in the mixing chamber of the nozzle to ensure highly efficient mixing prior to dispersing into the particle-forming vessel via a restricted orifice. Such a nozzle facilitates intense atomization and rapid mass transfer rates causing precipitation and disintegration of small particles.

1.3.4 Precipitation Technologies

Other technologies used for the preparation of drug nanoparticles include precipitation from solution. The precipitation process involves nucleation and crystal (particles) growth of drug particles from a supersaturated solution. The supersaturated solution is a solution in which the concentration of solute exceeds the saturation or equilibrium solute concentration at a given temperature. Thus, a supersaturated solution is not at equilibrium, and crystallization of the solute occurs in order to move the solution towards equilibrium. After initial particle nucleation, both nucleation and crystal growth attempt to bring the supersaturated solution to equilibrium. The time required for crystallization depends on the driving force of supersaturation. The particles are formed in a supersaturated solution through nucleation mechanisms. Nucleation of particles occurs as a function of the supersaturation, as described by [29],

$$S = \frac{C_o}{C_f}, \qquad \text{Eq. (3)}$$

where C_o and C_f are the concentration of drug before and after mixing the two solutions. If mixing is done rapidly, a higher level of supersaturation is created before significant nucleation occurs. The rate of primary nucleation is given by the equation [71],

$$B_0 = A \exp[(-16\pi\sigma^3 v^2)/(3k^3T^3(\ln S)^2)] \qquad \text{Eq. (4)}$$

where B_0 is the nucleation rate, σ is interfacial tension, ν is molar volume, A is frequency factor , T is temperature and S is supersaturation. The nucleation rate increases with increasing temperature and degree of supersaturation, but decreases with increasing surface energy. High nucleation rates offer the potential to produce a large number of submicron particles in the final dispersion, as long as the growth can be arrested by stabilizers.

Precipitation technologies are used in both the chemical and pharmaceutical industries for the production of nanoparticles [29, 72]. The conventional precipitation technologies, including solvent evaporation and salting out, have in common the disadvantages of poor control over particle morphology and particle size and size distribution producing a wide range of particle sizes [72]. Innovative technologies have been introduced to overcome these problems in the past several years, including solvent displacement, evaporative precipitation into aqueous solution and controlled precipitation. Each technology requires solvation of the drug into a solvent and then precipitation in an antisolvent or evaporation of the solvent leading to precipitation. These technologies differ by the type of solvent/antisolvent used and the process parameters (such as temperature and pressure) at which the technology is carried out. The physical state of the drug can be varied from crystalline to amorphous.

1.3.4.1 Solvent Displacement or Nanoprecipitation

The concept of nanoprecipitation based on interfacial polymer deposition following solvent displacement was developed and patented by Fessi and co-workers [73, 74]. It requires the use of two miscible solvents. This technology is suitable for hydrophobic compounds which are soluble in ethanol or acetone (the solvent), but with limited solubility in water (the non-solvent). Both the polymer and the drug are dissolved in the solvent, which is subsequently poured into the non-solvent while stirring. Nanoparticles are formed instantaneously by rapid solvent diffusion, and the organic solvent is then removed from the dispersion under reduced pressure. Nanoprecipitation enables the production of nanoparticles with average diameter ranging from 100–300 nm and narrow monomodal size distributions. The use of polymeric stabilizers was fundamental to obtain stable dispersions without significant particle aggregation. The wide range of polymers can be used, such as poly(lactic acid) (PLA) and copolymers of lactic acid with glycolic acid (PLGA), poly ε-caprolactone (PLCL) and cellulose derivatives.

Recently, Hyvonen et al were able to incorporate water insoluble drugs such as beclomethasone dipropionate into low molecular weight poly(L-lactic acid) nanoparticles using nanoprecipitation [75]. However, the major limitation of this method is related to drug solubility that is required for efficient encapsulation [76]. Guzman et al. reported that drug loading efficiency of cyclosporine in poly ε-caprolactone nanoparticles was only 0.46 mg/g of polymer [77]. Similar

findings of low drug encapsulation efficiency of other water insoluble drugs such as indomethacin (2.0% w/w) and dexamethasone (0.9% w/w) into PLGA nanoparticles was also found by Fessi et al.[74]. In addition, this method is not suited for the encapsulation of water-soluble drugs, which rapidly diffuse from the organic phase into water resulting in loss of drug into the aqueous phase [78].

1.3.4.2 Evaporative Precipitation into Aqueous Solution (EPAS)

EPAS particle engineering technology was developed to engineer small particles with high dissolution rates. This technology is patented by The University of Texas at Austin and licensed to The Dow Chemical Company. EPAS creates small particles through rapid phase separation. Evaporation of the primary solvent results in loss of solvent power and precipitation of very small particles of the dissolved solute. In this technology, drug dissolved in a water immiscible organic solvent is sprayed through an atomizing nozzle into an aqueous solution containing a hydrophilic stabilizer to produce an aqueous dispersion [79]. Rapid evaporation of the organic solvent at elevated temperatures produces very high supersaturation and rapid precipitation of the drug in the form of suspended particles. The particles may be stabilized by a variety of stabilizers present in either or both the organic and aqueous phases. The stabilizers diffuse to the surface of the growing particles to prevent particle growth during re-crystallization. The enhanced dissolution rates characteristic of EPAS can generally be accounted for by one of the following mechanisms:

increased surface area available for dissolution by decreasing the particle size of drug, precipitation as a metastable crystalline form or a decrease in substance crystallinity and/or by optimizing the wetting characteristics of the drug surface due to adsorption of hydrophilic stabilizer [80]. Nanoparticle suspensions of cyclosporine A with a particle size ranging from 130 nm to 460 nm was produced by the EPAS technology [81]. A variety of hydrophilic stabilizers were found to diffuse to the surface of the growing particles rapidly enough to prevent growth of the nanoparticles. The EPAS technology has been successfully used to produce high potency formulations with rapid dissolution rates of hydrophobic drugs such as danazol [82] and itraconazole [83, 84]. The resulting stabilizer-coated drug particles had high drug-to-stabilizer ratios greater than 12, corresponding to potencies (wt drug/wt drug + wt surfactant) as high as 93%. The relatively small amount of adsorbed stabilizer was sufficient to stabilize the particle and produce high wettability and dissolution rates during EPAS technology.

1.3.4.3 Controlled Precipitation (CP)

More recently, the controlled precipitation technology was developed by The Dow Chemical Company. It involves growing the particles in a controlled fashion to attain the desired particle size and morphology. Briefly, the drug is dissolved in a water miscible organic solvent, which is then rapidly mixed with an aqueous phase (antisolvent) in a controlled manner. This ensures sudden high supersaturation, resulting in rapid nucleation and the formation of small particles.

Stabilizers can be added in either the organic or aqueous phase for preventing particle agglomeration during solvent evaporation and storage. The addition of aqueous solution leads to the lost of solvent power, thus causing the precipitation or re-crystallization of the dissolved drug. The dispersion of drug nanoparticles can be further processed to remove the solvent using vacuum distillation apparatus. Upon solvent removal, the stripped dispersion can be dried by spray drying or lyophilization. The main idea behind this technology is that the anti-solvent should be highly soluble in the solvent, while the solute is insoluble or insignificantly soluble in the anti-solvent in order to promote precipitation. In the recent research, CP has found success in the nanoparticle production of danazol and naproxen [27]. The particle sizes of both drugs increased as the was temperature increased from 3°C to 50°C in the mixing zone. The nanoparticles obtained by CP yields better dissolution profile in comparison to the physical mixtures, micronized and wet-milled drugs. Scale-up of this technology was shown to be successful for large-scale production of nanoparticles on the kilogram scale with good recovery and low residual solvent levels. The ability for large-scale production is an important requirement for the nanoparticle technologies to be introduced into the pharmaceutical industry applications.

1.3.5 Cryogenic Spray-freezing Technologies

Cryogenic technologies have been developed to produce small particles without the introduction of mechanical forces or heat which can cause degradation of the drug. The basic advantage of this technology is its applicability to drugs that are poorly water soluble. In addition, techniques are especially suitable in thermosensitive drugs such as proteins and peptides micronization. The freeze drying technique reported in the literature is spray-freeze drying (SFD). It typically involves the spray of protein or drug solution into a cold vapor phase over a cryogenic liquid to form fine droplets. For the spray-freeze-drying process at atmospheric pressure, the frozen droplets are dried during the following atmospheric freeze drying in the cold desiccated air stream by sublimation. It has however a number of disadvantages, which is related to the poor heat transfer [85]. As the result, the droplets may not be freeze immediately. Webb et al. reported the aggregation and precipitation of recombinant human interferon-γ produced by SFD [86]. The passage of the droplets may allow freezing to begin during the time of flight through the cold vapor phase which takes about one second before reaching cryogenic liquid phase where completely freeze occurred. Therefore this occurrence allowed protein to diffuse and aggregate at the air–liquid interface.

The relatively new process of spray freezing into liquid (SFL) was developed to overcome this problem. In the SFL technology, the feed solution

containing drugs and excipient(s) is atomized through a nozzle below the surface of liquid nitrogen. The droplets are immediately frozen upon contact with the cryogenic liquid phase. The frozen particles are then lyophilized to obtain dry, free flowing powders. The ultra-rapid freezing rates prevent the phase separation of solutes within the feed solution and induce formation of amorphous structures. The success of the SFL technology results from intense atomization of a feed liquid directly into a cryogenic liquid to produce the molecular dispersion of amorphous nanostructured particles with high surface areas and enhanced dissolution rates [87]. Their utility for engineering of microparticles and microparticulate drug carrier systems has been very well established. SFL has been successfully used to produce micron-sized aggregates of nanoparticles in various compounds such as insulin [88, 89], bovine serum albumin [90] and poorly water soluble drugs [26, 91-93].

1.4 POTENTIAL THERAPEUTIC APPLICATIONS OF NANOPARTICLE-BASED DRUG DELIVERY TECHNOLOGIES

Nanoparticle-based technologies are changing the way drug delivery is being approached, offering new ways to deliver drugs effectively, to reduce the amount of those drugs used, to localize the delivery of potent compounds and, therefore, to reduce side effects. They have become important in several areas of drug delivery, potentially via numerous administration routes, including

parenteral, oral, brain and pulmonary routes. The unique characteristics of nanoparticles have enabled their application to delivering a wide range of compounds such as hydrophilic drugs, hydrophobic drugs, peptides, proteins, vaccines, etc. Examples of the most recent research carried out using different nanoparticulate systems are reviewed in Table 1.2 [94]. The general aspects on nanoparticles have been extensively reviewed [95-97] and the present chapter will focus on the recent findings in drug delivery systems.

1.4.1 Injectable Drug Delivery

Parenteral administration of drugs by injection is the most common route of administration to achieve rapid therapeutic drug levels for the treatment of acute treatment [98]. Because of their small size below 1 μm, nanoparticles are primarily developed for intravenous administration to prevent blocking the fine capillaries leading to embolism [98, 99]. They can be injected either intravenously, intramuscularly or subcutaneously or direct injection into solid tissues or organs. When given intravenously, nanoparticles are taken up by direct endocytosis or phagocytosis into monocytes, macrophages, leukocytes and other cells of the RES whose function is to scavenge foreign particles and microorganisms. One of the main interests of nanoparticles is their higher intracellular uptake compared to microparticles, which makes nanoparticles potential candidates for delivering drug to infected macrophages for effective microbial killing [100-102]. Treatment of many intracellular infections in the

MPS is often fails to eradicate the organism because of the inability of drugs to penetrate infected cells [100]. Therefore, there may be promising applications of nanoparticles for treatment of infectious diseases when administered intravenously. For examples, Forestier et al. studied the efficacy of ampicillin-loaded poly(isobutylcyanoacrylate) (PIBCA) nanoparticles against the activity of *L. monocytogenes* in macrophages compared with that of free ampicillin [103]. Ampicillin-bound nanoparticles showed more effective than free ampicillin for inhibiting intracellular growth of *L. monocytogenes*. After 30 h of incubation, nanospheres-bound ampicillin inhibited bacterial growth by 99% with a lag period of 9 h while free ampicillin was ineffective. This effect was attributed to high cellular uptake of the ampicillin-loaded nanoparticles and the diffusion of the drug through the cell.

Also nanoparticles can provide slow release of the drug when accumulated in the in phagocytic cells or administered subcutaneously [104]. Such particles that slowly dissolve may enable passive targeting of the lung, liver and spleen via the RES, followed by sustained release. Subcutaneous administration of nanoparticles was achieved mainly for the delivery of peptides and vaccines [104]. It allows sustained release depot of the drugs therefore reducing the number of administrations, increasing blood half-life of the active drug, and finally, in some cases, reducing side effects. The rate of release may be controlled by the nature of the carrier materials and particle size.

1.4.2 Oral Drug Delivery

Nanoparticles have been successfully used as carriers for oral drug delivery to increase bioavailability of many drugs with poor absorption characteristics ranging from anticoagulants[105], antihypertensives [106, 107], anti-cancer drugs [50, 108], antibiotics [109] and hormones [26, 28, 82]. In addition, these studies have revealed a great potential of nanoparticle technologies in tackling problems associated with delivery of poorly water-soluble drugs regarding low oral bioavailability, high intersubject variability and poor or suboptimal therapeutic response. Different effects have been observed depending on the particle technology used. Vaughn et al. have compared the properties of nanoparticles (composed of danazol and PVP K-15) formed by EPAS and SFL and correlated to the in vivo performance of the drug [87]. The differences in particle morphology and degree of miscibility of the drug and polymer were found using Z-contrast scanning transmission electron microscopy (STEM). The results indicated that the SFL technology produced amorphous solid solutions particles with mean size of 30 nm. On the other hand, the EPAS technology results in formation of solid dispersion with partially crystalline form of larger nanoparticles (500 nm). The result was attributed to the differences in the particle formation mechanisms for the EPAS and SFL technologies, precipitation versus rapid freezing, respectively. Both EPAS and SFL formulations, however, were able to achieve 27% and 33% supersaturation, respectively compared to the

physical mixture (crystalline microparticles with PVP K-15) and remained above supersaturation for 60-90 minutes. An in vivo study has been conducted in mice and demonstrated an increased in the rate and extent of absorption for danazol produced by EPAS and SFL compared to the physical mixture and commercial Danocrine® capsules.

Nanoparticles are generally stabilized using different types of polymers and surfactants which can change the surface charge of the particle preventing electrostatic forces from causing aggregation. Various polymers have been used to fabricate nanoparticles include synthetic polymers such as polylactide–polyglycolide copolymers, polyacrylates and polycaprolactones or natural polymers such as albumin, gelatin, alginate and chitosan. The release of drug from nanoparticles can be controlled by modulating polymer characteristics to achieve desired therapeutic level in target tissue for required duration and optimal therapeutic efficacy [110]. Recently, it was shown that the use of nanoparticles containing rifampicin, isoniazid and pyrazinamide were achieved high concentrations and maintained in the plasma for 8 days following a single oral administration in mice [109]. Therapeutic drug concentrations of these nanoparticles were also found in the organs including lungs, liver and spleen for 10 days whereas free drugs were cleared by 24–48 hrs.

Nanoparticles have also shown a certain degree of success for the oral delivery of macromolecules, such as peptides, proteins, oligonucleotides and

plasmids to the systemic circulation and to the immune system [95, 111, 112]. The oral delivery of these compounds is unresolved challenge leading to low bioavailability mainly because of their poor penetration across biological membranes and their susceptibility to enzymatic degradation. The major obstacle for using nanoparticles as an oral delivery system is the prerequisite that particles need to be absorbed from the gastrointestinal tract with a sufficient rate and extent. The adhesion of the particles to the mucosal surface is an essential step before the translocation of the particles can take place [113, 114]. Therefore, mucoadhesion may play an important role in the uptake process. Ponchel et al. have studied the adsorption of poly (styrene) latexes in different particle sizes [114] . The adsorption isotherms followed Langmuir-behavior as shown in Figure 1.5. The adsorption of nanoparticles rapidly increased (sharp initial slope) before reach the plateau suggesting that nanoparticles exhibits stronger affinity with the mucus layer than those of micron size particles. This demonstrated that nanoparticles were able to penetrate into the mucous layer more efficiently than micron sized particles of the same material. Mucoadhesive polymers have been used to prolong contact times of nanoparticle systems at the absorption site allowing high drug adsorption [113]. Typical mucoadhesive polymers include polysaccharides such as chitosan and xanthan gum; cellulose based polymers such as hydroxypropylmethyl cellulose (HPMC); acrylate polymers such as poly(acrylic acid) and carbomers; and sodium alginate. The improvement of oral

absorption for protein and peptide drugs including insulin and calcitonin has been well reported using the specialized delivery system of mucoadhesive nanoparticles [115].

1.4.3 Pulmonary Drug Delivery

The pulmonary route has been used for decades to administer drug to the lung for the treatment of asthma and other respiratory diseases [116]. Currently, this route has attracted great attention because it may become an important non-invasive route for systemic drug delivery. In general, non-invasive routes have higher patient compliance than parenteral routes but achieving rapid onset of therapeutic drug levels can be challenging. The recent example of pulmonary administration for systemic drug delivery is insulin inhalation. The first commercial pulmonary formulation of rapid-acting insulin (Exubera®) is now approved by the FDA. It is manufactured by Pfizer using Nektar Therapeutics proprietary inhalation technology. This is considered a significant step forward and a breakthrough approach in the treatment of type 1 and type 2 diabetics by delivering insulin to the lungs via inhalation. Inhaled insulin enters the blood circulation more rapidly than by subcutaneous injection while increasing patient compliance [117].

Pulmonary administration of drugs can be expected to achieve faster onset of action and higher systemic bioavailability than other noninvasive routes because of the huge surface area with highly vascularized regions and relatively low drug-metabolizing enzyme activity in the lung [118]. In addition, the pulmonary route is not subject to first pass metabolism, so this is especially useful for many drugs which undergo extensive metabolism in liver. For example, pulmonary delivery has long been viewed as a promising approach for improving the systemic bioavailability of immunosuppressive drugs and reducing their toxicity [119-121]. It is well known that the oral absorption of these drugs is variable and incomplete because of the drug efflux back into the intestine by the membrane pump p-glycoprotein and drug metabolism in the intestine and hepatic by CYP3A family of enzymes [122] . Many studies have demonstrated that aerosolized cyclosporine (CsA) is an effective therapeutic for preventing allograft rejection at a reduced dose compared to intravenous or oral dosage forms [123-125]. In early clinical studies, CsA was simply dissolved in the solvents such as ethanol or propylene glycol [126-129]. However, the results were unsatisfactory due to the irritating properties of these solvents. More importantly, the nebulization procedure was complicated due to the precipitation of CsA within the nebulization chamber.

Until recently, research has been focused on new aerosol delivery systems using inhaled nanoparticles as therapeutic carriers [130-132]. This is an active

area of research by numerous groups because of the appealing aspect of inhaled nanoparticles in significantly improving the systemic bioavailability of the drug. This was attributed to the rapid dissolution rate of nanoparticles in the airway epithelium via surface energetics in comparison with microparticles. In addition, nanoparticles may also be considered as drug targeting approach to facilitate intracellular delivery particularly to alveolar macrophages and lymphocytes for treating infections of the MPS system [133-135]. Some microorganisms, particularly in the lung macrophages, including mycobacteria and aspergillus fungus, are difficult to reach with a normal treatment. The delivery of an antifungal agent directly to the lung has recently been evaluated as a promising way to improve the treatment of invasive fungal infections compared to the conventional treatment. It has been recently reported that nanoparticles of itraconazole (ITZ) processed using SFL were taken up by pulmonary macrophages [136]. Further, aerosolized nanoparticles of ITZ were able to achieve high and sustained levels in the lung tissue. The efficacy studies conducted against the *Aspergillus fumigatus* in mice was also shown to significantly prolong survival of infected mice through the inhalation of ITZ nanoparticles compared to the commercial product using Sporanox ® oral solution [137].

However, a potential limitation of using nanoparticles for pulmonary delivery is their extremely low inertia causing the particles to escape from lung

deposition. As a result, a large portion of the inhaled particles would be exhaled from the lungs after inspiration. Various particle technologies and designs have been investigated in order to deliver nanoparticles to the deep lung [138-141]. The nebulization technology was used to produce the aerosolized droplets of nanoparticles which can then be inhaled [142]. The aerodynamic diameters of these droplets are within the 1-5 μm range which is optimum for delivery into the lung. Similar concepts of incorporating nanoparticles into the matrix of micron sized carrier particles using both spray-drying and freeze-drying techniques has also been reported [139, 140, 143]. Sham et al. have successfully produced nanoparticle-loaded microspheres using lactose as the carrier [143]. They used the spray drying technique to form microparticles which contain gelatin or polybutylcyanoacrylate nanoparticles. The aerodynamic diameter of the spray dried particles was 3.0±0.2 μm while the average particle size of the nanoparticles was 242±14 nm for gelatin and 173±63 nm for polybutylcyanoacrylate. Further, Tsapis et al. have also utilized large porous particles as carriers for nanoparticles (trojan particles) [141]. Such particles have the potential in delivering nanoparticles to the alveolar region and avoid elimination from the lungs because of their large size and low density. Another approach is to use bioadhesive and biodegradable polymers in order to retain the nanoparticles within the lungs [117, 144]. A polymer also allows for the slow and sustained release of drugs, which leads to a less frequent and attenuated drug treatment regimen. To date, these

approaches are not presently being explored commercially or clinically, as the technologies are relatively new and are still being developed.

1.4.4 Brain Drug Delivery

One of the more recent applications includes employing nanoparticles as drug delivery systems to the brain (143-145). The administration of drugs to the central nervous system (CNS) is a significant challenge because many drugs have great difficulty crossing the blood–brain barrier (BBB). The blood brain barrier is a complex structure composed of endothelial cells connected by highly restrictive tight junctions (146). This unique structure protects the brain against peripheral neurotransmitters, cytotoxins and microorganisms. However, it also restricts the passage of potential drugs for the treatment of neurological or psychiatric disorders, and of other brain pathologies (such as infections and tumors). Conventional methods for delivering drugs to the CNS involves invasive surgical procedures (147). Attempts have been made to disrupt the BBB (increased paracellular diffusion) in order to enhance delivery of drug to the brain using vasoactive agents such as leukotrienes, histamine, bradykinin, and the synthetic bradykinin analog RMP-7 (receptor-mediated permeabilizer (147). However, junctional openings of the BBB may break down the self-defense mechanism of the brain allowing entry of toxins and unwanted molecules. Recently, nanoparticles have been revealed as efficient carriers to deliver drugs through the

BBB into the brain (145, 148, 149). It was reported that the use of poly (butylcyanoacrylate) nanoparticles (PBCA) coated with surfactants, especially polysorbate 80 led to a high drug concentrations in the brain following intravenous administration (150). Drugs that have successfully been delivered across the BBB using PBCA nanoparticles include hexapeptide dalargin, the dipeptide kytorphin, tubocurarine and doxorubicin (147). The mechanism by which the nanoparticles deliver drugs into the brain has not yet been fully elucidated. The possible transport mechanism has been suggested to be cellular endothelial endocytosis following adsorption of plasma proteins especially apolipoprotein E (apo E) after intravenous injection (36). The polysorbate-coated nanoparticles interact with the low density lipoproteins (LDL) receptors on the endothelial cells, resulting in their uptake by brain endothelial cells into the brain. On the other hand, the particles without the surfactant coating remained in the blood vessels.

1.5 CONCLUSION

Nanoparticle technology represents a valuable tool for optimizing and enhancing drug formulations by improving their efficacy, safety, convenience and compliance. The integration of nanoparticle technologies into the pharmaceutical drug development process is beginning to demonstrate tremendous potential in drug development including success of commercial applications, patent protection and successful investment from governments around the globe. The use of

nanoparticle technology in drug development is presently in its infancy and still being explored. However, recent works have shown promise for nanoparticle-based technologies as potential methods to enhance drug bioavailability and enable drugs to be incorporated into formulations for targeted drug delivery. Also, nanoparticle-based technologies have been used with various routes of administration, including oral, injectable, brain and the lungs. It is often difficult or impossible to obtain drug nanoparticles by conventional technologies using jet and ball milling, spray drying, and recrystallization using solvent evaporation. Currently, the engineering of drug nanoparticles using mechanical, emulsification, precipitation, supercritical fluids and cryogenic has been successfully demonstrated. The technologies such as wet milling and high-pressure homogenization have enabled successful commercialization of drug nanoparticles. There are, however, some challenges facing the successful implementation for the widespread use of nanoparticle technologies in pharmaceutical industry including large scale production and harvesting of particles with the desired characteristics.

1.6 REFERENCES

1. Kubik T, Bogunia-Kubik K, Sugisaka M. (2005) Nanotechnology on duty in medical applications. Curr. Pharm. Biotechnol. **6:** 17-33.
2. Ferrari M. (2005) Cancer nanotechnology: Opportunities and challenges. Nat. Rev. Cancer **5:** 161-171.

3. Hilt JZ. (2004) Nanotechnology and biomimetic methods in therapeutics: molecular scale control with some help from nature. Adv. Drug Deliv. Rev. **56:** 1533-1536.

4. Roco MC. (2005) International perspective on government nanotechnology funding in 2005. J. Nanopart. Res. **7:** 707-712.

5. Fox JL. (2000) Researchers discuss NIH's nanotechnology initiative **18:** 821.

6. Roco MC. (2001) International strategy for nanotechnology research and development. J. Nanopart. Res. **3:** 353-360.

7. Hughes GA. (2005) Nanostructure-Mediated Drug Delivery. Dis. Mon. **51:** 342-361.

8. Sahoo SK, Labhasetwar V. (2003) Nanotech approaches to drug delivery and imaging. Drug Discov. Today **8:** 1112-1120.

9. Stylios GK, Giannoudis PV, Wan T. (2005) Applications of nanotechnologies in medical practice. Injury **36:** S6-S13.

10. Lee VHL. (2004) Nanotechnology: challenging the limit of creativity in targeted drug delivery. Adv. Drug Deliv. Rev. **56:** 1527-1528.

11. Henrymichelland S, Alonso MJ, Andremont A, Maincen P, Sauzieres J, Couvreur P. (1987) Attachment of Antibiotics to Nanoparticles - Preparation, Drug-Release and Antimicrobial Activity Invitro. Int. J Pharm. **35:** 121-127.

12. Mukherji G, Murthy RSR, Miglani BD. (1989) Preparation and evaluation of polyglutaraldehyde nanoparticles containing 5-fluorouracil. Int. J Pharm. **50:** 15-19.

13. Oppenheim RC. (1981) Solid Colloidal Drug Delivery Systems - Nanoparticles. Int. J Pharm.**8:** 217-234.

14. Kawashima Y. (2001) Nanoparticulate systems for improved drug delivery. Adv. Drug Deliv. Rev. **47:** 1-2.

15. Lockman PR, Mumper RJ, Khan MA, Allen DD. (2002) Nanoparticle technology for drug delivery across the blood-brain barrier Drug Dev. Ind. Pharm., pp. 1-13.

16. Huang Z, Chen HC, Yan LJ, Roco MC. (2005) Longitudinal nanotechnology development (1991-2002): National Science Foundation funding and its impact on patents. J. Nanopart. Res. **7:** 343-376.

17. Lipinski CA, Lombardo F, Dominy BW, Feeney PJ. (1997) Experimental and computational approaches to estimate solubility and permeability in drug discovery and development settings. Adv. Drug Deliv. Rev. **23:** 3-25.

18. Horter D, Dressman JB. (2001) Influence of physicochemical properties on dissolution of drugs in the gastrointestinal tract. Adv. Drug Deliv. Rev. **46:** 75-87.

19. Fleisher D, Bong R, Stewart BH. (1996) Improved oral drug delivery: solubility limitations overcome by the use of prodrugs. Adv. Drug Deliv. Rev. **19:** 115-130.

20. Loftsson T, Brewster ME. (1996) Pharmaceutical applications of cyclodextrins. 1. Drug solubilization and stabilization. J. Pharm. Sci. **85:** 1017-1025.

21. Leuner C, Dressman J. (2000) Improving drug solubility for oral delivery using solid dispersions. Eur. J. Pharm. Biopharm. **50:** 47-60.

22. Torchilin VP. (2001) Structure and design of polymeric surfactant-based drug delivery systems. J. Control. Release **73:** 137-172.

23. Venkatesh S, Lipper RA. (2000) Role of the development scientist in compound lead selection and optimization. J. Pharm. Sci. **89:** 145-154.

24. Bowers VD, Locker S, Ames S, Jennings W, Corry RJ. (1991) The Hemodynamic-Effects of Cremophor-El. Transplantation **51:** 847-850.

25. Hecq J, Deleers M, Fanara D, Vranckx H, Amighi K. (2005) Preparation and characterization of nanocrystals for solubility and dissolution rate enhancement of nifedipine. Int. J Pharm. **299:** 167-177.

26. Hu J, Johnston KP, Williams I, Robert O. (2004) Rapid dissolving high potency danazol powders produced by spray freezing into liquid process. Int. J Pharm. **271:** 145-154.

27. Rogers TL, Gillespie IB, Hitt JE, et al. (2004) Development and characterization of a scalable controlled precipitation process to enhance the dissolution of poorly water-soluble drugs. Pharm. Res. **21:** 2048-2057.

28. Liversidge GG, Cundy KC. (1995) Particle size reduction for improvement of oral bioavailability of hydrophobic drugs: I. Absolute oral bioavailability of nanocrystalline danazol in beagle dogs. Int. J Pharm.**125:** 91-97.

29. Sohnel O, Garside J. (1992) Precipitation: Basic Principles and Industrial Applications. Butterworth Heinemann.

30. Raghavan SL, Trividic A, Davis AF, Hadgraft J. (2000) Effect of cellulose polymers on supersaturation and in vitro membrane transport of hydrocortisone acetate Int. J Pharm., pp. 231-237.

31. Jasti BR, Berner B, Zhou S-L, Li X. (2004) A Novel Method for Determination of Drug Solubility in Polymeric Matrices J. Pharm. Sci. pp. 2135-2141.

32. Gao P, Rush BD, Pfund WP, et al. (2003) Development of a supersaturable SEDDS (S-SEDDS) formulation of paclitaxel with improved oral bioavailability. J. Pharm. Sci. **92:** 2386-2398.

33. Pedersen M. (1997) The bioavailability difference between genuine cyclodextrin inclusion complexes and freeze-dried or ground drug

cyclodextrin samples may be due to supersaturation differences. Drug Dev. Ind. Pharm.**23:** 331-335.

34. Gao P, Guyton ME, Huang T, Bauer JM, Stefanski KJ, Lu Q. (2004) Enhanced Oral Bioavailability of a Poorly Water Soluble Drug PNU-91325 by Supersaturatable Formulations. Drug Dev. Ind. Pharm.**30:** 221-229.

35. Brannon-Peppas L, Blanchette JO. (2004) Nanoparticle and targeted systems for cancer therapy. Adv. Drug Deliv. Rev. **56:** 1649-1659.

36. Roney C, Kulkarni P, Arora V, et al. (2005) Targeted nanoparticles for drug delivery through the blood-brain barrier for Alzheimer's disease. J. Control. Release **108:** 193-214.

37. Mykhaylyk O, Dudchenko N, Dudchenko A. (2005) Doxorubicin magnetic conjugate targeting upon intravenous injection into mice: High gradient magnetic field inhibits the clearance of nanoparticles from the blood. J. Magn. Magn. Mater. **293:** 473-482.

38. Peracchia MT, Fattal E, Desmaele D, et al. (1999) Stealth(R) PEGylated polycyanoacrylate nanoparticles for intravenous administration and splenic targeting. J. Control. Release **60:** 121-128.

39. Li Y-P, Pei Y-Y, Zhang X-Y, et al. (2001) PEGylated PLGA nanoparticles as protein carriers: synthesis, preparation and biodistribution in rats. J. Control. Release **71:** 203-211.

40. Moghimi SM, Hunter AC, Murray JC. (2001) Long-Circulating and Target-Specific Nanoparticles: Theory to Practice. Pharmacol Rev **53:** 283-318.

41. Fang C, Shi B, Pei Y-Y, Hong M-H, Wu J, Chen H-Z. (2006) In vivo tumor targeting of tumor necrosis factor-[alpha]-loaded stealth nanoparticles: Effect of MePEG molecular weight and particle size. Eur. J. Pharm. Sci. **27:** 27-36.

42. Harries M, Ellis P, Harper P. (2005) Nanoparticle albumin-bound paclitaxel for metastatic breast cancer. J. Clin. Oncol. **23:** 7768-7771.

43. Mandal S, Phadtare S, Sastry M. (2005) Interfacing biology with nanoparticles. Curr. Appl. Phys. **5:** 118-127.

44. Takeuchi H, Yamamoto H, Kawashima Y. (2001) Mucoadhesive nanoparticulate systems for peptide drug delivery Adv. Drug Deliv. Rev., pp. 39-54.

45. Hu J, Johnston KP, Williams III RO. (2004) Nanoparticle Engineering Processes for Enhancing the Dissolution Rates of Poorly Water Soluble Drugs. Drug Dev. Ind. Pharm. **30:** 233-245.

46. Liversidge GG, Cundy KC, Bishop J, Czekai D. (1991) Surface modified drug nanoparticles. US Patent No. 5145684.

47. Merisko-Liversidge E, Liversidge GG, Cooper ER. (2003) Nanosizing: a formulation approach for poorly-water-soluble compounds. Eur. J. Pharm. Sci. **18:** 113-120.

48. Kondo N, Iwao T, Masuda H, et al. (1993) Improved oral absorption of a poorly water-soluble drug, HO-221, by wet-bead milling producing particles in submicron region. Chem. Pharm. Bull. **41:** 737-740.

49. Kayser O, Olbrich C, Yardley V, Kiderlen AF, Croft SL. (2003) Formulation of amphotericin B as nanosuspension for oral administration. Int. J Pharm.**254:** 73-75.

50. Peters K, Leitzke S, Diederichs JE, et al. (2000) Preparation of a clofazimine nanosuspension for intravenous use and evaluation of its therapeutic efficacy in murine Mycobacterium avium infection. J. Antimicrob. Chemother. **45:** 77-83.

51. Muller RH, Mader K, Gohla S. (2000) Solid lipid nanoparticles (SLN) for controlled drug delivery - a review of the state of the art. Eur. J. Pharm. Biopharm. **50:** 161-177.

52. Müller RH, Becker R, Kruss B, Peters K. (1998) Pharmaceutical nanosuspensions for medicament administration as system of increased saturation solubility and rate of solution. US Patent No. 5858410.

53. Lamprecht A, Ubrich N, Hombreiro Perez M, Lehr C-M, Hoffman M, Maincent P. (1999) Biodegradable monodispersed nanoparticles prepared by pressure homogenization-emulsification. Int. J Pharm. **184:** 97-105.

54. Kriwet B, Walter E, Kissel T. (1998) Synthesis of bioadhesive poly(acrylic acid) nano- and microparticles using an inverse emulsion polymerization method for the entrapment of hydrophilic drug candidates. J. Control. Release **56:** 149-158.

55. Lawrence MJ, Rees GD. (2000) Microemulsion-based media as novel drug delivery systems. Adv. Drug Deliv. Rev. **45:** 89-121.

56. Solans C, Izquierdo P, Nolla J, Azemar N, Garcia-Celma MJ. (2005) Nano-emulsions. Curr. Opin. Colloid Interface Sci. **10:** 102-110.

57. Jaiswal J, Kumar Gupta S, Kreuter J. (2004) Preparation of biodegradable cyclosporine nanoparticles by high-pressure emulsification-solvent evaporation process. J. Control. Release **96:** 169-178.

58. Quintanar-Guerrero D, Allemann E, Fessi H, Doelker E. (1999) Pseudolatex preparation using a novel emulsion-diffusion process involving direct displacement of partially water-miscible solvents by distillation. Int. J Pharm. **188:** 155-164.

59. Trotta M, Gallarate M, Carlotti ME, Morel S. (2003) Preparation of griseofulvin nanoparticles from water-dilutable microemulsions. Int. J Pharm. **254:** 235-242.

60. Vonderscher J, Meinzer A. (1994) Rationale for the Development of Sandimmune-Neoral. Transplant. Proc. **26:** 2925-2927.

61. Marr R, Gamse T. (2000) Use of supercritical fluids for different processes including new developments--a review. Chem. Eng. Process. **39:** 19-28.

62. Subramaniam B, Rajewski RA, Snavely K. (1997) Pharmaceutical processing with supercritical carbon dioxide. J. Pharm. Sci. **86:** 885-890.

63. Turk M, Hils P, Helfgen B, Schaber K, Martin H-J, Wahl MA. (2002) Micronization of pharmaceutical substances by the Rapid Expansion of Supercritical Solutions (RESS): a promising method to improve bioavailability of poorly soluble pharmaceutical agents. J. Supercrit. Fluid **22:** 75-84.

64. Young TJ, Mawson S, Johnston KP, Henriksen IB, Pace GW, Mishra AK. (2000) Rapid Expansion from Supercritical to Aqueous Solution to Produce Submicron Suspensions of Water-Insoluble Drugs. Biotechnol. Prog. **16:** 402-407.

65. Jung J, Perrut M. (2001) Particle design using supercritical fluids: Literature and patent survey J. Supercrit. Fluid, pp. 179-219.

66. Knez Z, Weidner E. (2003) Particles formation and particle design using supercritical fluids. Curr. Opin. Solid State Mater. Sci. **7:** 353-361.

67. Yeo S-D, Kiran E. (2005) Formation of polymer particles with supercritical fluids: A review. J. Supercrit. Fluid **34:** 287-308.

68. Reverchon E. (1999) Supercritical antisolvent precipitation of micro- and nano-particles. J. Supercrit. Fluid **15:** 1-21.

69. Palakodaty S, York P. (1999) Phase behavioral effects on particle formation processes using supercritical fluids. Pharm. Res. **16:** 976-985.

70. Sohnel O, Garside J. (1992) Precipitation: Basic Principles and Industrial Applications. Butterworth Heinemann.

71. Kind M. (2002) Colloidal aspects of precipitation processes. Chem. Eng. Sci. **57:** 4287-4293.

72. Fessi HC, Devissaguet JP. (1992) Process for the preparation of dispersible colloidal systems of a substance in the form of nanoparticles. US Patent 5,118,528.

73. Fessi H, Puisieux F, Devissaguet JP, Ammoury N, Benita S. (1989) Nanocapsule formation by interfacial polymer deposition following solvent displacement. Int. J Pharm. **55:** R1-R4.

74. Hyvonen S, Peltonen L, Karjalainen M, Hirvonen J. (2005) Effect of nanoprecipitation on the physicochemical properties of low molecular weight poly(l-lactic acid) nanoparticles loaded with salbutamol sulphate and beclomethasone dipropionate. Int. J Pharm. **295:** 269-281.

75. Layre A-M, Gref R, Richard J, et al. (2005) Nanoencapsulation of a crystalline drug. Int. J Pharm.**298:** 323-327.

76. Guzman M, Molpeceres J, Garcia F, Aberturas MR, Rodriguez M. (1993) Formation and Characterization of Cyclosporine-Loaded Nanoparticles. J. Pharm. Sci. **82:** 498-502.

77. Bilati U, Allemann E, Doelker E. (2005) Development of a nanoprecipitation method intended for the entrapment of hydrophilic drugs into nanoparticles. Eur. J. Pharm. Sci. **24:** 67-75.

78. Palakodaty S, York P. (1999) Phase behavioral effects on particle formation processes using supercritical fluids. Pharm. Res. **16:** 976-985.

79. Sarkari M, Brown J, Chen X, Swinnea S, Johnston KP, Williams III RO. (2002) Enhanced drug dissolution using evaporative precipitation into aqueous solution. Int. J Pharm. **243:** 17-31.

80. Chen X, Young TJ, Sarkari M, Williams I, Robert O., Johnston KP. (2002) Preparation of cyclosporine A nanoparticles by evaporative precipitation into aqueous solution. Int. J Pharm. **242:** 3-14.

81. Chen X, Vaughn JM, Yacaman MJ, Williams III RO, Johnston KP. (2004) Rapid dissolution of high-potency danazol particles produced by evaporative precipitation into aqueous solution. J. Pharm. Sci. **93:** 1867-1878.

82. Chen X, Benhayoune Z, Williams III RO, Johnston KP. (2004) Rapid dissolution of high potency itraconazole particles produced by evaporative precipitation into aqueous solution. J. Drug Del. Sci. Technol. **14:** 299-304.

83. Sinswat P, Gao X, Yacaman MJ, Williams III RO, Johnston KP. (2005) Stabilizer choice for rapid dissolving high potency itraconazole particles formed by evaporative precipitation into aqueous solution. Int. J Pharm. **302:** 113-124.

84. Pikal MJ, Dellerman KM, Roy ML, Riggin RM. (1991) The effects of formulation variables on the stability of freeze-dried human growth hormone. Pharm. Res. **8:** 427-436.

85. Webb SD, Golledge SL, Cleland JL, Carpenter JF, Randolph TW. (2002) Surface adsorption of recombinant human interferon-[Gamma] in lyophilized and spray-lyophilized formulations. J. Pharm. Sci. **91:** 1474-1487.

86. Vaughn JM, Gao X, Yacaman M-J, Johnston KP, Williams III RO. (2005) Comparison of powder produced by evaporative precipitation into aqueous solution (EPAS) and spray freezing into liquid (SFL) technologies using novel Z-contrast STEM and complimentary techniques. Eur. J. Pharm. Biopharm. **60:** 81-89.

87. Rogers TL, Hu J, Yu Z, Johnston KP, Williams III RO. (2002) A novel particle engineering technology: spray-freezing into liquid. Int. J Pharm. **242:** 93-100.

88. Yu Z, Rogers TL, Hu J, Johnston KP, Williams III RO. (2002) Preparation and characterization of microparticles containing peptide produced by a novel process: spray freezing into liquid. Eur. J. Pharm. Biopharm. **54:** 221-228.

89. Yu Z, Garcia AS, Johnston KP, Williams I, Robert O. (2004) Spray freezing into liquid nitrogen for highly stable protein nanostructured microparticles. Eur. J. Pharm. Biopharm. **58:** 529-537.

90. Rogers TL, Nelsen AC, Hu J, Johnston KP, Williams III RO. (2002) A novel particle engineering technology to enhance dissolution of poorly water soluble drugs: spray-freezing into liquid. Eur. J. Pharm. Biopharm. **54:** 271-280.

91. Rogers TL, Overhoff KA, Shah P, Johnston KP, Williams III RO. (2003) Micronized powders of a poorly water soluble drug produced by a spray-freezing into liquid-emulsion process. Eur. J. Pharm. Biopharm. **55:** 161-172.

92. Rogers TL, Nelsen AC, Sarkari M, Young TJ, Johnston KP, Williams III RO. (2003) Enhanced aqueous dissolution of a poorly water soluble drug

by novel particle engineering technology: Spray-freezing into liquid with atmospheric freeze-drying. Pharm. Res.**20:** 485-493.

93. Orive G, Gascon AR, Hernandez RM, Dominguez-Gil A, Pedraz JL. (2004) Techniques: New approaches to the delivery of biopharmaceuticals. Trends Pharmacol. Sci. **25:** 382-387.

94. Yamada T, Iwasaki Y, Tada H, et al. (2003) Nanoparticles for the delivery of genes and drugs to human hepatocytes. Nat Biotech.**21:** 885-890.

95. Lu Y, Chen SC. (2004) Micro and nano-fabrication of biodegradable polymers for drug delivery. Adv. Drug Deliv. Rev. **56:** 1621-1633.

96. Couvreur P, Puisieux F. (1993) Nano- and microparticles for the delivery of polypeptides and proteins. Adv. Drug Deliv. Rev. **10:** 141-162.

97. Wissing SA, Kayser O, Muller RH. (2004) Solid lipid nanoparticles for parenteral drug delivery. Adv. Drug Deliv. Rev. **56:** 1257-1272.

98. Kipp JE. (2004) The role of solid nanoparticle technology in the parenteral delivery of poorly water-soluble drugs. Int. J Pharm. **284:** 109-122.

99. Pinto-Alphandary H, Andremont A, Couvreur P. (2000) Targeted delivery of antibiotics using liposomes and nanoparticles: research and applications. Int. J. Antimicrob. Agents **13:** 155-168.

100. Ahsan F, Rivas IP, Khan MA, Torres Suarez AI. (2002) Targeting to macrophages: role of physicochemical properties of particulate carriers--

liposomes and microspheres--on the phagocytosis by macrophages. J. Control. Release **79:** 29-40.

101. Chellat F, Merhi Y, Moreau A, Yahia LH. (2005) Therapeutic potential of nanoparticulate systems for macrophage targeting. Biomaterials **26:** 7260-7275.

102. Forestier F, Gerrier P, Chaumard C, Quero AM, Couvreur P, Labarre C. (1992) Effect of Nanoparticle-Bound Ampicillin on the Survival of Listeria Monocytogenes in Mouse Peritoneal Macrophages. J. Antimicrob. Chemother. **30:** 173-179.

103. Gautier JC, Grangier JL, Barbier A, et al. (1992) Biodegradable nanoparticles for subcutaneous administration of growth hormone releasing factor (hGRF). J. Control. Release **20:** 67-77.

104. Jiao Y, Ubrich N, Marchand-Arvier M, et al. (2002) In vitro and in vivo evaluation of oral heparin-loaded polymeric nanoparticles in rabbits. Circulation **105:** 230-235.

105. Ahlin P, Kristl J, Kristl A, Vrecer F. (2002) Investigation of polymeric nanoparticles as carriers of enalaprilat for oral administration. Int. J Pharm.**239:** 113-120.

106. Kim YI, Fluckiger L, Hoffman M, Lartaud-Idjouadiene I, Atkinson J, Maincent P. (1997) The antihypertensive effect of orally administered

nifedipine-loaded nanoparticles in spontaneously hypertensive rats. Br. J. Pharmacol. **120:** 399-404.

107. Dong Y, Feng S-S. (2005) Poly(d,l-lactide-co-glycolide)/montmorillonite nanoparticles for oral delivery of anticancer drugs. Biomaterials **26:** 6068-6076.

108. Pandey R, Zahoor A, Sharma S, Khuller GK. (2003) Nanoparticle encapsulated antitubercular drugs as a potential oral drug delivery system against murine tuberculosis. Tuberculosis **83:** 373-378.

109. Brannon-Peppas L. (1995) Recent advances on the use of biodegradable microparticles and nanoparticles in controlled drug delivery. Int. J Pharm. **116:** 1-9.

110. Panyam J, Labhasetwar V. (2003) Biodegradable nanoparticles for drug and gene delivery to cells and tissue. Adv. Drug Deliv. Rev. **55:** 329-347.

111. Fishbein I, Chorny M, Rabinovich L, Banai S, Gati I, Golomb G. (2000) Nanoparticulate delivery system of a tyrphostin for the treatment of restenosis. J. Control. Release **65:** 221-229.

112. Peppas NA, Huang Y. (2004) Nanoscale technology of mucoadhesive interactions. Adv. Drug Deliv. Rev. **56:** 1675-1687.

113. Ponchel G, Montisci M-J, Dembri A, Durrer C, Duchene D. (1997) Mucoadhesion of colloidal particulate systems in the gastro-intestinal tract. Eur. J. Pharm. Biopharm. **44:** 25-31.

114. Takeuchi H, Yamamoto H, Kawashima Y. (2001) Mucoadhesive nanoparticulate systems for peptide drug delivery. Adv. Drug Deliv. Rev. **47:** 39-54.

115. Yu JW, Chien YW. (1997) Pulmonary drug delivery: Physiologic and mechanistic aspects. Crit Rev Ther Drug Carrier Syst **14:** 395-453.

116. Kawashima Y, Yamamoto H, Takeuchi H, Fujioka S, Hino T. (1999) Pulmonary delivery of insulin with nebulized -lactide/glycolide copolymer (PLGA) nanospheres to prolong hypoglycemic effect. J. Control. Release **62:** 279-287.

117. Hoover JL, Rush BD, Wilkinson KF, et al. (1992) Peptides are better absorbed from the lung than the gut in the rat. Pharm. Res. **9:** 1103-1106.

118. Mitruka SN, Pham SM, Zeevi A, et al. (1998) Aerosol cyclosporine prevents acute allograft rejection in experimental lung transplantation. J. Thorac. Cardiovasc. Surg. **115:** 28-37.

119. Koshkina NV, Golunski E, Roberts LE, Gilbert BE, Knight V. (2004) Cyclosporin A aerosol improves the anticancer effect of paclitaxel aerosol in mice. J. Aerosol Sci. **17:** 7-14.

120. Ingu A, Komatsu K, Ichimiya S, et al. (2005) Effects of Inhaled FK 506 on the Suppression of Acute Rejection After Lung Transplantation: Use of a Rat Orthotopic Lung Transplantation Model. J. Heart Lung Transplant. **24:** 538-543.

121. Fahr A. (1993) Cyclosporin clinical pharmacokinetics. Clin. Pharmacokinet. **24:** 472-495.

122. Blot F, Tavakoli R, Sellam S, et al. (1995) Nebulized cyclosporine for prevention of acute pulmonary allograft rejection in the rat: Pharmacokinetic and histologic study. J. Heart Lung Transplant. **14:** 1162-1172.

123. Letsou GV, Safi HJ, Reardon MJ, et al. (1999) Pharmacokinetics of liposomal aerosolized cyclosporine A for pulmonary immunosuppression. Ann. Thorac. Surg. **68:** 2044-2048.

124. Keenan RJ, Duncan AJ, Yousem SA, et al. (1992) Improved immunosuppression with aerosolized cyclosporine in experimental pulmonary transplantation. Transplantation **53:** 20-25.

125. Keenan RJ DA, Yousem SA , et al. (1992) Improved immunosuppression with aerosolized cyclosporine in experimental pulmonary transplantation Transplantation . pp. 20-25.

126. Dowling RD ZM, Burckart GJ, et al. (1990) Aerosolized cyclosporine as single-agent immunotherapy in canine lung allografts. Surgery, pp. 198-204.

127. Blot F, Tavakoli R, Sellam S, et al. (1995) Nebulized cyclosporine for prevention of acute pulmonary allograft rejection in the rat:

Pharmacokinetic and histologic study J. Heart Lung Transpl. pp. 1162-1172.

128. Iacono AT, Keenan RJ, Duncan SR, et al. (1996) Aerosolized cyclosporine in lung recipients with refractory chronic rejection Am. J. Respir. Crit. Care Med., pp. 1451-1455.

129. Geys J, Coenegrachts L, Vercammen J, et al. (2006) In vitro study of the pulmonary translocation of nanoparticles: A preliminary study. Toxicol. Lett. **160:** 218-226.

130. Eerikainen H, Kauppinen EI. (2003) Preparation of polymeric nanoparticles containing corticosteroid by a novel aerosol flow reactor method. Int. J Pharm. **263:** 69-83.

131. Bivas-Benita M, Zwier R, Junginger HE, Borchard G. (2005) Non-invasive pulmonary aerosol delivery in mice by the endotracheal route. Eur. J. Pharm. Biopharm. **61:** 214-218.

132. Fawaz F, Bonini F, Maugein J, Lagueny AM. (1998) Ciprofloxacin-loaded polyisobutylcyanoacrylate nanoparticles: pharmacokinetics and in vitro antimicrobial activity. Int. J Pharm. **168:** 255-259.

133. Hoeben B. J., McConville J. T., Najvar L. K., Talbert R. L., Peters J. I., Wiederhold N. P., Frei B. L., Graybill J. R., Bocanegra R., Sinswat P., Johnston K. P., and Williams R. O. (2006) In Vivo Efficacy of Aerosolized Nanostructured Itraconazole Formulations for the Prevention

of Invasive Pulmonary Aspergilliosis. Antimicrob. Agents Chemother.-submitted.

134. Evora C, Soriano I, Rogers RA, Shakesheff KM, Hanes J, Langer R. (1998) Relating the phagocytosis of microparticles by alveolar macrophages to surface chemistry: the effect of 1,2-dipalmitoylphosphatidylcholine. J. Control. Release **51:** 143-152.

135. Vaughn JM, K. P. Johnston and R. O. Williams III. Single Dose and Multiple Dose Studies of Aerosolized Itraconazole Nanoparticles, in press. 2005.

136. Vaughn JM, K. P. Johnston and R. O. Williams III. Single Dose and Multiple Dose Studies of Aerosolized Itraconazole Nanoparticles, in press. 2005.

137. Sham JO-H, Zhang Y, Finlay WH, Roa WH, Lobenberg R. (2004) Formulation and characterization of spray-dried powders containing nanoparticles for aerosol delivery to the lung. Int. J Pharm. **269:** 457-467.

138. Pohlmann AR, Weiss V, Mertins O, Da Silveira NP, Guterres SS. (2002) Spray-dried indomethacin-loaded polyester nanocapsules and nanospheres: Development, stability evaluation and nanostructure models. Eur. J. Pharm. Sci. **16:** 305-312.

139. Grenha A, Seijo B, Remunan-Lopez C. (2005) Microencapsulated chitosan nanoparticles for lung protein delivery. Eur. J. Pharm. Sci. **25:** 427-437.

140. Tsapis N, Bennett D, Jackson B, Weitz DA, Edwards DA. (2002) Trojan particles: Large porous carriers of nanoparticles for drug delivery. Proceedings of the National Academy of Sciences of the United States of America **99:** 12001-12005.

141. Dailey LA, Schmehl T, Gessler T, et al. (2003) Nebulization of biodegradable nanoparticles: impact of nebulizer technology and nanoparticle characteristics on aerosol features. J. Control. Release **86:** 131-144.

142. Pandey R, Sharma A, Zahoor A, Sharma S, Khuller GK, Prasad B. (2003) Poly (DL-lactide-co-glycolide) nanoparticle-based inhalable sustained drug delivery system for experimental tuberculosis. J. Antimicrob. Chemother. **52:** 981-986.

143. Garcia-Garcia E, Andrieux K, Gil S, Couvreur P. (2005) Colloidal carriers and blood-brain barrier (BBB) translocation: A way to deliver drugs to the brain? Int. J Pharm. **298:** 274-292.

144. Koziara JM, Lockman PR, Allen DD, Mumper RJ. (2004) Paclitaxel nanoparticles for the potential treatment of brain tumors. J. Control. Release **99:** 259-269.

145. Kreuter J. (2001) Nanoparticulate systems for brain delivery of drugs. Adv. Drug Deliv. Rev. **47:** 65-81.

146. Huynh GH, Deen DF, Szoka J, Francis C. (2006) Barriers to carrier mediated drug and gene delivery to brain tumors. J. Control. Release **110:** 236-259.

147. Scherrmann J-M. (2002) Drug delivery to brain via the blood-brain barrier. Vascular Pharmacology **38:** 349-354.

148. Calvo P, Gouritin B, Chacun H, et al. (2001) Long-circulating pegylated polycyanoacrylate nanoparticles as new drug carrier for brain delivery. Pharm. Res. **18:** 1157-1166.

149. Lockman PR, Mumper RJ, Khan MA, Allen DD. (2002) Nanoparticle technology for drug delivery across the blood-brain barrier. Drug Dev. Ind. Pharm. **28:** 1-13.

150. Kreuter J, Alyautdin RN, Kharkevich DA, Ivanov AA. (1995) Passage of peptides through the blood-brain barrier with colloidal polymer particles (nanoparticles). Brain Research **674:** 171-174.

1.7 DISSERTATION OBJECTIVES AND OUTLINE

In the past decades, there is a growing demand for more effective and versatile technologies to overcome formulation and bioavailability problems associated with poorly-water-soluble drugs. Nanoparticle engineering technologies represent an important strategy to deliver and enhance drug performance by improving the dissolution rate and bioavailability of these drugs. The basic concepts of different nanoparticle engineering technologies, technological advantages and disadvantages and their current applications in drug delivery systems are discussed in Chapter 1. These technologies include mechanical technologies, supercritical fluid technologies, freezing technologies, and precipitation technologies.

Physicochemical properties of engineered particles are dependent on the technology employed and on the properties and proportion of the excipient used. Drug potency (wt drug/wt drug + wt stabilizer) for most formulations is 50% or less. Typically, the ratio of drug-to- stabilizer ranges from 1:10 to 1:1. It is challenging to achieve rapid release with a high drug-to- stabilizer ratio or payload, especially for low potent compounds with high dose requirements. Such formulation can offer several advantages such as low administration dose improving patient compliance and less potential of toxicity and interactions from an excipient.

Evaporative precipitation into aqueous solution (EPAS) is a particle engineering technology by which a drug solution in a water immiscible organic solvent is sprayed through an atomization nozzle into a heated aqueous solution containing hydrophilic stabilizer (s) at high temperature. The rapid evaporation of the small organic droplets results in fast nucleation leading to submicron to micron particles dispersions. The adsorption of water soluble stabilizers on the drug particle surfaces facilitates the dissolution rates of the final powder after drying. This is also a key factor to achieve high potency formulation while at the same time maintain high dissolution rates of the drug. High-potency (≥ 90%) drug particles with high dissolution rates produced using EPAS technology, followed by removing the non-adsorbed stabilizer were successfully developed and investigated in Chapter 2. The hypothesis is that the high potency ITZ powders can be produced by an optimum choice of stabilizer(s) which adsorb very rapidly onto the ITZ particle surfaces during the very short spray times employed in the EPAS process. The very small amount of adsorbed stabilizers was sufficient to form a hydrophilic layer on the particle surface resulting in increased particle wettability and dissolution.

Poorly-water-soluble compounds are often difficult to develop as drug products using conventional formulation techniques. The rapidly disintegrating and dissolving tablets containing ITZ particles produced by EPAS were prepared by direct compression altering the stabilizer species and levels, and the factors

affecting the drug release properties from the matrix tablets were investigated in Chapter 3. We hypothesized that the high dissolution properties of EPAS particles can be maintained after incorporate into tablets. The ability to maintain rapid dissolution rates of tablets containing ITZ EPAS powders offers great promise for pharmaceutical development and manufacturing to improve dissolution rates of poorly water soluble drugs for oral delivery systems.

Controlled precipitation (CP) is another precipitation technology where a drug solution in a water miscible organic solvent is mixed with an aqueous solution containing a surfactant(s). Upon mixing, the supersaturated solution leads to nucleation and growth of drug particles, which may be stabilized by surfactant or polymer. Enhanced in vitro dissolution and supersaturation can be achieved by forming high energy, amorphous drug particles with high surface areas. The stabilization of amorphous drug to prevent crystallization upon contact aqueous media and during storage was studied in Chapter 4. The objective of this study is to investigate the influence of different water-soluble polymers, including HPMC E5, PVP K15, PVA and PEG 8000, on the dissolution rate and supersaturation behavior of amorphous REP particles formed by CP.

Ultra-rapid freezing (URF), is a cryogenic technology which enhances the dissolution of poorly water soluble drugs by producing nanostructured particles with high degrees of porosity. URF technology involves dissolving the drug and excipient in a suitable organic solvent or aqueous co-solvent and applying to the

surface of cryogenic solid substrate. A solution of drug is frozen instantaneously onto the surface of cryogenic solid substrate in a continuous manner, giving the final product a uniform character. URF powders exhibit desirable properties for enhancing bioavailability such as high surface area and increased drug dissolution rates. In Chapter 5, the feasibility of URF in producing nanostructured drug particles which suitable for administering via inhalation were studied in a mouse model. More specific objective was to compare the effects of the differences in the properties of two types of particles (amorphous vs crystalline) on supersaturation and drug absorption. Lung and whole blood concentrations following single pulmonary were also evaluated. The application of particle engineering technology for pulmonary drug delivery represents new potential opportunities for therapeutic application not only for immunosuppressive drugs but also other poorly water soluble drugs. The successful delivery system may provide a convenient, noninvasive method for the administration of drugs to the lungs to treat local diseases and/or to provide systemic drug delivery without the need for painful injections.

CHAPTER 2: Stabilizer Choice for Rapid Dissolving High Potency Itraconazole Particles Formed by Evaporative Precipitation Into Aqueous Solution

2.1 ABSTRACT

The objective of this study was to investigate the influence of stabilizer type on the physicochemical properties, including dissolution, of ultra-high potency powders containing itraconazole (ITZ) formed by Evaporative Precipitation Into Aqueous Solution (EPAS). ITZ was dissolved in dichloromethane, which was then atomized through a heated coil at 80°C into an aqueous solution over precise periods of time. Stabilizers were present in either the aqueous, organic or both phases. The dispersions were centrifuged and the supernatant was removed. Three hydrophilic stabilizers were investigated, including polysorbate 80, polyvinyl pyrrolidone and poloxamer 407. Rapid dissolving ultra-high potency of ITZ powders was successfully produced. Greater than 80% of ITZ was dissolved in 5 min. compared to only 13% of ITZ bulk powders. The resulting stabilizer-coated drug particles had high drug-to-stabilizer ratios greater than 12, corresponding to potencies (wt drug/wt drug + wt surfactant) as high as 93%. An increase in dissolution rate was correlated with the amount of stabilizer adsorbed and the wettability. The combination of polysorbate 80 and poloxamer 407 present in the aqueous and organic phases,

respectively, was superior in achieving high wetting and rapid dissolving ITZ powders. The ability to control the adsorption behavior of stabilizers by using synergistic combinations affords the opportunity to achieve high dissolution rates with higher potencies compared to previously reported values.

2.2 INTRODUCTION

Itraconazole (ITZ) is an orally active triazole antifungal agent with a potent broad spectrum of activity against *Candida* species and *Aspergillus* species which are the two most common human fungal pathogens. It has a molecular formula $C_{35}H_{38}Cl_2N_8O_4$ and molecular weight of 705.64. ITZ is categorized as a Class II compound by the Biopharmaceutics Classification System (BCS), and is water insoluble (Solubility ~ 1 ng/mL at neutral pH) but highly permeable [1]. This compound is a weak base (pK_a=3.7) and reportedly has an octanol:water partition coefficient (log P) of greater than 5 at pH 6 [2]. ITZ was chosen as the model drug for this study due to its low solubility and poor wetting in water, and hence low and variable bioavailability [3]. There have been many attempts to improve the bioavailability and dissolution rate of poorly water soluble drugs like ITZ. These include reducing the particle size by mechanical means to increase surface area [4]; solubilization in surfactant systems [5,6]; formation of water-soluble complexes [7] and manipulation of solid state of the drug substance by

inhibiting crystallization to form amorphous particles [8]. Particle size reduction is a promising way to increase dissolution rates of poorly water soluble drugs [9,10].

Evaporative precipitation into aqueous solution (EPAS) is a particle engineering technology reported to produce submicron to micron-sized drug particles stabilized by surfactants or polymers and dispersed in an aqueous medium [11-13]. During processing, drug dissolved in an organic solvent is sprayed through an atomizing nozzle into an aqueous solution containing a hydrophilic stabilizer to produce an aqueous dispersion (Figure 2.1). Rapid evaporation of the organic solvent at elevated temperature produces very high supersaturation and rapid precipitation of the drug in the form of suspended particles. The particles may be stabilized by a variety of stabilizers present in either or both the organic and aqueous phases. The stabilizers adsorb onto the newly formed drug particle surfaces consequently decreasing the surface energy and providing steric and/or electrostatic repulsion between particles. This process may be dictated by the thermodynamic and kinetic aspects of stabilizer adsorption: the stabilizer must adsorb on the newly created surface and attain a conformation that is conducive to steric stabilization. The primary objective of this study is to prepare rapid dissolving ultra-high potency ITZ powders by the EPAS process. We desire to have extremely high drug-to-stabilizer ratios greater than 12, corresponding to potencies (wt drug/wt drug + wt surfactant) above 90%.

In a previous study, Chen et al.[14], reported potencies of ITZ produced by the EPAS process ranging from 40 up to only 72%. We believe that by choosing the optimal stabilizer type, and by optimizing the phase that the stabilizer is present in, that even higher potencies can be achieved for highly wettable and rapidly dissolving ITZ powders. It is challenging to increase the drug-to-stabilizer ratio to values of up to 12, while at the same time maintaining high surface areas, stabilized particles with enhanced wetting and high dissolution rates. We hypothesize that the ultra-high potency ITZ powders, greater than those reported by Chen et al., with low levels of adsorbed stabilizer can be produced by an optimum choice of stabilizer(s) which can adsorb very rapidly onto the ITZ particle surfaces during the very short spray times employed in the EPAS process. The very small amount of adsorbed stabilizers was sufficient to form a hydrophilic layer on the particle surface resulting in increased particle wettability and dissolution.

2.3 MATERIALS AND METHODS

2.3.1 Materials

ITZ was purchased from Hawkins, Inc. (Minneapolis, MN). The stabilizers including a nonionic surfactant (polysorbate 80; MW = 1,310) and a homopolymer; polyvinyl pyrrolidone (PVP K-15, MW =15,000) were purchased

from Spectrum Chemicals (Gardena, CA). The polyoxyethylene-polyoxypropylene copolymer (poloxamer 407, MW =11,700) was purchased from BASF (Mount Olive, NJ). HPLC grade acetonitrile was obtained from EM Industries Inc. (Gibbstown, NJ) and dichloromethane was purchased from Fisher Scientific Co. (Houston, TX). Other chemicals and solvents were of analytical reagent grade. Purified water was obtained from an ultra-pure water system (Milli-QUV plus, Millipore S. A., Molsheim Cedex, France).

2.3.2 Particle Formation using EPAS Process

A schematic diagram of the EPAS apparatus is shown in Figure 2.1. The EPAS process consisted of spraying a 15.0% (w/w) solution of ITZ containing 2% w/v stabilizer dissolved in dichloromethane via an HPLC pump (Model PU-2086, Jasco Inc., Baltimore, MD) through a 1/16 inch outer diameter (o.d.) × 0.030 inch inner diameter (i.d.) preheating coil contained within a 1-1/2 inch o.d. × 15 inch long plastic water jacket (Model 95023D, Alltech Associates Inc., Deerfield, IL) into 50 mL of 2.0 w/w% aqueous solution of stabilizers. Water was circulated through the jacket with a temperature controller (Julabo MP, Julabo USA Inc., Allentown, PA). The temperature of the water bath and the heating jacket was maintained at 80 °C. The nozzle was made by cutting stainless steel tubing (1/16 inch o.d. ×0.030 inch i.d.) [15] to form an elliptical conical

orifice. The crimped end of the nozzle was filed back until the desired flow rate of 1 mL/min was achieved giving a pressure drop of about 20 MPa across the orifice. This type of nozzle produces very high pressure drops resulting in intense atomization of the organic drug solution at the tip of the nozzle. The nozzle was submerged approximately 10 cm under the surface of the aqueous solution. After atomizing for 5 min., an aqueous dispersion containing a drug-to-stabilizer ratio of 0.68 was recovered. The dispersions were centrifuged (Model J2-21, Beckman, Fullerton, CA) at 10000 rpm for 20 min. to concentrate the particles, as described previously for particles formed by EPAS [13]. The supernatant was decanted to remove the unbound stabilizer in order to increase the potency (wt drug/wt drug + wt surfactant) in the precipitate. The particles were frozen by submerging in liquid nitrogen and then lyophilized.

2.3.3 Potency Test

The potency of dry powders (wt drug/wt drug + wt surfactant) was determined by dissolving a known amount of dry powder (ca. 10mg) into 50mL of mobile phase and then determining ITZ concentration by HPLC. Reverse-phase HPLC was conducted using a Shimadzu VP-AT series LC10 HPLC (Columbia, MD) to measure the quantity of ITZ in the prepared sample. The mobile phase consisted of acetonitrile: water (70:30 v/v) containing 0.02% diethylamine. The flow rate was 1.0 mL/min and the detector wavelength was 263 nm. ITZ was eluted from

an Inertsil 5um ODS-2 column (4.6 mm i.d. x 150 mm; Alltech Associates, Inc., Deerfield, IL) at 5 min using an injection volume of 50 µl.

2.3.4 Adsorption Studies

To measure the amount of stabilizer adsorbed onto the particles immediately after EPAS processing, 15% w/v itraconazole solution containing 2% stabilizer dissolved in dichloromethane was sprayed into 50 mL aqueous solution containing 2% stabilizer at a flow rate of 1 mL/min. After 5 min. of spraying, the EPAS dispersion with a drug-to-stabilizer ratio of 0.68 (drug: organic stabilizer: aqueous stabilizer of 0.75:0.1:1), and total concentration of itraconazole of 15 mg/mL was recovered. The pressure drop was 20 MPa and the temperature of both organic and aqueous phases was 80^{o}C. Immediately after the dispersions were formed, aliquots of 4 mL of the dispersion were centrifuged at 10,000 rpm for 20 min for complete separation of the solids, leaving a clear supernatant at the top. After centrifugation, the supernatant and precipitate were weighed before and after drying at 40^{o}C to determine the amount of stabilizer adsorbed gravimetrically.

A separate set of experiments was designed to determine the equilibrium adsorption isotherm for each pure stabilizer as a function of stabilizer concentration. 2% (w/v) ITZ dissolved in dichloromethane was sprayed into 15 mL aqueous solution containing stabilizer at a flow rate of 1 mL/min. Various

concentrations (from 0.1% to 3%) of stabilizers dissolved in the organic phase were used to prepare the EPAS samples in triplicate. After 5 min. of spraying, the EPAS dispersion was agitated at 37 ^{o}C for 24 hr, to allow adsorption to reach equilibrium. Aliquots of 4 mL of the dispersion were centrifuged at 10,000 rpm for 20 min. to concentrate the solids. After centrifugation, the supernatant and precipitate were weighed before and after drying at 40^{o}C to determine the amount of stabilizer adsorbed gravimetrically.

Stabilizer adsorption was measured gravimetrically based on the mass balance between the supernatant and particles. The composition of the small amount of supernatant left on the precipitate was assumed to be the same as that in the bulk supernatant and the amount of ITZ in the precipitate was at least 50 times more than ITZ dissolved in micelles. The amount of adsorbed stabilizer on ITZ particles is given by the following equation:

$$W_{surf,ads} = W_{ppt,dry} - W_{drug,ppt} - (W_{ppt,wet} - W_{ppt,dry}) \times \left(\frac{W_{\sup,dry}}{W_{\sup,wet} - W_{\sup,dry}}\right)$$

where:

$W_{sup,wet}$ = weight of the supernatant before drying

$W_{sup,dry}$ = weight of the supernatant after drying to remove water

$W_{ppt,wet}$ = weight of the precipitate before drying

$W_{ppt,dry}$ = weight of the precipitate after drying

$W_{drug,ppt}$ = amount of ITZ in the precipitate measured by HPLC

$W_{surf,ads}$ = amount of adsorbed surfactant or stabilizer on ITZ

2.3.5 Dissolution Testing

Dissolution testing (Vankel 7000, Vankel Technology Group, Cary, NC) was conducted on isolated ITZ EPAS powders using the United States Pharmacopoeia (USP) apparatus II (paddles) at 50 rpm. Dry powder containing approximately 10 mg of ITZ was weighed out and placed into 900 ml of dissolution media that contained enzyme-free simulated gastric fluid with 0.5% sodium lauryl sulfate (pH 1.2). The dissolution media was maintained at 37 °C and degassed prior to use by sonication for 2 min. Sink conditions were maintained throughout the testing. Aliquots of the dissolution media (5 mL) were collected at 2, 5, 10, 20, 30, 60 and 120 min. intervals. After 60 min, the paddle speed was increased to 200 rpm to approximate complete dissolution of ITZ at the 2 hour time point. The samples were filtered using 0.45µm filters (Gelman GHP Acrodisc 0.45µm, VWR, West Chester, PA). To ensure that no precipitation occurred during HPLC analysis, 0.1 mL of acetonitrile was added to 4 mL of filtered samples. These were mixed using a vortex mixer for approximately 5 sec. and again filtered through a 0.45µm filter into an HPLC vial for drug content

analysis by reverse phase HPLC. Dissolution profiles for ITZ EPAS powders were determined in replicates of 6.

2.3.6 Transmission Electron Microscopy (TEM)

A JEOL 2010F field emission transmission (JEOL) with Energy Dispersive X-ray Spectroscopy (EDS) (Peabody, MA) was used to examine the primary particle size and determine the chemistry of the sample. The dry powders were redispersed in water and placed on a Cu grid, fixed on the TEM holder and inserted into the TEM column.

2.3.7 Contact Angle Measurement

Dry powder was compressed at 1000 kg compression force using a Carver Laboratory Press (Model M, ISI Inc., Round Rock, TX) with 6mm diameter flat-faced punches. A droplet of water (3 µl) was placed onto the surface of the compact and observed using a low power microscope. The contact angle was determined by measuring the tangent to the curve of the droplet on the surface of the compact using a Goniometer (Model No.100-00-115, Ramè-Hart Inc., Mountain Lakes, NJ).

2.3.8. Surface Area Analysis

The specific surface area was determined using a Nova 3000 surface area analyzer (Quantachrome Corporation, Boynton Beach, FL) to measure N2 sorption at 77.40oK. The surface area per unit powder mass was calculated from the fit of adsorption data to the Brunauer, Emmett, and Teller (BET) equation.

2.3.9 Powder X-Ray Diffraction

Powder X-ray diffraction was conducted using $CuK\alpha_1$ radiation with a wavelength of 1.54054 Å at 40 kV and 20 mA from a Philips 1720 X-ray diffractometer (Philips Analytical Inc., Natick, MA). The sample powders were placed in a glass sample holder. Samples were scanned from 5^o to 50^o (2θ) at a rate 0.05^o/sec. For comparative purposes, the three highest values for relative line intensity and the corresponding 2θ angle were compared.

2.4 RESULTS AND DISCUSSION

2.4.1 Adsorption Studies

2.4.1.1 Adsorption Isotherms of Stabilizers onto ITZ Particle Surface after 24 Hours Equilibration

The adsorption isotherm for each of the stabilizers investigated with ITZ particles produced by EPAS is shown in Figure 2.2. The adsorption isotherms for poloxamer 407 and PVP followed Langmuir-behavior characterized by a steep

initial slope at low concentration and a plateau, indicating the point where most of the adsorption sites on the ITZ particle surface are occupied. In the adsorption of polysorbate 80, the shape of the isotherm was more complex with changes in concavity. The adsorption increased rapidly to an initial plateau and then further gradually increased toward a second plateau. This adsorption behavior could be related to the increase of aggregate concentration typical of micelle formation. As can be seen in Figure 2.2, the polysorbate 80 adsorption exhibited a strong affinity to ITZ particle surfaces as indicated by the sharp initial slope and a higher adsorption at all concentrations. Polysorbate 80 molecules would be expected to adsorb onto the hydrophobic ITZ surfaces with the PEO groups extended into water to provide steric stabilization. Luckham et al. [16] found that lower molecular weight ethoxylated polymers adsorb on carbon black surfaces more strongly than higher molecular weight polymers. The nonadsorbing ethylene oxide block hinders the adsorption of the higher molecular weight stabilizers. This may explain why polysorbate 80, which has shorter PEO chains, adsorbed onto the particle surfaces to a greater extent than poloxamer 407 with PEO chains about 100 segments long. In addition, polysorbate 80 with a lower HLB value (HLB=15) would be expected to adsorb more strongly onto the hydrophobic surface than poloxamer 407 and PVP. The homopolymer PVP is very hydrophilic and has a small thermodynamic driving force for adsorption [17]. Sato and Kohnosu [18] reported that the amount of PVP adsorbed onto the hydrophobic

surface of TiO_2 is low in aqueous solution, which is in agreement with the results obtained by Pattanaik and Bhaumik [19]. Therefore, low adsorption of PVP found in this study was also consistent with previously reported studies.

2.4.1.2 Adsorption of Stabilizers onto ITZ Particle Surface after EPAS Process

The adsorption ($W_{surf,ads}/W_{drug,ppt}$) of stabilizers in each EPAS formulations was measured immediately after forming the dispersions, and the results are listed in Table 2.1. The results demonstrated that the combination of poloxamer 407 and polysorbate 80, present in the organic and aqueous phases, respectively, showed the highest adsorption (10.72% w/w) after the short spray time of 5 minutes. The much larger adsorption for this surfactant blend produced greater wettability and hence a faster dissolution rate in contrast with much smaller adsorption values for compositions containing poloxamer 407 in both phases, where only 6.46% w/w stabilizer-to-drug was adsorbed. Chen et al [13] found that the adsorption dynamics of the copolymer poloxamer 407 is rather slow when added alone in the aqueous phase. Chen et al showed that adsorption of poloxamer 407 increased from 3.87 to 11.21% w/w surfactant-to-drug after storage at 25^{o}C for 72 hours. This increase might be caused by slow surface rearrangement of the adsorbed polymer layer to provide space for further adsorption [20]. Moreover, the increase in viscosity of poloxamer 407 at high

temperature could also cause the longer diffusion time. However, in the present study, we found that the combination of poloxamer 407 and polysorbate 80, present in the organic and aqueous phases, respectively, showed the highest adsorption immediately upon particle formation. Poloxamer 407 is added in the same (organic) phase as the ITZ where it precipitates from the evaporating organic droplets, and, hence, requires a relatively short time to diffuse and adsorb onto the nucleating particle surfaces. Moreover, employing a second surfactant like polysorbate 80 may facilitate orientation of poloxamer 407 at the solid-liquid interface, and enable a much shorter equilibration time to attain optimal surfactant conformation. Chen et al required much longer equilibration times using poloxamer 407 alone, which resulted in larger particles. Polysorbate 80 is a much smaller molecule (MW: 1310) than poloxamer 407 (MW: 11,700). The small size of polysorbate 80 may be expected to lead to faster diffusion [21] to the particle surface and faster adsorption kinetics at the surface, to inhibit the otherwise rapid crystallization. In addition, the adsorption for pure polysorbate 80 was substantially larger than for the other stabilizers as was shown in Figure 2.2.

Several authors have reported results of the interactions of Pluronic block copolymer with surfactant systems [22,23]. In particular, Couderc et al. [24] reported on the synergistic behavior in mixed micelle formation of binary surfactant mixtures of poloxamer 407 and nonionic surfactant containing an EO group ($C_{12}EO_6$). Polymer–surfactant association is influenced by many factors

including interactions with ions, hydrogen bonding, the hydrophobicity of the polymer and the non-polar tail of the surfactant, and the structural conformation and flexibility of the polymer. It has also been reported that some non-ionic surfactants may significantly increase emulsifying capacity of polymeric surfactants [25]. Thus the highest adsorption produced with polysorbate 80 and poloxamer 407 is consistent with the previously observed favorable interactions between these stabilizers. However, this interaction was not found in the combination of polysorbate 80 and PVP K15 which yielded low adsorption (5.86% w/w). It may possible that a layer of PVP K15 which was present in the organic phase with ITZ coated the nuclei first and that polysorbate 80 could not adsorb on the polymer layer. Moreover the small adsorption could also due to the competitive adsorption of these stabilizers onto surfaces of the ITZ particles [26]. It is constructive to further compare the different intermolecular interactions of the surface of ITZ particles with poloxamer 407 and PVP K15. A small amount of adsorbed stabilizers was observed (5.70% w/w) compared to the combination of poloxamer 407 and polysorbate 80. This may be attributed to the lower adsorption after 24 hours for both poloxamer 407 and PVP K15, relative to polysorbate 80. Since PVP has higher molecular weight than poloxamer 407, it will take longer to diffuse and adsorb onto the ITZ particle surfaces. The combination of PVP K15 by itself also yielded low adsorption (5.38% w/w).

2.4.2 Dissolution Testing

Dissolution profiles of ITZ EPAS powders are presented in Figure 2.3. The dissolution rate of all formulations is significantly greater than that compared to the bulk powder. A high dissolution rate was observed for all EPAS formulations in spite of the fact that the crystallinity of each of the EPAS powders was observed to be high, as will be discussed later in this paper. The dissolution rate was also correlated to the amount of stabilizer adsorbed. It was much higher for the formulation containing polysorbate 80 and poloxamer 407 than the other stabilizers. In five min., 80% of ITZ prepared by EPAS was dissolved as compared to 13% determined for the bulk powder. Results presented below (Sections 3.3 and 3.4) indicate that this observation of the highest dissolution rate is consistent with the high wettability (lowest contact angle) and very small primary particle size of ITZ produced by EPAS, respectively.

2.4.3 Transmission Electron Microscopy (TEM)

TEM was used to investigate the primary particles and morphology of ITZ particles after redispersion of the dried EPAS powders in water. In Figure 2.4, the TEM micrograph of ITZ with polysorbate 80 and poloxamer 407 indicate aggregation of small particles after being redispersed in water. The particles were composed of small primary particles which aggregated during the drying process. This explains why the highest dissolution occurred in the formulation containing

polysorbate 80 and poloxamer 407 even though the particle size of dry powders was about 7 μm measured by laser diffraction, which most probably represented aggregates being measured by laser light diffraction. Since these aggregates were not easily deaggregated into their discrete particles, laser diffraction was not used to quantitate particle size. Energy dispersive spectroscopy (EDS) was used to qualitatively determine and confirm the elemental compositions of particles in this image. The EDS spectrum was obtained, the constituent elements identified and the occurrence classified into a compositional type. The EDS spectrum showed the presence of C, N, O and Cl , as shown in Figure 2.5. The presence of both N and Cl atoms which are only present in the ITZ molecule, is indicative that the large particle is ITZ which consisted of very small aggregated primary particles. It clearly showed that the bright spots of highest elemental intensity could be overlaid on the pattern of the ITZ structure. Other elements of Cu and Si were present on the film and supporting grid. The rapid evaporation of the heated organic solution in the EPAS process produces high supersaturation and rapid precipitation of ITZ in the form of a nanoparticle dispersion that is stabilized by a variety of stabilizers. The results also further confirmed the potential of EPAS process in producing nanoparticles of poorly water soluble drugs.

2.4.4 Contact Angle Measurement

Surfactants or stabilizers generally improve wetting by adsorbing on the surface to cause a reduction in the solid-liquid interfacial energy. The contact angle results are shown in Table 2.2. Adsorbed hydrophilic stabilizer on the particle surface reduced the contact angle indicating improved wettability compared to bulk powder. It is likely that different stabilizers and their combination may display variation in wetting particle surface. The decrease in contact angle correlated with an increase in dissolution rate as reported in Table 2.2. For the EPAS formulation of polysorbate 80 and poloxamer 407, the contact angles were lowest due to high adsorption and wetting of particle surfaces resulting in the highest dissolution rate profile. Reduction in contact angle from 61.6^{o} for bulk ITZ to 30.3^{o} was achieved at a high drug potency of 90%, with a corresponding increase in drug dissolution from 14 to 80% in 5 minutes. This may be expected as the ITZ surface is largely hydrophobic in nature so the bulk powder does not break the interfacial tension of the dissolution media at the air/liquid boundary. The ITZ particles without stabilizers float on the surface throughout the dissolution experiment. The contact angle of the corresponding physical mixture of ITZ with polysorbate 80 and poloxamer 407 was 52.3°, indicating a much less hydrophilic surface. Therefore increasing the accessibility for wetting by the dissolution media is an important factor to enhance the dissolution rate of ITZ. Miyazaki et al. [27] reported that the dissolution rate enhancement of phenylbutazone was mostly due to the enhanced wetting.

2.4.5 Surface Area Analysis

The surface areas of the dry powders were determined by BET and the results are shown in Table 2.2. The surface areas of ITZ EPAS formulations were higher than that of the bulk powder except for the formulations containing polysorbate 80. Polysorbate 80 is a liquid at room temperature, and consequently, it caused aggregation of the dry powder at room temperature, and subsequently low surface area as shown in Table 2.2. The calculated surface area for monodisperse spheres of ITZ with particle diameter about 8 μm would be 2.3 m^2/g. The larger surface area for the powders suggests that the particles were not uniform spheres but were aggregates composed of smaller primary particles as can be seen from the TEM results. This morphology results in high dissolution of all EPAS formulations compared to the bulk powders. The dissolution rates for the systems with higher surface areas on the order of 5-6 m^2/g, were lower than for the formulation of polysorbate 80 and poloxamer 407 which had somewhat lower surface areas. The reduced wetting and dissolution can be attributed to the observation that these powder samples remained for a longer time on the top of dissolution medium before being wetted completely.

2.4.6 Powder X-Ray Diffraction

X-ray diffraction was used to analyze the crystallinity of the dry powders. As shown in Figure 2.6, all profiles show no change in crystallinity. The

crystalline peak positions were the same as for the bulk ITZ. The degree of crystallinity for these samples did not appear to correlate with dissolution results. As shown by the dissolution results, all EPAS formulations yielded very good dissolution profiles, indicating that high dissolution rates may be achieved for high surface area crystalline powders. Moreover, in terms of thermodynamics, the crystalline solids are preferable since they are more physically and thermodynamically stable compared to amorphous solids which may re-crystallize. Amorphous or disordered material is a metastable state and tends to revert back to the more stable crystalline state under unfavorable humidity and temperature conditions. Water, from the atmosphere, can be absorbed and reduce the glass transition temperature [28] thus decreasing the energy barrier to re-crystallization [29]. However, the stability of amorphous materials can be enhanced by storage well below the glass transition temperature (Tg) and by using high Tg material such as polyvinylpyrrolidone, polyethylene glycol and various cellulose derivatives like hydroxypropyl methylcellulose, hydroxypropylcellulose, etc. [30,31].

2.4.7 Potency of ITZ Powders and Drug-to-Stabilizer Ratio after Centrifugation

The potencies of the powders after centrifugation are listed in Table 2.2. The potency of ITZ in the dry powders was greater than 90%, corresponding to a drug-to-stabilizer ratio greater than 9:1. The high potencies result from the

removal of a large amount of non-adsorbed stabilizer in the supernatant. This concept has been successfully used to produce high potency danazol and ITZ in the EPAS studies [13,14]. Chen et al reported the potency of itraconazole particles was increased to only 70% after 25 minutes of spraying followed by removal of the unbound surfactant. In the present study, we were able to increase the potency up to 90%, while maintaining high dissolution rates and small primary particle sizes. In the present study, we used high ITZ concentration in the feed solution (drug-to-organic stabilizer ratio of 7.5) with a short spray time only 5 min. These conditions allow less time for stabilizers to adsorb onto the particles and can led to the extremely high potency values up to 93% with rapid dissolution. The final drug-to-stabilizer ratios varied from 9:1 to 15:1. In general, the ratio of drug-to-stabilizer ranges from 1:10 to 1:1 when drugs are dissolved in micelles, vesicles or liposomes [32,33]. There are several advantages of the formulation with high drug-to-stabilizer ratio such as low administration dose and less potential interactions from the excipients. Potential stability problems can result from interactions of drug substances with excipients in solid dosage forms [34].

2.5 CONCLUSIONS

Rapid dissolving formulations containing ultra high potency of ITZ powders were achieved using the EPAS process. Polysorbate 80, poloxamer 407, PVP K-15 and their combinations showed differences in the degree of improving wettability and dissolution of ITZ depending on their adsorption onto the particle

surface. The adsorption of stabilizers is influenced by the HLB of the stabilizer and the hydrophobicity of the particle surface. For very lipophilic compounds, such as ITZ (log P>5), polysorbate 80, with a lower HLB value, was adsorbed more strongly than poloxamer 407 and PVP. The synergistic stabilization effect was demonstrated to be optimal for combinations of polysorbate 80 and poloxamer 407, when incorporated into the aqueous and organic phases, respectively. The stabilization observed for this mixed stabilizer system has been explained in terms of strong adsorption for the small polysorbate 80 to compensate for the limited amount of adsorption for the copolymer poloxamer 407 after 24 hours. EPAS followed by removal of free stabilizer produced high potencies up to 93% and rapid dissolution rates. The highest dissolution rates, i.e. 80% in 5 minutes were obtained for ITZ produced by EPAS with polysorbate 80 and poloxamer 407, as stabilizers in the aqueous and organic phases respectively. The dissolution rates are enhanced due to the small primary particle size and by adsorbed stabilizers that raise the surface hydrophilicity, as shown by a decrease in the contact angle. The optimum choice of stabilizer(s) which adsorb rapidly onto the ITZ particle surfaces during the very short spray times employed in the EPAS process can help produce the extremely high drug-to-stabilizer ratios greater than 12, corresponding to potencies above 90%. The very small amount of adsorbed stabilizers was sufficient to form a hydrophilic layer on the particle surfaces resulting in increased particle wettability and dissolution. These results

provide evidence that the selection of appropriate stabilizer(s) is an important consideration in formulation development.

This study also demonstrated the usefulness of the EPAS process as a method in controlling particle characteristics and enhancing drug dissolution. This process is a very versatile drug delivery platform and is suitable for many commonly used routes of administration such as oral, nasal and pulmonary delivery.

2.6 ACKNOWLEDGMENTS

The authors gratefully acknowledge financial support from The Dow Chemical Company (Midland, MI). The authors would also like to thank Drs. Jason McConville for his helpful discussion and Xiaoxia Chen for her skilled assistance with the adsorption study.

2.7 REFERENCES

1. Amidon GL, Lennernas H, Shah VP, Crison JRA. (1995) Theoretical basis for biopharmaceutical drug classification: The correlation of in vitro drug product dissolution and in vivo bioavailability. Pharm. Res. **12:** 413-420.
2. Peeters J, Neeskens P, Tollenaere JP, Van Remoortere P, Brewster ME. (2002) Characterization of the interaction of 2-hydroxypropyl- -cyclodextrin with itraconazole at pH 2, 4, and 7. J. Pharm. Sci. **91:** 1414-1422.

3. Woestsnborghs R, Heykants J, Gasparini R, Gauwenbergh G. (1989) The effects of food and dose on the oral systemic availability of itraconazole in healthy subjects. Eur. J. Clin. Pharmacol. **36:** 423-426.

4. Kubo H, Osawa T, Takashima K, Mizobe M. (1996) Enhancement of oral bioavailability and pharmacological effect of 1-(3,4-dimethoxyphenyl)-2,3 bis(methoxycarbonyl)-4-hydroxy-6,7,8-trimethoxynapthalene (TA-7552), a new hypocholesterolemic agent by micronization in co-ground mixture with D-mannitol. Biol. Pharm. Bull. **19:** 741-747.

5. Martis L, Hall NA, Thakkar AL. (1972) Micelle formation and testerone solubilization by sodium glycocholate. J. Pharm. Sci. **61:** 1757-1761.

6. Rees A, Collett JH. (1974) The dissolution of salicylic acid in micellar solutions of polysorbate-20. J. Pharm. Pharmacol. **26:** 956-960.

7. Cassella R, Williams DA, Jambhekar SS. (1998) Solid-state-cyclodextrin complexes containing indomethacin, ammonia and water. II. Solubility studies. Int. J. Pharm. **165:** 15-22.

8. Leuner C, Dressman J. (2000) Improving drug solubility for oral delivery using solid dispersions. Eur. J. Pharm. Biopharm. **50:** 47-60.

9. Hu J, Johnston KP, Williams III RO. (2004) Nanoparticle Engineering Processes for Enhancing the Dissolution Rates of Poorly Water Soluble Drugs. Drugs. Drug Dev. Ind. Pharm. **30:** 233-245.

10. Rogers TL, Johnston KP, Williams III RO. (2001) Solution-based particle formation of pharmaceutical powders by supercritical or compressed fluid CO2 and cryogenic spray-freezing technologies. Drugs. Drug Dev. Ind. Pharm. **27:** 1003-1015.

11. Sarkari M, Brown J, Chen X, Swinnea S, Williams I, Robert O., Johnston KP. (2002) Enhanced drug dissolution using evaporative precipitation into aqueous solution. Int. J Pharm.**243:** 17-31.

12. Chen X, Young TJ, Sarkari M, Williams I, Robert O., Johnston KP. (2002) Preparation of cyclosporine A nanoparticles by evaporative precipitation into aqueous solution. Int. J Pharm. **242:** 3-14.

13. Chen X, Vaughn JM, Yacaman MJ, Williams III RO, Johnston KP. (2004) Rapid dissolution of high-potency danazol particles produced by evaporative precipitation into aqueous solution. J. Pharm. Sci. **93:** 1867-1878.

14. Chen X, Benhayoune Z, Williams III RO, Johnston KP. (2004) Rapid dissolution of high potency itraconazole particles produced by evaporative precipitation into aqueous solution. J. Drug Del. Sci. Technol. **14:** 299-304.

15. Young TJ, Mawson S, Johnston KP, Henriksen IB, Pace GW, Mishra AK. (2000) Rapid Expansion from Supercritical to Aqueous Solution to

Produce Submicron Suspensions of Water-Insoluble Drugs. Biotechnol. Prog. **16:** 402-407.

16. Luckham PF, Bailey AI, Miano F, Tadros TF. (1995) Effectiveness of surfactants as steric stabilizers. In: (Eds) RS (ed.) in: Surfactant adsorption and surface solubilization ACS symposium series 615. American Chemical Society, Washington, DC, pp. 166-182.
17. Gennes DP. (1987) Polymers at an interface: a simplified view. Adv Colloid Interface Sci. **27:** 189-209.
18. Sato T, Kohnosu S. (1994) Effect of polyvinylpyrrolidone on the physical properties of titanium dioxide suspensions. Colloids and Surfaces A-Physicochem. Eng. Aspects. **88:** 197-205.
19. Pattanaik M, Bhaumik S. (2000) Adsorption behaviour of polyvinyl pyrrolidone on oxide surfaces. Materials Letters **44:** 352-360.
20. Tripp CP, Hair ML. (1996) Kinetics of the adsorption of a polystyrene-poly(ethylene oxide) block copolymer on silica: a study of the time dependence in surface/segment interactions. Langmuir. **12:** 3952-3956.
21. Kim DW, Shin S, Oh S-G. (2000) Preparation and stabilization of silver colloids in aqueous sufactant solutions. In: (Eds) KLMaDOS (ed.) in:*A*dsorption and aggregation of surfactants in solution. Surfactant Science Series. New York: Marcel Dekker, pp. 255-268.

22. Ivanova R, Alexandridis P, Lindman B. (2001) Interaction of poloxamer block copolymers with cosolvents and surfactants. Colloids and Surfaces A-Physicochem. Eng. Aspects. **183:** 41-53.

23. Na GC, Yuan BO, Stevens HJ, Weekley BS, Rajagopalan N. (1999) Cloud point of nonionic surfactants: Modulation with pharmaceutical excipients. Pharm. Res. **16:** 562-568.

24. Couderc S, Li Y, Bloor DM, Holzwarth JF, Wyn-Jones E. (2001) Interaction between the nonionic surfactant hexaethylene glycol mono-n-dodecyl ether (C12EO6) and the surface active nonionic ABA block copolymer pluronic F127 (EO97PO69EO97)-formation of mixed micelles studied using isothermal titration calorimetry and differential scanning calorimetry. Langmuir **17:** 4818-4824.

25. Carlotti ME, Pattarino F, Gasco MR, Cavalli R. (1995) Use of polymeric and non-polymeric surfactants in o/w emulsion formulation. Int. J. Cosmetic Sci. **17:** 13-25.

26. Noskov BA, Akentiev AV, Miller R. (2002) Dynamic surface properties of poly(vinylpyrrolidone) solutions. J. Colloid Interface Sci. **255:** 417-424.

27. Miyazaki S, Yamahira T, Morimoto Y, Nadai T. (1981) Micellar interaction of indomethacin and phenylbutazone with bile-salts. Int. J. Pharm. **8:** 303-310.

28. Elamin AA, Sebhatu T, Ahlneck C. (1995) The use of amorphous model substances to study mechanically activated materials in the solid state. Int. J. Pharm. **119:** 25-36.

29. Carstensen JT, Van Scooik K. (1990) Amorphous-to-crystalline transformation of sucrose. Pharm. Res. **12:** 1278-1281.

30. Hancock BC, Zografi G. (1997) Characteristics and significance of the amorphous state in pharmaceutical systems. J. Pharm. Sci. **86:** 1-12.

31. Saleki-Gerhardt A, Zografi G. (1994) Non-isothermal and isothermal crystallization of sucrose from the amorphous state. Pharm. Res. **11:** 1166-1173.

32. Lee EJ, Lee SW, Choi HG, Kim CK. (2001) Bioavailability of cyclosporin A dispersed in sodium lauryl sulfate-dextrin based solid microspheres. Int. J. Pharm. **218:** 125-131.

33. Kushida I, Ichikawa M, Asakawa N. (2002) Improvement of dissolution and oral absorption of ER-34122, a poorly water-soluble dual 5-lipoxygenase/cyclooxygenase inhibitor with anti-inflammaory activity by preparing solid dispersion. J. Pharm. Sci. **91:** 258-266.

34. Mroso PN, Li Wan Po A, Irwin WJ. (1982) Solid state stability of aspirin in the presence of exciplents: kinetic interpretation, modelling and prediction. J. Pharm. Sci. **71:** 1096-1101.

CHAPTER 3: Rapidly Disintegrating and Dissolving Tablets Containing Itraconazole Particles Formed by Evaporative Precipitation Into Aqueous Solution

3.1 ABSTRACT

In this study, the rapidly disintegrating and dissolving tablets containing itraconazole (ITZ) particles produced by evaporative precipitation into aqueous solution (EPAS) were prepared by direct compression. The objective was to examine the effects of formulation factors including stabilizer types and levels used in EPAS process on the physicochemical properties of these tablets. During EPAS process, ITZ (15%w/v) and stabilizer (2%w/v) were dissolved in dichloromethane solution. This ITZ/stabilizer/organic feed solution was pumped through a heating coil at 80°C and atomized by a crimped nozzle into an aqueous solution containing stabilizer (2%w/v). Different stabilizers were investigated, including polyvinyl pyrrolidone K15, poloxamer 407 and poloxamer 188. The resulting EPAS dispersion was dried to powder. The dissolution rate, contact angle, surface area, X-ray diffraction, scanning electron microscopy and particle size were determined for each EPAS micronized powder composition. Tablets were prepared by direct compression using a single-punch tabletting machine. Rapidly disintegrating and dissolving tablet formulation contained ITZ EPAS

powders (40%w/w), microcrystalline cellulose (34% w/w), lactose monohydrate (20% w/w), sodium starch glycolate (5%w/w), silicone dioxide (0.5%w/w) and magnesium stearate (0.5%w/w). The tablets were characterized by hardness, friability, disintegration and dissolution. Rapidly disintegrating and dissolving tablets were successfully developed using EPAS processed powders containing nanoparticles of ITZ. Greater than 70-80% of ITZ was dissolved at 5 min, compared to only 14% and 80% of the bulk ITZ at 5 and 120 min, respectively. EPAS processed powders containing ITZ with poloxamer 407 yielded the highest surface area (8.79 ± 0.42 m^2/g) and the lowest contact angle (30.2 ± 0.62^o) subsequently achieving the highest dissolution rate. Tablets compacted from EPAS processed powders showed the similar release profiles with a complete dissolution of ITZ within the test time. All tablets had friability about 0.14-0.23%, hardness about 10-12 kg and disintegration time about 20-25 s. EPAS processed powders demonstrated to be suitable as matrix material for preparing rapidly disintegrating and dissolving tablets with sufficient mechanical integrity and well reproducible drug dissolution profiles.

3.2 INTRODUCTION

Development of solid dosage forms for poorly water-soluble drugs has been a major challenge and often results in low bioavailability since the rate of drug absorption from the gastrointestinal tract can be severely limited by dissolution

rate (1-3). There has been an increasing interest in the development of nanoparticles during the past few decades. Small particle engineering processes enable poorly soluble drugs to increased solubility and dissolution rate, resulting improving drug bioavailability. There are various reviews for particle engineering technologies (4-7). Evaporative precipitation into aqueous solution (EPAS) technology is a promising approach to engineer small particles with high dissolution rates offers a great potential in the development of oral drug delivery and overcome this problem. EPAS is a particle formation process developed to produce submicron to micron-sized hydrophobic drug particles. EPAS has been successfully used to enhance dissolution for numerous drugs including cyclosporine, carbamazepine, itraconazole and danazol (8-13). The EPAS process creates small particles through rapid phase separation. Evaporation of the primary solvent results in loss of solvent power and precipitation of very small particles of the dissolved solute. Briefly, drug dissolved in an organic solvent is sprayed through an atomizing nozzle into an aqueous solution containing a hydrophilic stabilizer to produce an aqueous dispersion. Rapid evaporation of the organic solvent at elevated temperature produces very high supersaturation and rapid precipitation of the drug in the form of suspended particles. The particles may be stabilized by a variety of stabilizers from either or both of organic and aqueous phases. The stabilizers adsorb onto the newly formed drug particle surfaces consequently decreasing the surface energy and providing steric and/or

electrostatic repulsion between particles to minimize particle aggregation. The enhanced dissolution rate characteristic of EPAS can generally be accounted for by one of the following mechanisms; increase the surface area available for dissolution by decreasing the particle size of drug, precipitation as a metastable crystalline form or a decrease in substance crystallinity and by optimizing the wetting characteristics of the drug surface due to adsorption of hydrophilic stabilizer. EPAS dispersion can be administered in the form of an aqueous dispersion as the final dosage form or incorporate into solid dosage forms for oral delivery.

Among the currently used solid dosage forms, rapidly disintegrating and dissolving tablets offer the major advantage over traditional tablets and capsules through their convenience in administration and suitability for patients who have swallowing difficulties such as children, elderly patients, and psychotic or disabled patients. Also, patients who are traveling, or who have little or no access to water are good candidates for rapidly disintegrating and dissolving tablets. These tablets in the market are prepared by various techniques including lyophilization, molding and direct compression. The commercially available tablets which disintegrate in less than 1 min are brittle, friable and have low physical resistance. These products require special packaging resulting in higher costs.

In this study, the rapidly disintegrating and dissolving tablets of ITZ with sufficient mechanical integrity were developed, involving the use of EPAS process to improve drug dissolution for the production of tablets. The main objective was to investigate the influence of the stabilizer types and levels on the physicochemical properties of EPAS processed powder and its corresponding tablet. We hypothesized that the high dissolution properties of EPAS particles can be maintained after incorporate into tablets using direct compression method. Itraconazole (ITZ), a Biopharmaceutics Classification System Class II (BCS) drug, was selected as the model drug in this study due to its extremely low water solubility. The absolute bioavailability of ITZ given orally is reported to be about 16% (18-19). Previously, we have also demonstrated the effect of design stabilizer on the properties and dissolution rates of ITZ particles produced by EPAS process. The resulting stabilizer-coated drug particles achieved high dissolution rates even with unusually high potencies by using a synergistic combination of properly chosen stabilizers.

3.3 MATERIALS AND METHODS

3.3.1 Materials

ITZ was purchased from Hawkins, Inc. (Minneapolis, MN). The stabilizers including a homopolymer; polyvinyl pyrrolidone (PVP K-15, MW =15,000) was

purchased from Spectrum Chemicals (Gardena, CA). The polyoxyethylene-polyoxypropylene copolymer (poloxamer 407, MW =11,700) and (poloxamer 188, MW =11,700) were purchased from BASF (Mount Olive, NJ). Lactose Monohydrate and magnesium stearate were purchased from Spectrum Quality Products Inc. (Gardena, CA). Microcrystalline cellulose (Avicel PH101) was obtained from FMC BioPolymer (Newark, DE) and sodium starch glycolate (Explotab) were purchased from Penwest Pharmaceuticals Co. (Patterson, NY). Colloidal silicon dioxide (Cab-o-sil) was obtained from Cabot Corporation (Tuscola, IL). HPLC grade acetonitrile was obtained from EM Industries Inc. (Gibbstown, NJ) and dichloromethane was purchased from Fisher Scientific Co. (Houston, TX). Other chemicals and solvents were of analytical reagent grade. Purified water was obtained from an ultra-pure water system (Milli-QUV plus, Millipore S. A., Molsheim Cedex, France).

3.3.2 Particle Formation Using EPAS Process

A schematic diagram of the EPAS apparatus is shown in Figure 3.1. The EPAS process consisted of spraying a 15.0% (w/w) solution of ITZ containing 2% w/v stabilizer dissolved in dichloromethane via an HPLC pump (Model PU-2086, Jasco Inc., Baltimore, MD) through a preheating coil (1/16 inch outer diameter (o.d.) × 0.030 inch inner diameter (i.d.) contained within a 1-1/2 inch

o.d. × 15 inch long plastic water jacket (Model 95023D, Alltech Associates Inc., Deerfield, IL) into 50 mL of 2.0 w/w% aqueous solution of stabilizers. Water was circulated through the jacket with a temperature controller (Julabo MP, Julabo USA Inc., Allentown, PA). The temperature of the water bath and the heating jacket was maintained at 80 °C. The nozzle was made by cutting stainless steel tubing (1/16 inch o.d. ×0.030 inch i.d.) (10) to form an elliptical conical orifice. The crimped end of the nozzle was filed back until the desired flow rate of 1 mL/min was achieved giving a pressure drop of about 20 MPa across the orifice. This type of nozzle produces very rapid pressure drops resulting in intense atomization of the organic drug solution at the tip of the nozzle. The nozzle was submerged approximately 10 cm under the surface of the aqueous solution. After atomizing for 5 min., an aqueous suspension containing a drug-to-stabilizer ratio of 0.68 was recovered. For higher potency, the suspensions were centrifuged (Model J2-21, Beckman, Fullerton, CA) at 10000 rpm for 20 min. to concentrate the particles, as done previously for particles formed by EPAS (11-13). The supernatant was decanted off to remove the unbound stabilizer in order to increase the potency in the precipitate. The particles were frozen by submerging in liquid nitrogen and lyophilized.

3.3.3 Characterization of EPAS Powders

3.3.3.1 Scanning Electron Microscopy (SEM)

A Hitachi Model S-4500 field emission scanning electron microscope (Hitachi Instruments, Irvine, CA) was used to visualize the particles and evaluate surface morphology of the particles. Samples were sputter coated with gold after being deposited on carbon tape on a microscope stage. The samples were sputter coated for 30 seconds.

3.3.3.2 Particle Size Analysis

The particle size was determined by light scattering with a Mastersizer-S (Model MAM2145, Malvern Instruments Inc., Southborough, MA). The particle size distribution was calculated on a volume weighted basis. To measure the particle size distribution, 5 mL of the suspension was diluted with 500 mL saturated ITZ solution, to produce a light obscuration in the range of 10-30%. The diluted suspension was sonicated for 30 sec. to break up any agglomerated particles. To study the redispersibility of the dry powders after centrifugation and lyohilization, about 20 mg dry powder were redispered into 500 mL saturated ITZ solution to produce an obscuration in the range 10-30%. After 1 min, the particle size distribution was measured. Ultrasound was used in the measurement to break up the agglomerated particles.

3.3.3.3 Potency Test

The potency of dry powders was determined by dissolving a known amount of dry powder (ca. 10mg) into 50 mL of mobile phase and then determining measuring ITZ concentration by HPLC. Reverse-phase HPLC was carried out using a Shimadzu VP-AT series LC10 HPLC (Columbia, MD) to measure the amount of ITZ. The mobile phase consisted of acetonitrile: water (70:30 v/v) containing 0.02% diethylamine. The flow rate was 1.0 mL/min and the detector wavelength was 263 nm. ITZ was eluted from an Intertsil 5um ODS-2 column (4.6 mm i.d. x 150 mm; Alltech Associates, Inc., Deerfield, IL) at 5 min using an injection volume of 50 µl.

3.3.3.4 Contact Angle

Dry powder was compressed at 1000 kg compression force using a Carver Laboratory Press (Model M, ISI Inc., Round Rock, TX) with flat-faced 6mm diameter punches. A droplet of dissolution medium (3 µl) was placed onto the surface of the compact and observed using a low power microscope. The contact angle was determined by measuring the tangent to the curve of the droplet on the surface of the compact using a Goniometer (Model No.100-00-115, Ramè-Hart Inc., Mountain Lakes, NJ).

3.3.3.5 Surface Area Analysis

The specific surface area of EPAS powders was determined using a Nova 3000 surface area analyzer (Quantachrome Corporation, Boynton Beach, FL) to measure N_2 sorption at 77.40 deg K. The surface area per unit powder mass was calculated from the fit of adsorption data to the Brunauer, Emmett, and Teller (BET) equation. Samples were degassed by applying vacuum at room temperature for 24 hr. prior to determination of the specific surface area. Three samples of each EPAS formulation were analysed.

3.3.3.6 Powder X-Ray Diffraction

Powder X-ray diffraction was conducted using $CuK\alpha_1$ radiation with a wavelength of 1.54054 Å at 40 kV and 20 mA from a Philips 1720 X-ray diffractometer (Philips Analytical Inc., Natick, MA). The sample powders were placed in a glass sample holder. Samples were scanned from 5^o to 50^o (2θ) at a rate 0.05^o/sec. For comparative purposes, the three highest values for relative line intensity and the corresponding 2θ angle were compared.

3.3.4 Preparation of Tablets

The tablets with a theoretical weight of 200 mg containing ITZ EPAS powders were prepared with 30 mg drug content .The model formula of tablet formulations used in this study comprised ITZ EPAS powders, directly compressible diluents, and magnesium stearate was used as lubricant. Diluents

used are: avicel PH-101 and lactose monohydrate as the fillers; sodium starch glycolate as a disintegrant and cab-o-sil as a glidant. The powder mixtures, except for magnesium stearate, were geometrically diluted and introduced into a V- Blender (York Model, Patterson-Kelly Company, East Stroudsburg, PA) and mixed for 10 min. Magnesium stearate was then added and mixed for an additional 5 minute. The blended powders were compressed using a single-punch tabletting machine (Strokes-F, Philadelphia, PA) equipped with 9 mm shallow concave punches. The prepared tablets were stored in a desiccators at room temperature for at least 48 h before being subjected to any characterization to remove any residual humidity. The uniformity of tablet weight was investigated. The average tablet weight was determined from 20 individually weighed tablets. The tablets were characterized by evaluation of hardness, friability, disintegration and dissolution. Means and relative standard deviations were calculated.

3.3.5 Characterization of Tablets

3.3.5.1 Tablet Friability

Tablet friability was calculated as the percentage weight loss of tablets after 100 rotations in a friabilator (Vanderkamp, Model 10801, Van-kel Industrial Inc., Chatham, NJ). According to section <1216> of the USP 24/NF19 (20), the tablet friability was determined for 33 tablets (corresponding to 6.5 g). The tablets

were carefully dedusted prior to testing. Accurately weigh the tablet sample, and place the tablets in the drum. Rotate the drum at a speed of 25 rpm for 4 min., and remove the tablets. Remove any loose dust from the tablets as before, and accurately weigh. Tablet friability (n=3) was calculated as the percentage weight loss of 20 tablets after 100 rotations in a friabilator.

3.3.5.2 Tablet Tensile Strength

The tablet tensile strength was calculated from its diametral crushing force measured using a hardness tester (Herberlein). Ten tablets from each formulation were analysed.

3.3.5.3 Disintegration Time

The disintegration time (n=6) was tested using the disintegration test apparatus (Vander, Model 71A-174A-3, Chatham, N.J.).Water kept at 37 °C was used as a medium and the basket was raised and lowered at a constant frequency of 30 cycles/min. Six tablets from each formulation were evaluated.

3.3.6 Dissolution Study

Dissolution testing of ITZ from the EPAS processed powders and the tablets was determined using the United States Pharmacopoeia (USP) apparatus II

(Vankel 7000, Vankel Technology Group, Cary, NC) at 50 rpm. The dissolution media was composed of 900 mL of enzyme-free simulated gastric fluid containing 0.5% SLS (pH 1.2) and was degassed prior to use. The dissolution media was maintained at 37 °C. Sink conditions were maintained throughout the testing. Aliquots of the dissolution media (5 mL) were collected at 2, 5, 10, 20, 30, 60 and 120 min. intervals. After 60 min, the paddle speed was increased to 200 rpm for 2 hours time point. These samples were filtered using 0.45µm filters (Gelman GHP Acrodisc 0.45µm, West Chester, PA). To ensure that no precipitation occurred during HPLC analysis, 0.1 mL of acetonitrile was added to 4 mL of filtered samples. These were mixed using a vortex mixer for approximately 5 sec. and then filtered using a 0.45µm filter into an HPLC vial for drug content analysis by reverse phase HPLC. The mean of six determinations was used to calculate the drug release from each of the formulations.

3.3.7 Statistical Analysis

Statistical evaluation of the data was compared using a student's t-test of the two samples assuming equal variances to evaluate the differences. The significance level ($\alpha = 0.05$) was based on the 95% probability value ($p < 0.05$).

3.4 RESULTS AND DISCUSSION

3.4.1 Characterization of EPAS Powders

The main composition of EPAS formulations other than drug is stabilizers. Several EPAS formulations containing different stabilizers were prepared and their compositions were given in Table 3.1. The type of stabilizer was varied from formulation E1 to formulation E3. The stabilizers included polyvinyl pyrrolidone K15 (PVP K15) as homopolymer, poloxamer 407 and poloxamer 188 as copolymers. The purpose behind the design of these two series of triblock copolymers was to evaluate the effect of both EO and PO block length (where EO is polyethylene oxide, PO is polypropylene oxide) on physicochemical of EPAS particles. The favorable effect of poloxamer 407 on dissolution rate has also been previously demonstrated (13). Therefore, it was worthy to extend our investigations and compare the performance of these polymers in improving dissolution behavior of ITZ. Poloxamers are nonionic triblock copolymers of poly (ethylene oxide) and poly (propylene oxide) used primarily in pharmaceutical formulations as surface active agents (21-22). The poly (ethylene oxide) segment is hydrophilic while the poly (propylene oxide) segment is hydrophobic. The two different types of poloxamers were investigated in this study. Poloxamer 407 and poloxamer 188 are chemically similar in composition, differing only in the relative amounts of EO and PO added during manufacture. Their physical and surface-active properties vary over a wide range and a number of different types are commercially available.

3.4.1.1 Particle Morphology, Size and Potency

The particle morphology of bulk ITZ and EPAS powder samples with different stabilizers (E1-E3) was examined by SEM (Figure 3.2). Bulk ITZ is shown to have a long needle-shaped crystal habit (Figure 3.2a). Large crystals of 10-20 μm in length, with smaller crystals exhibiting a wide particle size distribution. In contrast, all cases of EPAS samples, the particles are composed of nanostructured aggregates containing nanoparticles of ITZ with stabilizer (Figure 3.2b-3.2d). These aggregates have also been taken for the particle size determining by laser diffraction. Physicochemical characteristics of the EPAS processed powders are summarized in Table 3.2.The mean particle size of the EPAS processed powders ranged from 7 to 10 μm. According to the SEM micrographs, these particle sizes were very likely to represent the aggregate sizes of submicron particles. Different potencies of EPAS samples containing poloxamer 407 as stabilizer (E4-E6) are presented in Table 3.2. The high potencies result from the removal of a large amount of non-adsorbed stabilizer in the supernatant (11). The resulting EPAS powders had high drug-to-stabilizer ratios up to 10, corresponding to potencies up to 91%. There was no significant difference in particle size ($p>0.05$) when potencies and drug-to-stabilizer ratio were increased.

3.4.1.2 Contact Angle and Surface Area

The wettability of EPAS processed powders was assessed from the contact angle of dissolution media on the compacted surface of EPAS powders. The contact angle values for various samples are reported in Table 3.2. The mean contact angle value for bulk ITZ was 61.6° against water and it was observed that the powders were poorly wet in aqueous media. On the other hand, the measured contact angle of EPAS samples were in range of 30-40° indicating a high hydrophilic surface. Reduction in contact angle was achieved even in the highest potency sample with a drug-to-stabilizer ratio of 10.76. In all cases, EPAS samples had a significantly lower ($p < 0.05$) contact angle compared to bulk ITZ indicating the better wetting ability of EPAS samples. It was much lower in EPAS samples containing poloxamer 407 (E1 and E4-E6). The result showed that poloxamer 407 acts as a good wetting agent for ITZ. Wong et al. (23) also revealed that the spray dried griseofulvin particles with poloxamer 407 had the highest dissolution rate and hence improving the absolute oral bioavailability of the drug in rats.

The BET surface areas of various dry powders were analyzed and the results are illustrated in Table 3.2. The surface areas of EPAS samples were at least two times higher than that of the bulk ITZ. The large surface areas of the EPAS samples reflect the submicron primary particle domains of the nanostructured aggregates as observed in the SEM micrographs. The surface area was the highest for EPAS processed powders with poloxamer 407 system (8.79 m^2/g), which was

significantly greater ($p<0.05$) than those of EPAS processed powders made by the other stabilizers investigated as reported in Table 3.2. This could be due to the stabilizing effect of the poloxamer 407 against particle growth during the particle formation step. The presence of stabilizer in EPAS process inhibits crystal growth by adsorbing onto the newly created surface of the precipitated drug.

3.4.1.3 Dissolution Study

Dissolution testing of various dry powder samples were carried out and given in Figure 3.3a and 3.3b. The in vitro dissolution rates of EPAS samples (E1-E6) were significantly increased compared to bulk ITZ ($p<0.05$). The dissolution of ITZ was nearly 95% within the first 5 min for formulation E1 containing ITZ with poloxamer 407, compared to 83% for formulation E2 (poloxamer 188), 87% for formulation E3 (PVP K15) and 14% for the bulk ITZ, respectively. This observation of the high dissolution rates was consistent with high surface area produced by the intense atomization with rapid evaporation in the EPAS process along with improve wettability due to the presence of stabilizer on ITZ particle surface. The decrease in contact angle correlated with an increase in dissolution rate as reported in Table 3.2. This significantly improves wettability allowing for close proximity of the drug to the dissolution media resulting in a further increase in the dissolution of ITZ.

With the use of poloxamers, the dissolution rates of ITZ were greater for poloxamer 407 with the lower EO/PO ratio of 3.61 or less hydrophilicity of

stabilizers than poloxamer 188 with EO/PO ratio of 5.93. This indicates that lipophilicity and hydrophilicity of surfactant has an influence in the dissolution rate of ITZ. The finding in the present study is in agreement with our previous study (13) that the stabilizer adding during EPAS process must adsorb strongly onto particle surfaces in order to prevent particle agglomeration and the adsorption is greatly influenced with respect to its hydrophobicity. ITZ is highly hydrophobic drug and therefore a non-ionic stabilizer with high hydrophobicity or low HLB can be highly adsorbed onto ITZ particle surfaces allowing for sufficient wetting The PO block of poloxamer adsorbs onto the hydrophobic surface of ITZ while the EO block may be solvated by water providing highly hydrophilic surface in replace, as indicated by the reduction of contact angle values as discussed earlier in section 3.1.2. In the previous study, it was found that enhanced dissolution of ITZ is mainly due to high surface area and enhanced wettability of the EPAS processed powder. Based on the dissolution results, the amphiphilic character of poloxamer 407 appears to be sufficiently well-balanced to provide both adsorption onto the drug particle and steric stabilization. On the other hand, the lower dissolution rate of ITZ was observed in E3 sample than E1 and E2 samples. In 10 min., 70% ITZ dissolved from sample E3 as compared to 90% and 80% determined for the sample E1 and E2, respectively. The decreased in dissolution rate can be attributed to the observation that this sample remained for a longer time on the top of dissolution medium before being wetted

completely. We also observed that PVP Kl5 dissolves in water more slowly than the other stabilizers when preparing aqueous solutions. It is, therefore, important to ascertain which stabilizer type should be employed to obtain rapid dissolution of ITZ using EPAS process.

In this section, the effect of different stabilizer levels on the amount of dissolved drug was evaluated. The formulation E1 composed of ITZ and poloxamer 407 demonstrated the best rapid dissolution profile among the three EPAS formulations investigated by altering the types of stabilizer. Therefore, this formulation was chosen to conduct this additional experiment. Formulations E4, E5 and E6 were prepared by varying drug-to-stabilizer ratio from 3.57 to 10.76. At 5 min, the amounts of ITZ dissolved from E1 was nearly 83% which higher than those of E6 (81%), E5 (78%) and E4 (75%) for the 3.57, 5.36 and 10.76 drug-to-stabilizer ratios, respectively. However, no significant difference in the dissolution rates was observed indicating that only a small amount of stabilizer required to achieve high dissolution rates in EPAS process ($p>0.05$). This result was also consistent with our previous studies that showed the rapidly dissolving, high potency formulations of ITZ were able to prepare by EPAS (13, 24).

3.4.1.4 Powder X-Ray Diffraction

The solid-state physical structure by powder X-ray diffraction (PXRD) was established to analyze the crystallinity of the dry powders. The diffractogram of bulk ITZ powders from 5 to 45°θ (Figure 3.4) showed numerous distinctive peaks

that indicated a high crystallinity. The PXRD patterns of all EPAS samples also exhibited the identical characteristic diffraction peaks of crystalline bulk ITZ. This indicated that ITZ existed in the crystalline state in EPAS samples. The degree of crystallinity for these samples did not appear to be correlated to their dissolution rates. As we seen from the dissolution results, all EPAS samples yielded very rapid dissolution profiles, indicating that high dissolution rates may be achieved for high surface area crystalline powders.

3.4.2 Characterization of Tablets

Optimized composition of tablet formulations (200 mg tablet) containing EPAS processed powders of ITZ are given in Table 3.3. The content of ITZ was maintained at 30 mg per tablet. Table 3.4 shows the physical characterization of the prepared tablets from each formulation. As can be seen, all examined tablets revealed the narrow range of weight variation with the coefficient of variation less than 1% and no significant differences ($p>0.05$) were observed between each formulations. Tablet hardness was in the range of 10-12 kg indicating a good handling property without breakage or excessive friability problems (23) thus confirming the excellent compactability properties of the EPAS processed powders for direct compression. The percentage weight loss in the friability test was 0.09-0.16% which were below 1% indicating the sufficient mechanical integrity and strength of the prepared tablets. All the tablets formulations rapidly

disintegrated within 23 seconds, indicating that the tablets disintegrated very fast after they contacted the dissolution media. Figure 3.5 shows the dissolution characteristics of tablets prepared with different stabilizers in EPAS compositions. In terms of dissolution, tablets formulated employing EPAS processed powders gave higher dissolution rates than Sporanox® capsule used as powders. Within the first 10 min, the EPAS tablet samples had dissolved more than 70% whereas, Sporanox® had dissolved 55% of ITZ. In contrast, all EPAS tablet samples revealed the similar dissolution profiles with their corresponding EPAS processed powders. The ability of EPAS processed powders consisting of ITZ nanoparticles to maintain high dissolution rates after compacted into tablets is very useful for developing rapidly disintegrating and dissolving tablets of ITZ in order to maintain the advantages of nanoparticles to improve biovailability of poorly water soluble drug, such as ITZ.

3.5 CONCLUSIONS

Poorly-water-soluble compounds are often difficult to develop as drug products using conventional formulation techniques. In this study, EPAS has been proved to be an useful process to produce a rapid release dosage form for ITZ. High dissolution rates of ITZ were obtained from EPAS processed powders consisting of ITZ nanoparticles. Several reasons may explain the faster dissolution rates. The rapid evaporation and atomization in the EPAS process,

may lead to smaller primary particles resulting in high surface area along with the close proximity of the aqueous stabilizer to the ITZ surface particles. The type of stabilizer was shown to be an important factor to obtain dissolution rate of ITZ from EPAS processed powders by adsorbing onto the hydrophobic surface of ITZ resulting in a hydrophilic surface. This phenomenon combined with high surface area leads to a rapid wetting and dissolution of the EPAS processed powders upon contact with aqueous media. In contrast, the level of stabilizer range from 0.62-10.76 has no effect on the dissolution rate of ITZ indicating that high dissolution rate of EPAS processed powders can be achieved using small amount of stabilizer. Additionally, EPAS processed powders were able to be direct compressed into tablets with desirable mechanical properties and maintained high dissolution rates of ITZ. The ability to maintain rapid dissolution rates of EPAS processed powders in tablet formulation offers great promise for pharmaceutical development and manufacturing to improve dissolution rates of a poorly water soluble drug for oral delivery system.

3.6 ACKNOWLEDGMENTS

The authors would like to gratefully acknowledge the financial support from The Dow Chemical Company (Midland, MI).

3.7 REFERENCES

1. Liversidge GG, Cundy KC. (1995) Particle size reduction for improvement of oral bioavailability of hydrophobic drugs: I. Absolute oral bioavailability of nanocrystalline danazol in beagle dogs. Int. J Pharm.**125:** 91-97.
2. Chiba, Y., Kohri N, Iseki K, and K., M. (1991) Improvement of dissolution and bioavailability for mebendazole, an agent for human echinococcosis, by preparing solid dispersion with polyethylenen-glycol. Chem. Pharm. Bull.**39**: 2158-2160.
3. Zhao YH, Abraham MH, Le J, Hersey A, Luscombe CN, Beck G, Sherborne B, Cooper I. Rate-limited steps of human oral absorption and QSAR studies. Pharm Res **19**: 1446-1457.
4. Hu J, Johnston KP, Williams III RO. (2004) Nanoparticle Engineering Processes for Enhancing the Dissolution Rates of Poorly Water Soluble Drugs. Drug Dev. Ind. Pharm. **30:** 233-245.
5. Rogers TL, Nelsen AC, Sarkari M, Young TJ, Johnston KP, Williams III RO. (2003) Enhanced aqueous dissolution of a poorly water soluble drug by novel particle engineering technology: Spray-freezing into liquid with atmospheric freeze-drying. Pharm. Res.**20:** 485-493.

6. Tom, J. W., and Bebenedetti., P. G. (1991) Particle formation with supercritical fluids- a review. J. Aerosol Sci. **22**: 555-584.
7. Merisko-Liversidge E, Liversidge GG, Cooper ER. (2003) Nanosizing: a formulation approach for poorly-water-soluble compounds. Eur. J. Pharm. Sci. **18:** 113-120.
8. Chen X, Young TJ, Sarkari M, Williams RO, Johnston KP (2002) Preparation of Cyclosporine A Nanoparticles by Evaporative Precipitation into Aqueous Solution (EPAS). Int J Pharm **242**:3-14.
9. Sarkari M, Brown J, Chen X, Swinnea S, Williams RO, Johnston KP (2002) Enhanced Drug Dissolution Using Evaporative Precipitation into Aqueous Solution. Int J Pharm **243**:17-31.
10. Young TJ, Mawson S, Johnston KP, Henriksen IB, Pace GW, Mishra AK. (2000) Rapid Expansion from Supercritical to Aqueous Solution to Produce Submicron Suspensions of Water-Insoluble Drugs. Biotechnol. Prog. **16:** 402-407.
11. Chen X, Williams RO and Johnston KP. (2004) Rapid Dissolution of High Potency Danazol Particles Produced by Evaporative Precipitation into Aqueous Solution. J. Pharm. Sci. **93:**1867-1878.
12. Chen X, Benhayoune Z, Williams III RO, Johnston KP. (2004) Rapid dissolution of high potency itraconazole particles produced by evaporative

precipitation into aqueous solution. J. Drug Del. Sci. Technol. **14:** 299-304.

13. Sinswat P, Gao X, Yacaman MJ, Williams III RO, Johnston KP. (2005) Stabilizer choice for rapid dissolving high potency itraconazole particles formed by evaporative precipitation into aqueous solution. Int. J Pharm. **302:** 113-124.
14. Jain S and Sehgal V (2001) Itraconazole: an effective oral antifungal for onchomychosis. Int. J. Dermatol. **40:** 1-5.
15. De Beule K, Van Gestel J (2001) Pharmacology of itraconazole. Drugs. **61:** 27-37.
16. Peeters J, Neeskens P, Tollenaere JP, Remoortere VP and Brewster ME.(2002) Characterization of the interaction of 2-hydroxypropyl- β-cyclodextrin with itraconazole at pH 2, 4, and 7. J. Pharm. Sci. **91:** 1414-1422.
17. Heykants J., Van Peer, A., Van de Velde, V., Van Rooy, P., Meuldermans, W., Lavrijsen, K., Woestenborghs, R. and Cauwenbergh, G. (1989) The clinical pharmacokinetics of itraconazole: an overview. Mycoses **32**: 67–87.
18. Yoo, S.D., Kang, E., Jun, H., Shin, B.S., Lee, K.C. and Lee, K.H (2000) Absorption, first-pass metabolism, and disposition of itraconazole in rats. Chem. and Pharmaceutical Bulletin **48:** 798-801.

19. Hardin TC, Graybill JR, Fetchick R, Woestenborghs R, Rinaldi MG, Kuhn JG. (1988) Pharmacokinetics of itraconazole following oral administration to normal volunteers. Antimicrob Agents Chemother **32:** 1310-1313.
20. US Pharmacopeia XXIV (2005) US Pharmacopeial Convention, Rockville, MD
21. Strickley RG (2004) Solubilizing excipients in oral and injectable formulations Source. Pharm. Res. **21:** 201-230.
22. Schmolka, I.R.(1966) Polyalkylene oxide block copolymers, in: M.J. Schick (Ed.), Nonionic Surfactants, Marcel Dekker, New York, pp. 300–371.
23. Marshall, K., Rudnick, E.M., 1990. Tablet dosage form. In: Banker, G.S., Rhodes, C.T. (Eds.), Drugs and The Pharmaceutical Sciences—Modern Pharmaceutics, vol. 40. Marcel Dekker, New York, pp. 355–426.

CHAPTER 4: Dissolution Rates and Supersaturation Behavior of Amorphous Repaglinide Particles Produced by Controlled Precipitation

4.1 ABSTRACT

Rapidly dissolving nanostructured particles containing amorphous repaglinide (REP) were produced by controlled precipitation. Rapid in vitro dissolution rates and high levels of supersaturation (drug concentration/crystalline equilibrium solubility) were achieved using different stabilizing polymers including hydroxypropylmethylcellulose (HPMC) E5, polyvinylpyrrolidone (PVP) K15, polyvinyl alcohol (PVA) and polyethylene glycol (PEG) 8000. The dissolution and supersaturation characteristics of amorphous REP depended on the surface area of the particles and the miscibility of REP with the polymer employed to prevent drug crystallization in the solid phase. Each of the polymers contained hydrogen bonding groups to favor miscibility with the drug. Of the various formulations investigated, REP/HPMC E5 had the highest surface area leading to the highest dissolution rate in aqueous media under sink conditions. For each of the polymers, except for PVA, the level of supersaturation was on the order of 5 and decayed only slightly for up to 24 hr. In addition, the amorphous REP/HPMC E5 system produced high supersaturation after 3 months storage at 25 °C/60% RH indicating it was stable against crystallization. This understanding

of the effect of polymer stabilizers on drug morphology and subsequently, dissolution rates and supersaturation, may be used to facilitate rational design of dosage forms with the potential for improved bioavailability.

4.2 INTRODUCTION

Oral drug delivery is the dominant route of administration, especially when repeated or routine administration is required [1]. However, oral bioavailability of poorly water soluble drugs is often limited by their dissolution rate when the drug can be readily absorbed across the gastrointestinal membrane following dissolution [2, 3]. Therefore, the enhancement in dissolution rate of these drugs in order to attain desirable blood levels has become one of the major challenges in pharmaceutical technology. The problems associated with low solubility drugs that contribute to insufficient dissolution rates of drug from oral dosage forms have important consequences impacting drug absorption leading to poor and variable drug absorption [4]. Many approaches to improve dissolution rates aim to increase surface area available for dissolution by reduction of particle size [5-9]. In addition, enhancement of particle surface wettability by adsorption of surfactants or hydrophilic polymers during particle formation may further increase the dissolution rate. Particle size [10] reduction by mechanical milling or high pressure homogenization often requires long times, introduces impurities,

and limits flexibility in controlling particle morphology [11]. Solubility can be enhanced with co-solvents, surfactants, or complexing agents [12-14] as well as the formation of emulsions and solid dispersions [10, 15]. However, use of excipients limits the drug potency in the final product, in some instances to below 50% (%w/w). Additionally, formation of an amorphous material may increase the solubility up to 100-times compared to that of its crystalline form[16]. An increase in the solubility (C_{sat}) of the drug increases the dissolution rate driving force dramatically, according to the Noyes-Whitney equation:

$$rate = \frac{DA}{h}\left(C_{sat} - C\right) \qquad \text{Eq. 1}$$

where C is concentration of drug in the bulk media away from the drug surface, D is diffusivity, A is the surface area, and h is the boundary layer thickness for the concentration gradient.

Controlled precipitation (CP) of water insoluble drugs from solution offers the ability to manipulate and control particle size distribution as well as morphology. The drug dissolved in an organic solvent is rapidly mixed with an antisolvent in the presence of polymeric and/or non-polymeric stabilizers. If mixing is done rapidly, a higher level of supersaturation is created before significant nucleation occurs [17]. The rate of primary nucleation is given by the following equation [17]:

$$B^0 \propto \exp\left(-\frac{16\pi\gamma^3 V_M{}^2 N_A}{3(RT)^3(\ln(1+S_0))^2}\right) \quad \text{Eq. 2}$$

where B^0 is the nucleation rate, γ is interfacial tension, V_M is molar volume, S_0 is degree of supersaturation (C/equilibrium crystalline solubility) and N_A is Avogadro's number. Once nucleation occurs, particles can grow by condensation of drug molecules onto the surface and by coagulation of particles. The nucleation rate depends more strongly on S than does the rate of condensation, which is linear in S [18]. High nucleation rates offer the potential to produce a large number of submicron particles in the final suspension, if the growth can be quickly arrested by the adsorption of stabilizers to the nuclei.

By forming amorphous drug particles with high surface areas, dissolution rates may be enhanced, and high supersaturation levels (metastable solubilities) may be achieved compared to the crystalline form of the drug. In the case of dissolution, supersaturation (S_d) may be defined as follows:

$$S_d = \frac{C(t)}{C_{eq}} \quad \text{Eq. 3}$$

where C(t) is the measured concentration at time t and C_{eq} is the equilibrium solubility of crystalline drug in the dissolution media. Amorphous drugs have been used to form supersaturated solutions that show large increases in membrane flux when compared to saturated solutions [19-22]. Drug molecules may precipitate from a supersaturated state by nucleation and growth to reach the

equilibrium solubility. In order to maintain supersaturation created by an amorphous drug, a crystallization inhibitor may be used to prevent precipitation from the aqueous media after dissolution. Several water soluble polymers, such as PVP and HPMC, have been used successfully to maintain supersaturated solutions for up to 24 hours [23-25]. Raghavan et al. have suggested H-bonding between the polymer and drug may play a primary role in the mechanism for crystallization inhibition [26]. Additionally, polymers may help maintain supersaturation by coating and passivating small embryos to arrest growth by preventing condensation of drug molecule onto the surfaces embryos. Extension of the time for high levels of supersaturation in the stomach and intestinal fluids may have a profound impact on increasing the bioavailability of poorly water soluble drugs, as has been suggested recently [27, 28].

Repaglinide (REP) is an oral prandial glucose regulator agent for the management of type 2 diabetes mellitus [29, 30]. It lowers blood glucose levels by stimulating the release of insulin from the pancreas. REP was chosen as the model drug for this study due to its low solubility and poor wettability in water [29]. It has a relatively low and variable bioavailability, as the absolute bioavailability of REP administered as a tablet was 62.5% (49.2% - 79.5%) relative to an intravenous infusion of the same dose [31]. High inter-individual variability in REP plasma concentrations has been reported in clinical trials [32, 33].

The objective of this study is to investigate the influence of different water-soluble polymers, including HPMC E5, PVP K15, PVA and PEG 8000, on the dissolution rate and supersaturation behavior of amorphous REP particles formed by CP. The mechanisms of drug dissolution and supersaturation are discussed from the view point of miscibility, as characterized by thermal analysis, and the ability of the polymer to form hydrogen bonds with REP. Also, the degree of crystallinity, morphology, and surface area of the REP particles were considered in order to understand the dissolution behavior under sink and supersaturated conditions.

4.3 MATERIALS AND METHODS

4.3.1 Materials

REP ($C_{27}H_{36}N_2O_4$; molecular weight = 452.6) and HPMC type 2910 (methoxyl content: 28–30%; hydroxypropyl content: 7–12%) with nominal viscosity for a 2% (w/v) aqueous solution of 5 mPas (Methocel Cellulose Ethers E5LV Premium) were kindly provided by The Dow Chemical Company (Midland, MI). PVP (K15 grade, M_w = 10, 000), PEG 8000 and PVA were purchased from Spectrum Chemical Mfg. Corp. (Gardena, CA). The chemical structures of REP and these polymers are presented in Table 4.1. Stabilized 1,3

dioxolane was obtained from ACROS Organics (Morris Plains, NJ). All other solvents used were of HPLC grade unless noted otherwise.

4.3.2 Controlled Precipitation

A schematic of the Controlled Precipitation apparatus is shown in Figure 4.1[8] . A 5% (wt./tot. wt.) solution of REP in dioxolane was prepared at room temperature and stirred until completely dissolved. An aqueous solution of polymer used in formulation, in deionized water was prepared at room temperature, and 100 g was pre-cooled in the precipitation apparatus to 3°C. Using a 60 mL syringe, 20 g of organic solution was delivered to the temperature-controlled mixing zone through 1/16" stainless steel tubing within approximately 15 s. The mixing rate of the loop was controlled by a centrifugal pump with the maximum fluid velocity measured at approximately 13 ft/sec. The suspension product was then fed at 25 mL/min directly into a vacuum distillation apparatus for removal (stripping) of dioxolane at a pressure and temperature of 7-10 torr and 38°C, respectively. After completion of solvent removal, particle size of the stripped suspension was measured by static light scattering with a Malvern Mastersizer-S (Malvern Instruments Ltd., U. K.). In some cases the suspension was sonicated in 30 s intervals within the Malvern unit and corresponding particle size measurements were taken. In order to obtain dry powders, the stripped

suspension was frozen drop-wise into liquid nitrogen and freeze-dried using a Virtis Advantage Tray Lyophilizer (Virtis Company, Gardiner, NY).

4.3.3 Scanning Electron Microscopy (SEM)

A Hitachi S-4500 scanning electron microscope (SEM) (Hitachi Instruments Inc., Irvine, CA) at an accelerating voltage of 15 kV with a secondary electron detector was used to obtain digital images of the samples. Powders were gently applied to adhesive carbon tape on an aluminum SEM stage. The stage was then coated with Au for 25 s using a Pelco Model 3 sputter-coaler under an Ar atmosphere before viewing.

4.3.4 Specific Surface Area Measurement

Specific surface area was measured using a NOVA-2000 instrument (Quantachrome Corporation, Boynton Beach, FL). A known amount of bulk REP or CP REP powder (~0.03 g) was loaded into a Quantachrome sample cell and degassed for approximately 12 hours prior to analysis. With nitrogen as the adsorbent, the surface area per gram of degassed sample weight was determined using a relative pressure range from 0.05 – 0.35.

4.3.5 X-Ray Diffraction (XRD)

X-ray diffraction was performed using a Philips PW 1720 X-ray generator (Philips Analytical Inc., Natick, MA) with CuK α_1 radiation at a wavelength of 1.54054 Å at 40 kV and 20 mA. Reflected intensities were detected by a Philips goniometer. Diffraction patterns were obtained for the bulk materials as well as CP samples. Dry powders were gently pressed onto a glass slide to a thickness of approximately 1 mm. XRD patterns were taken at a rate of 20 degrees/min with a step length of 0.05 degrees from 5-45 degrees.

4.3.6 Thermal Analysis

The glass transition temperature (T_g) of CP powders was determined by modulated differential scanning calorimeter (MDSC) carried out using a TA Instrument (City, State) differential scanning calorimeter (Model 2920). Approximately 5 mg of sample was placed into an aluminum pan (Perkin-Elmer Instruments, Norwalk, CT) and crimped with an aluminum lid. The samples were initially heated to 200 °C at 10.00 °C/min to remove all residual moisture. Subsequently, the sample was cooled to -20^{o}C and then reheated up to 200 °C at heating rate of 3^{o}C/min. An empty pan was used as the reference, and calibrations for temperature and enthalpy have been carried out using an indium standard.

4.3.7 Dissolution Testing at Sink Conditions

A USP dissolution apparatus (Vankel 7000, Vankel Technology Group, Cary, NC) Type II (paddles) at a rotation speed of 50 rpm was used for in vitro testing of drug dissolution from the powders. An amount of powder equivalent to 2 mg of drug was weighed out and placed into 900 mL of dissolution medium containing citric acid/sodium phosphate dibasic buffer with a pH of 4.5. The dissolution media was maintained at 37.0±0.5 °C and degassed prior to use by sonication for 2 min. Sink conditions (10 percent of C_{eq}) were maintained throughout the testing based on REP solubility in the dissolution medium. A sample volume of 5 mL was collected at 2, 5, 10, 20, 30 and 60 minutes using a VK8000 autosampler (Varian, Inc. Cary, NC). The samples were then filtered through a 0.45µm filters (Gelman GHP Acrodisc 0.45µm, VWR, West Chester, PA) into an HPLC vial for drug content analysis using reverse phase HPLC. Dissolution profiles of powders were determined in replicates of 6.

4.3.8. Supersaturated Dissolution

Dissolution experiments to determine supersaturation were performed similarly to USP dissolution testing at sink conditions, except the volume of the dissolution apparatus was only 100 mL. It was equipped with a paddle stirring mechanism. Drug formulations were weighed out corresponding to approximately 10-times (21 mg REP in each sample) or 25 times (53 mg REP) the equilibrium solubility in 100 mL of dissolution medium (citric acid/sodium

phosphate dibasic pH 4.5). Paddle speed and bath temperature were maintained at 50 rpm and 37^{o}C, respectively. A 1 mL aliquot of sample was taken at 5, 10, 20, 30, 60, 120, and 1440 minutes. This aliquot was immediately filtered through a 0.2 μm nylon filter and a 0.5 mL portion of this solution was dissolved in 1 mL of acetonitrile. The collected samples were analyzed for REP concentration using HPLC as described above. All experiments were performed in triplicate.

4.4 RESULTS AND DISCUSSION

4.4.1 Particle Morphology

SEM was used to visually observe the primary particle size and surface morphology of the particles. SEM micrographs of the various formulations are shown in Figure 4.2. SEM micrographs show variable morphology, depending on the stabilizer used. The SEM micrograph of bulk REP (Figure 4.2a) revealed a large and long needle-shaped crystal habits that ranged in length from 20-23 μm. The SEM image of the HPMC E5 stabilized powders (Figure 4.2b) show distinct aggregates of particles with smooth surfaces and confirms the primary particle size of about 100 nm. The particles prepared in the presence of PVP K-15, PEG 8000 and PVA were larger (Figure 4.2c-4.2e).

4.4.2 Surface Area

The specific surface area of the CP powders for all compositions was higher than that of bulk REP (1.53 m^2/g). The surface areas of the HPMC E5, PVPK15, PEG 8000 and PVA stabilized powders were 9.35 m^2/g, 5.08 m^2/g, 4.97 m^2/g and 3.57 m^2/g, respectively (listed in Table 4.2). The large surface areas of CP powders reflect the submicron primary particle domains of the nanostructured aggregates observed in the SEM micrographs. For example, a surface area of 9.35m^2/g would correspond to 640 nm diameter particles, assuming spherical geometry and 1g/cm^3 density. The surface areas of REP/PEG 8000, REP/PVPK15 and REP/PVA were lower than that of REP/HPMC E5, consistent with the larger particle sizes and less porous morphologies observed by SEM. A number of studies have shown that increasing the surface area of a hydrophobic drug enhanced the dissolution in aqueous media [34, 35]. Because all CP micronized powders possessed higher surface areas, compared to bulk REP, faster dissolution profiles were expected.

4.4.3 X-ray Powder Diffraction

The degree of crystallinity of REP in the CP powders was determined by powder XRD. The XRD patterns of powder samples investigated in this study are shown in Figure 4.3A. Bulk powder is highly crystalline, as determined by

distinct peaks between 12 and 36 2θ degrees. No characteristic diffraction peaks of the crystalline forms of REP were seen in any of the CP formulations regardless of stabilizer type. The lack of diffraction peaks indicated that the REP was in a high energy amorphous form. Since the drug content was approximately 50% (47 $\pm$ 2%) in all cases, even small amounts of crystallinity would be apparent in the XRD pattern. For example, the characteristic crystalline peaks were readily apparent in the physical mixture of REP and HPMC E5 at 50% drug content. It was also found that REP/HPMC E5 remained stable in the amorphous form following storage at 25°C /60 % relative humidity (RH) for 3 months (Figure 4.3B). Problems related to physical stability of amorphous drugs, which have a great tendency to undergo conversion to crystalline forms, often limit their physicochemical advantages and their application in dosage form design. The presence of high T_g polymers such as HPMC E5 produced an increase in the physical stability of the amorphous REP by increasing the T_g of drug formulation as discussed in section 3.6. For this reason, a high T_g stabilizer was included in the formulation and is discussed in the next subsection.

3.4.4 Thermal Analysis

The MDSC measurement of T_g in the CP compositions was determined by constructing a tangent to the thermogram baseline above and below the glass transition. The glass transition for amorphous REP was observed at 51.8°C (data

not shown). In all CP formulations, REP was incorporated at the same drug loading of 50% w/w. The presence of a single T_g intermediate to those of the drug and polymer was observed in the binary mixtures of REP/HPMC E5 and REP/PVP K15 (Figure 4.4). These results suggest a high degree of miscibility between REP and these polymers. However, two glass transitions were found for the REP/PVA system, one associated with glassy REP at 45.7°C and one originating from the drug–polymer mixture at 100.7 °C (close to the T_g of pure PVA, 107°C). This result indicates only partial miscibility. In the case of REP: PEG 8000, a T_g peak was not observed, as the T_g of the polymer was very low.

The T_g of homogeneous binary mixtures can be described by Gordon Taylor equation [36] which is based on the free volumes of the individual components.

$$T_{gmix} = \frac{w_1 T_{g1} + K w_2 T_{g2}}{w_1 + K w_2} \qquad \text{Eq. 4}$$

where w_1 and w_2 are the weight fractions of the individual components and T_{g1} and T_{g2} are their glass transition temperatures. K is a constant that can be calculated using the Simha-Boyer equation [37],

$$K \approx \frac{\rho_1 T_{g1}}{\rho_2 T_{g2}} \qquad \text{Eq. 5}$$

where ρ_1 and ρ_2 are the densities components 1 and 2, respectively. Figure 4.5 shows the comparison between experimental and theoretical T_g values predicted

by the Gordon–Taylor equation. The experimental T_g values were higher than the predicted T_g values, resulting from relatively strong interactions (i.e. H-bonding) between electron donating and electron accepting functional groups of the individual components. The more H-bonding between drug and polymer would allow less H-bonding sites available to water which can cause crystallization of amorphous drug. It is well known that the presence of moisture leads to a decrease in the T_g due to plasticizing and increasing molecular mobility by absorbed water. The recent study by Tanaka et al. [38] showed a dramatic decrease in T_g of amorphous FK888 from 89 to 57 °C when exposed to 4.5% of moisture, leading to physical instability. The T_g of the amorphous solid is an important indicator for predicting its physical stability. The increase in the T_g of the formulation with the inclusion of the polymers is important for maintaining a rigid system to prevent relaxation from the amorphous state to the crystalline state, over long storage times. In this study, the T_gs of CP formulations are about two fold higher than that of bulk REP (51.8^{o}C). At the T_g, amorphous solid undergoes a transition from a glassy state to a rubbery state due to high molecular mobility resulting in the crystallization and crystal growth of particles. It is recommended that the T_g be 50°C above the highest storage temperature to prevent crystallization and to ensure physical stability of the amorphous formulations over the product shelf-life. In the present study, we also found that the T_g of REP/HPMC E5 was similar to its initial T_g value when stored at 25°C

/60% RH for three months. This result also supports the physical stability determined by XRD (Figure 4.3B), which revealed the typical amorphous halo pattern indicating that the amorphous sample did not significantly convert to the crystalline form of REP.

3.4.5 Dissolution Testing at Sink Conditions

Using a USP apparatus II, the dissolution rate of all formulations was measured and is shown in Figure 4.6. The bulk REP powder was observed to wet and dissolve poorly during dissolution. Only 13 % of the micronized bulk REP dissolved in 2 minutes after addition to the dissolution media. As was expected, the dissolution rate of all CP formulations was significantly greater than that of the bulk powder. In all cases, the powders were wet much more rapidly as was apparent from their immediate dispersion into the dissolution media. The dissolution characteristics of amorphous REP produced by CP depended on the polymer used to stabilize the drug during CP. The rank order of dissolution rates and extent was REP/HPMC E5>REP/PVPK15>REP/PEG 8000>REP/PVA>Bulk REP, in direct correlation with the powder surface areas. Both dissolution rate and extent were much higher for the formulation containing HPMC E5 than the other stabilizing polymers within the first 30 min upon addition to the dissolution media. In 5 min., 86% of REP from the REP/HPMC E5 composition was dissolved as compared to only 13% determined for the bulk REP powder. The

fast dissolution rates and high extents of REP particles produced by CP were primarily attributed to the formation of a high energy amorphous drug, to increased C_{sat} compared to crystalline, bulk drug.

The initial dissolution rate was calculated with Eq. 1 for all samples in Figure 4.6 and compared to the experimental value. Table 4.2 lists the parameters for each calculation, including the total surface area (BET specific surface area times the total sample weight) and the boundary layer thickness, h. The value of h, was estimated to be the same as the average primary particle diameter, which was determined from the BET specific surface area. To estimate the primary particle diameter, it was assumed that the particles were monodisperse spheres without any agglomeration. In Table 4.2, the calculated and experimental rates were reported relative to the 1:1 REP/PVA case, since the exact values for C_{sat} and D (both constants for all cases) were unknown. The agreement between the experimental and calculated rates was reasonable, except for the REP/HPMC E5 case. In this case where the particle size was the smallest according to BET and SEM, the effect of particle agglomeration on the diffusion layer thickness may be expected to be more significant than for the lower surface area formulations. The diffusional layer thickness is likely larger than the estimated value and thus, the calculated rate was too high. Additionally, the calculated rate does not take into account possible inhibition by polymer domains that block exposure of the REP to the media. In particular, the dissolution of HPMC is known to be slow as

hydration forms a gel layer [39]. Both of these factors may explain why the calculated relative rate was higher than the experimentally observed relative rate. Overall, the agreement between theory and experiment suggested that the dissolution rate was primarily a function of the surface area of CP powders, which varied with the properties of the polymeric stabilizer.

3.4.6 Supersaturation Dissolution

The supersaturation dissolution of REP formulations with various polymers was investigated to observe the effects of polymer stabilization of amorphous REP in the solid phase on maximum supersaturation levels. Figure 4.7 shows the supersaturated dissolution of REP containing about 10 times the solubility limit of REP. For all of the polymers, REP concentration exceeded its equilibrium solubility in the dissolution medium to form a supersaturated solution. The high degree of supersaturation of REP was due to the stabilizing effect of the polymers against particle crystallization and/or growth by condensation and coagulation during the particle formation step. The degrees of supersaturation were comparable among REP/HPMC E5, REP/PVPK15 and REP/PEG 8000. However, considering the REP/PVA composition, the supersaturation reached 4 within a few minutes, and then decreased slightly over 24 hours.

According to MDSC results, the REP/PVA formulation gave two glass transition peaks (Figure 4.4). A REP-rich phase and a PVA-rich phase were present, since the two observed T_gs were relatively close to those of bulk REP and PVA. The REP-rich phase is susceptible to crystallization in the dosage form and upon addition to aqueous media, producing a less a soluble form of the drug. Any crystallized portion of the undissolved solid phase would then be unavailable to contribute to supersaturation of the dissolution media, thus limiting the maximum supersaturation to less than that of other formulations, which would remain amorphous in the solid phase. It is therefore reasonable to consider drug miscibility with the polymer to be essential in crystallization inhibition of the solid phase and thus, an important factor for maximizing supersaturation.

In this study, HPMC E5 was slightly more efficient at achieving high supersaturation and maintaining it for 24 hr that the next best two formulations. For these reasons, the REP/HPMC E5 formulations were studied in greater detail. Dissolution media were dosed with two amounts of drug powder, 21 and 53 mg, corresponding to 10 and 25-times (noted 10X and 25X, respectively) the equilibrium solubility limit in the dissolution media. In the case of the 10X dose, S_d, defined by Eq. 3, quickly exceeded the equilibrium solubility and continued to increase to 5 over two hours. For the 25X dose, S_d reached only 2. In both cases, the supersaturation level changed little for up to 24 hours. After storage of the

REP/HPMC E5 dry powder for 3 months at 25°C and ambient humidity, the supersaturation profile was almost identical to that of the initial powder.

Since the supersaturation provides a strong driving force for homogeneous nucleation, as described by Eq. 2, precipitation of the drug might be expected. If there is surface area available for heterogeneous nucleation to occur, rates may be even faster than homogeneous nucleation [18]. When a large amount of amorphous material is added to the solution, it may raise the supersaturation. In addition, excess undissolved particles may facilitate heterogeneous nucleation. The two processes could compete, resulting in a metastable equilibrium value of S_d. In the case of the 10X dose, the supersaturation reached 5X which left 5X in excess particles (approximately 10mg). Similarly, 23X in excess particles (approximately 49 mg) remained undissolved in the case of 25X dose (Figure 4.8). This large difference in heterogeneous nucleation sites is likely to be the cause for a lower S_d in the higher dose case. In both cases, however, the supersaturation level was maintained for up to 24 hours, in agreement with other work utilizing HPMC as a crystallization inhibitor [40]. In contrast to previous studies, which focus on low surface area solid dispersions at 10-30% drug loading, the CP process is capable of producing high surface area amorphous powders at much higher drug content which can supersaturate aqueous media at a rapid rate. These levels of supersaturation would be expected to increase flux of drug across the gastrointestinal membrane 5-fold for increased bioavailability.

With the solid drug in a high energy amorphous state, there is a thermodynamic drying force to convert to the lower energy crystalline state. Use of a high T_g polymer, such as HPMC, prevents mobility of the drug molecules and slows down the rate of transformation from amorphous to crystalline morphology [42]. The stability of REP morphology is readily apparent from the identical supersaturation profile of the powder after storage for 3 months at 25^{o}C. Moreover, the ability of formulations to supersaturate the dissolution media has been used to enhance bioavailability of poorly water soluble drugs[41]. In a supersaturated system, the concentration of drug in solution is greater than its solubility allowing high free drug concentration to available for absorption. This indicates the important role of supersaturation in enhancing the drug delivery of a poorly soluble drug.

4.5 CONCLUSIONS

Amorphous REP particles with high surface area were produced by CP. Rapid in vitro dissolution and supersaturation were achieved with various water soluble polymers including HPMC E5, PVP K15, PEG 8000 and PVA. Under sink conditions, the dissolution rate increased as the particle surface area increased, in good agreement with relative rates predicted by the Noyes-Whitney equation. REP/HPMC E5 gave the highest surface area particles, leading to the highest dissolution rate. The presence of polymer in CP inhibits drug crystallization of the solid phase during particle formation and storage to preserve

amorphous drug. This high miscibility between drug and polymer in the solid state favors the amorphous state for REP, as indicated by high supersaturation values up to 5 for levels up to 24 hr. in the dissolution media. MDSC data indicated that HPMC E5, PVP K15, PEG 8000 were miscible with REP, while partial miscibility was found with PVA. Accordingly, the PVA formulation produced a lower maximum supersaturation than the others. In addition, REP/HPMC E5 was physically stable in the amorphous form, achieving a high degree of supersaturation after storage at 25 °C/60% RH for up to 3 months. The high physical stability was favored by a high T_g for the binary mixture. Therefore selection of a stabilizing polymer to achieve high miscibility with the drug and a high T_g favors amorphous drug domains with high stability. The amorphous state may be used to achieve high supersaturation, and ultimately enhanced bioavailability.

4.6 ACKNOWLEDGMENTS

The authors would like to kindly acknowledge financial support from The Dow Chemical Company. This material is based upon work supported in part by the STC Program of the National Science Foundation under Agreement No. CHE-9876674.

4.7 REFERENCES

1. J. Kreuter, Peroral administration of nanoparticles. Adv. Drug Deliv. Rev. 7, 71 (**1991**).
2. R. H. Muller, C. Jacobs and O. Kayser, Nanosuspensions as particulate drug formulations in therapy: Rationale for development and what we can expect for the future. Adv. Drug Deliv. Rev. 47, 3 (**2001**).
3. N. Hussain, V. Jaitley and A. T. Florence, Recent advances in the understanding of uptake of microparticulates across the gastrointestinal lymphatics. Adv. Drug Deliv. Rev. 50, 107 (**2001**).
4. C. A. Lipinski, Poor aqueous solubility--an industry wide problem in drug discovery. Am. Pharm. Rev. 5, 82 (**2002**).
5. C. Leuner and J. Dressman, Improving drug solubility for oral delivery using solid dispersions. Eur. J Pharm. Biopharm. 50, 47 (**2000**).
6. B. Rabinow, E., Nanosuspensions in drug delivery. Nat. Rev. Drug Discov. 3, 785 (**2004**).
7. G. G. Liversidge and K. C. Cundy, Particle size reduction for improvement of oral bioavailability of hydrophobic drugs: I. Absolute oral bioavailability of nanocrystalline danazol in beagle dogs. Int. J Pharm. 125, 91 (**1995**).

8. T. L. Rogers, I. B. Gillespie, J. E. Hitt, K. L. Fransen, C. A. Crowl, C. J. Tucker, G. B. Kupperblatt, J. N. Becker, D. L. Wilson, C. Todd and E. J. Elder, Development and characterization of a scalable controlled precipitation process to enhance the dissolution of poorly water-soluble drugs. Pharm. Res. 21, 2048 (**2004**).
9. B. K. Johnson and R. K. Prud'homme, Engineering the direct preciptiation of stabilized organic and block copolymer nanoparticles as unique composites. Poly. Mater. Sci. and Eng. 36, 744 (**2003**).
10. M. Nakano, Places of emulsions in drug delivery. Adv. Drug Deliv. Rev. 45, 1 (**2000**).
11. J. Hu, K. P. Johnston and R. O. Williams III, Nanoparticle Engineering Processes for Enhancing the Dissolution Rates of Poorly Water Soluble Drugs. Drug Dev. Ind. Pharm. 30, 233 (**2004**).
12. V. J. Stella and R. A. Rajewski, Cyclodextrins: their future in drug formulation and delivery. Pharm. Res. 14, 556 (**1997**).
13. M. M. Akers, Excipient-drug interactions in parenteral formulations. J Pharm. Sci. 91, 2283 (**2002**).
14. R. Loftsson and M. E. Brewster, Pharmaceutical applications of cyclodextrins. J Pharm. Sci. 85, 1017 (**1996**).
15. C. Leuner and J. Dressman, Improving drug solubility for oral delivery using solid dispersions. Eur. J. Pharm. Biopharm. 50, 47 (**2000**).

16. B. C. Hancock and M. Parks, What is the True Solubility Advantage for Amorphous Pharmaceuticals? Pharm. Res. 17, 397 (**2000**)
17. O. Sohnel and J. Garside. Precipitation: Basic Principles and Industrial Applications, Butterworth Heinemann, (**1992**).
18. W. L. McCabe, J. C. Smith and P. Harriott. Unit Operations of Chemical Engineering, McGraw-Hill, New York, (**2001**).
19. S. L. Raghavan, A. Trividic, A. F. Davis and J. Hadgraft, Effect of cellulose polymers on supersaturation and in vitro membrane transport of hydrocortisone acetate. Int. J Pharm. 193, 231 (**2000**).
20. M. Iervolino, S. L. Raghavan and J. Hadgraft, Membrane penetration enhancement of ibuprofen using supersaturation. Int. J Pharm. 198, 229 (**2000**).
21. M. Iervolino, B. Cappello, S. L. Raghavan and J. Hadgraft, Penetration enhancement of ibuprofen from supersaturated solutions through human skin. Int. J Pharm. 212, 131 (**2001**).
22. B. R. Jasti, B. Berner, S.-L. Zhou and X. Li, A Novel Method for Determination of Drug Solubility in Polymeric Matrices. J Pharm. Sci. 93, 2135 (**2004**).
23. K. Yamashita, T. Nakate, K. Okimoto, A. Ohike, Y. Tokunaga, R. Ibuki, K. Higaki and T. Kimura, Establishment of new preparation method for solid dispersion formulation of tacrolimus. Int. J Pharm. 267, 79 (**2003**).

24. K. Okimoto, M. Miyake, R. Ibuki, M. Yasumura, N. Ohnishi and T. Nakai, Dissolution mechanism and rate of solid dispersion particles of nilvadipine with hydroxypropylmethylcellulose. Int. J Pharm. 159, 85 (**1997**).

25. H. Suzuki and H. Sunada, Influence of water-soluble polymers on the dissolution of nifedipine solid dispersions with combined carriers. Chem. Pharm. Bull. 46, 482 (**1998**).

26. S. L. Raghavan, A. Trividic, A. F. Davis and J. Hadgraft. Crystallization of hydrocortisone acetate: influence of polymers, Int. J Pharm. 212, 213 (**2001**).

27. P. Gao, B. D. Rush, W. P. Pfund, T. Huang, J. M. Bauer, W. Morozowich, M.-s. Kuo and M. J. Hageman, Development of a supersaturable SEDDS (S-SEDDS) formulation of paclitaxel with improved oral bioavailability. J Pharm. Sci. 92, 2386 (**2003**).

28. P. Gao, M. E. Guyton, T. Huang, J. M. Bauer, K. J. Stefanski and Q. Lu, Enhanced Oral Bioavailability of a Poorly Water Soluble Drug PNU-91325 by Supersaturatable Formulations. Drug Dev. Ind. Pharm. 30, 221 (**2004**)

29. C. Culy, Jarvis, B., Repaglinide, a review of its therapeutic use in Type 2 diabetes mellitus. Drugs 61, 1625 (**2001**).

30. W. Malaisse, Repaglinide, a new oral antidiabetic agent: a review of recent preclinical studies. Eur. J. Clin. Invest. 29, 21 (**1999**).
31. V. Hatorp, S. Oliver and C.-A. P. F. Su, Bioavailabitity of repaglinide, a novel antidiabetic agent, administered orally in tablet or solution form or intravenously in healthy male volunteers. Int. J Clin. Pharmacol. Ther. 36, 636 (**1998**).
32. T. C. Marbury, J. L. Ruckle, V. Hatorp, M. P. Andersen, K. K. Nielsen, W. C. Huang and P. Strange, Pharmacokinetics of repaglinide in subjects with renal impairment. Clin. Pharmacol.Ther. 67, 7 (**2000**).
33. T. Marbury, W.-C. Huang, P. Strange and H. Lebovitz, Repaglinide versus glyburide: a one-year comparison trial. Diabetes Res. Clin. Prac. 43, 155 (**1999**).
34. J. Hecq, M. Deleers, D. Fanara, H. Vranckx and K. Amighi, Preparation and characterization of nanocrystals for solubility and dissolution rate enhancement of nifedipine. Int. J Pharm. 299, 167 (**2005**).
35. P. Borm, F. C. Klaessig, T. D. Landry, B. Moudgil, J. Pauluhn, K. Thomas, R. Trottier and S. Wood, Research Strategies for Safety Evaluation of Nanomaterials, Part V: Role of Dissolution in Biological Fate and Effects of Nanoscale Particles. Toxicol. Sci. 90, 23 (**2006**).

36. M. Gordon and J. S. Taylor, Ideal copolymers and the second order transition of synthetic rubbers 1. Non-crystalline co-polymers. J. Appl. Chem. 2, 493 (**1952**).

37. R. Simha and R. F. Boyer, General relation involving the glass transition temperature and coefficient of expansion of polymers. J. Chem. Phys. 37, 1003 (**1962**).

38. K. Tanaka, S. Kitamura and T. Kitagawa, Effect of structural relaxation on the physical and aerosol properties of amorphous form of FK888 (NK1 antagonist). Chem. Pharm. Bull. 53, 498 (**2005**).

39. M. E. Matteucci, B. K. Brettmann, R. O. W. III and K. P. Johnston, Stable Supersaturated Solutions of a Poorly Water Soluble Drug from Amorphous Nanoparticle Dissolution in preparation. J Control Release. To be submitted (**2006**).

40. S. A. Mitchell, T. D. Reynolds and T. P. Dasbach, A compaction process to enhance dissolution of poorly water-soluble drugs using hydroxypropyl methylcellulose. Int. J Pharm. 250, 3 (**2003**).

41. J. M. Vaughn, J. T. McConville, M. T. Crisp, K. P. Johnston and R. O. Williams III, Supersaturation Produces High Bioavailability of Amorphous Danazol Particles Formed by Evaporative Precipitation into Aqueous Solution and Spray Freezing into Liquid Technologies. Drug Dev. Ind. Pharm. 32, 559 (**2006**).

42. J. Hu, K. P. Johnston and R. O. Williams III, Stable amorphous danazol nanostructured powders with rapid dissolution rates produced by spray freezing into liquid. Drug Dev. Ind. Pharm. 30, 695 (**2004**).

CHAPTER 5: Nebulization of Nanoparticulate Amorphous or Crystalline Tacrolimus in Mice

5.1 ABSTRACT

The objectives of this study were to produce nanostructured aggregates of tacrolimus (TAC) intended for pulmonary delivery using ultra-rapid freezing (URF), and to investigate the physicochemical and pharmacokinetic characteristics of the nanostructured aggregates containing amorphous or crystalline nanoparticles of TAC. Two URF formulations were investigated for pulmonary delivery, and compared to bulk unprocessed TAC, these were: TAC and lactose (1:1 ratio; URF-TAC:LAC) and TAC alone (URF-TAC). TAC and water soluble excipient i.e. lactose were dissolved in acetonitrile and water, respectively. Two solutions were mixed to obtain 60:40 ratio of the resulting organic/aqueous co-solvent system which was then frozen on the cryogenic substrate. The cosolvent was then frozen on the URF cryogenic substrate and the frozen compositions were collected and lyophilized to form the dry powder for nebulization. *In vitro* results revealed similar physiochemical properties for both URF formulations. BET analysis showed high surface areas of 29.3 m^2/g and 25.9 m^2/g for the URF-TAC:LAC and URF-TAC, respectively, and 0.53 m^2/g for the unprocessed TAC, respectively. Scanning electron microscopy (SEM)

showed nanostructured aggregates containing nanoparticles of TAC. The dissolution of TAC was 83.6% at 1 hr for the URF-TAC:LAC, compared to 80.5% for the URF-TAC and 30% dissolved for the unprocessed TAC, respectively. Similar aerodynamic particle sizes of 2-3 μm, and fine particle fraction between 70-75% for the URF-TAC:LAC and URF-TAC were determined by cascade impactor data. X-ray diffraction (XRD) results indicated that URF-TAC was crystalline, whereas URF-TAC:LAC was amorphous. The supersaturated dissolution profiles were in agreement with these results. URF-TAC:LAC displayed the ability to supersaturate in the dissolution media to about 11-times crystalline equilibrium solubility. *In vivo* studies were conducted in mice by dispersing the URF formulations in deionized water and nebulizing the dispersed URF formulations using a specially designed nose-only dosing apparatus. The pharmacokinetic profiles obtained showed comparable $AUC_{(0-24)}$, higher C_{max}, and lower T_{max} for the URF-TAC:LAC compared to the URF-TAC . Therefore, rapidly dissolving, pulmonary formulations containing nanostructured aggregates of amorphous or crystalline TAC were developed using the URF technology. The URF processed formulations were demonstrated to be effectively delivered as an aqueous dispersion of TAC nanoparticle via nebulization, with a similar *in vivo* performance by displaying the comparable extent of drug absorption.

5.2 INTRODUCTION

Tacrolimus (TAC) is a widely used immunosuppressive agent isolated from *Streptomyces tsukubaensis*. It has proven to be a potent immunosuppressant in transplantation medicine for treatment of organ rejection and different immunological diseases such as pulmonary fibrosis and bronchiolar asthma [1-3]. TAC was first introduced as rescue therapy when cyclosporin A (CsA) therapy failed to prevent graft rejection. It has a mechanism of action similar to that of CsA, but its immunosuppressive activity is 10- to 100-times more potent than CsA [4,5]. TAC is currently available in both an intravenous and oral dosage form (commercially known as Prograf®). However, these current available dosage forms of the drug are poorly tolerated and provide a variable and/or low bioavailability [6]. The oral formulations of TAC present a considerable challenge as the drugs are practically insoluble in water and extensively metabolized from both CYP3A4 metabolism and p-glycoprotein efflux transport within the intestinal epithelium [7]. The oral bioavailability of TAC varies from 4% to 93% [8]. Inefficient or erratic drug absorption is primarily the result of incomplete absorption from the gastrointestinal tract and first-pass metabolism, which is subject to considerable inter-individual variation [8].

This study focused on investigating a pulmonary drug delivery system based on, nanoparticles of TAC in order to overcome the above mentioned problems to improve bioavailability. The appealing aspects of inhaled drug

nanoparticles include: Rapid dissolution of nanoparticles in the lung and the avoidance of hepatic first pass metabolism (which is especially useful for a drug that undergoes extensive metabolism in liver) [9,11]. Additionally, inhaled nanoparticles can increase local drug concentrations in the lung for potential therapeutic use in lung transplantation and pulmonary diseases. The treatment of lung transplant recipients is often limited due to poor penetration of drug into the lung following oral or intravenous administration [12]. Aerosolized drug will have direct access to the graft in lung transplant offering the possibility of much higher drug levels [13]. However, a major disadvantage of pulmonary delivery for drugs like TAC is limitations in the levels and types of excipients that are considered safe to use in pulmonary formulations. Although many surfactants or polymers such as cyclodextrins, poloxamers, polyethylene glycols (PEG) and glycerol have been studied in pulmonary formulations to aid drug solubilization in many research studies [14-16], these excipients have not been approved yet for commercial use by the FDA because of potential toxicity in the lung. Several clinical studies have demonstrated effective pulmonary delivery of CsA solutions in ethanol or propylene glycol prior to aerosolization in lung transplantation models [17-19]. However, the solvents have produced the results have shown unsatisfactory due to the irritating properties of these solventsation to the airways. In addition, the use of high levels of ethanol or propylene glycol in formulations intended for pulmonary delivery have yet to be widely studied in humans.

Recently, liposome technology has been investigated as a non-irritating alternative for pulmonary delivery of CsA, but the formulation had low drug loading and thus requires a lengthy nebulization period [20].

In this present study, pulmonary formulations containing TAC manufactured by ultra-rapid freezing (URF), without the inclusion of surfactants or polymeric excipients, were investigated. URF technology is a continuous, scalable cryogenic process produces nanostructured aggregates with high surface area resulting in high enhanced drug dissolution rates. Previously, spray freezing into liquid (SFL) was reported [21-26]. The rapid freezing rates achieved with the SFL process led to the production of amorphous nanostructured aggregates composed of primary particles, ranging from 100 to 200 nm, with high surface areas, high wettability and significantly enhanced dissolution rates. The URF process yields particles with similar properties as those produced by SFL. In URF a solution of the active and excipient in a suitable organic solvent or aqueous co-solvent is applied to the surface of a cryogenic solid substrate. The is frozen instantaneously, in 50 ms to 1s, onto the surface of cryogenic solid substrate in a continuous manner [27,28]. URF powders exhibit desirable properties for enhancing bioavailability such as high surface area, increased drug dissolution rates, and amorphous character.

The objective of this study was to demonstrate that nanostructured aggregates composed of amorphous or crystalline primary nanoparticles of TAC

produced by the URF process are suitable for pulmonary delivery by nebulization, resulting in high lung and blood concentrations. The hypothesis is that high surface area and rapid dissolution rate obtained from nanostructured aggregates of TAC promote high systemic drug absorption via the lung, whilst still maintaining a desirable pulmonary residence time for potential local therapy. Relevant physicochemical properties (e.g. surface area, dissolution, crystallinity) of TAC nanostructured aggregates were characterized in order to understand how they influence *in vivo* drug absorption following single-dose nebulization of the particle dispersions.

5.3 MATERIALS AND METHODS

5.3.1 Materials

TAC was kindly provided by The Dow Chemical Company (Midland, MI). Lactose, magnesium chloride hexahydrate, sodium chloride, potassium chloride, sodium phosphate dibasic anhydrous, sodium sulphate anhydrous, calcium chloride dihydrate, sodium acetate trihydrate, sodium bicarbonate and sodium citrate dihydrate were analytical grade and purchased from Spectrum Chemicals (Gardena, CA). Dipalmitoylphosphatidylcholine (DPPC) was purchased from Sigma-Aldrich Chemicals (Milwaukee, WI). High performance liquid chromatography (HPLC) grade acetonitrile (ACN) was purchased from EM

Industries, Inc. (Gibbstown, NJ). Liquid nitrogen was obtained from Boc Gases (Murray Hill, NJ). Deionized water was prepared by a Milli-Q purification system from Millipore (Molsheim, France).

5.3.2 Preparation of URF Formulations

TAC formulations were processed using URF. A schematic diagram of the URF process is illustrated in Figure 5.1. Two URF formulations considered for pulmonary delivery were TAC:lactose in a 1:1 ratio (URF-TAC:LAC) and TAC alone (URF-TAC). The compositions were prepared by dissolving TAC and hydrophilic excipient (if any) at a 1:1 ratio and 0.75% solids in a 60/40 mixture of acetonitrile and water. The solution of drug was applied to the surface of solid substrate, which is cooled using a cryogenic substrate maintained at -50^{o}C. The frozen compositions were then collected and the solvent was removed by lyophilization using VirTis Advantage Tray Lyophilizer (VirTis Company Inc., Gardiner, NY). The lyophilization recipes used in this study is outlined in Appendix A. The dried powders were stored at room temperature under vacuum.

5.3.3 *In Vitro* Characterization of Powders for Pulmonary

5.3.3.1 X-ray Powder Diffraction (XRD)

The XRD patterns of the powders were analyzed using a Philips 1710 x-ray diffractometer with a copper target and nickel filter (Philips Electronic Instruments, Inc., Mahwah, NJ). Each sample was measured from 5 to 45 2θ degrees using a step size of 0.05 2θ degrees and a dwell time of one second.

5.3.3.2 BET Specific Surface Area Analysis

Specific surface area was measured using a Nova 2000 v.6.11 instrument (Quantachrome Instruments, Boynton Beach, FL). A known weight of powder was added to a 12 mm Quantachrome bulb sample cell and degassed for a minimum of three hours. The data recorded were then analyzed according to BET theory using NOVA Enhanced Data Reduction Software v. 2.13.

5.3.3.3 Scanning Electron Microscopy (SEM)

A Hitachi S-4500 field emission scanning electron microscope (Hitachi High-Technologies Corp., Tokyo, Japan) was used to obtain SEM micrographs of the powder samples. Samples were mounted on conductive tape and sputter coated using a model K575 sputter coater (Emitech Products, Inc., Houston, TX, USA) with gold/palladium for 30 s. An accelerating voltage of 5-15 kV was used to view the images.

5.3.3.4 Dissolution Testing at Below Equilibrium Solubility

Dissolution testing at below equilibrium solubility was performed on the URF powder samples using a United States Pharmacopeia (USP) 27 Type 2 dissolution apparatus (VanKel VK6010 Dissolution Tester with a Vanderkamp VK650A heater/circulator, Varian, Inc. Palo Alto, CA). Powder samples (0.4 mg of TAC) equivalent to approximately 59% of the equilibrium solubility (6.8 μg/mL) were added to 100 mL of modified simulated lung fluids (SLF) with 0.02 % DPPC as dissolution media [29]. The dissolution media was maintained at 37.0 ± 0.2°C and stirred at a constant rate of 50 rpm. Samples (1 mL) were withdrawn at 10, 20, 30, 60 and 120 minute time points, filtered using a 0.45 μm GHP Acrodisc filter (VWR, Inc., West Chester, PA) and analyzed using a Shimadzu LC-10 liquid chromatograph (Shimadzu Corporation, Kyoto, Japan) equipped with an Alltech ODS-2, 5 μm C_{18} column (Alltech Associates, Inc., Deerfield, IL). The mobile phase consisted of a 70:30 (v/v) ACN: Water mixture, used at a flow rate of 1 mL/min. The maximum absorbance was measured at wavelength λ_{max}= 214 nm.

5.3.3.5 Dissolution Behavior in the Formation of Supersaturated Solutions

Supersaturated dissolution profiles were generated according to the method described above (Section 5.3.3.4) except using the small volume dissolution apparatus equipped with a paddle stirring mechanism. Each drug

formulation was weighed out which corresponded to approximately 15-times the aqueous crystalline solubility of TAC in 100 mL of the modified simulated lung fluid with 0.02% DPPC. Paddle speed and bath temperature were maintained at 100 rpm and 37^{o}C, respectively. An aliquot (1 mL) were removed from the small volume dissolution vessel at 10, 20, 30 and 60 minutes, then at 2, 4 and 24 hours. Each aliquot was filtered through a 0.2 μm nylon filter, and a 0.5 mL aliquot of each filtered solution was immediately mixed with 1 mL of acetonitrile (to ensure no re-crystallization of drug previously dissolved at 37°C). The samples were analyzed for TAC concentration using the same HPLC procedure described above (Section 5.3.3.4). All experiments were performed in triplicate.

5.3.3.6 In Vitro Aerosol Performance

The *in vitro* deposition characteristics of the dispersed and nebulized TAC formulations were investigated using a non-viable 8-stage cascade impactor (Thermo-Electron Corp., Symrna, GA, USA). The aerosolization behavior was described in terms of total emitted dose (TED), fine particle fractions (FPFs), mass median aerodynamic diameters (MMAD) and geometric standard deviation (GSD). The cascade impactor was assembled and operated in accordance with USP method 601 to assess the drug delivered. The powders were dispersed in water (10 mg/mL) and nebulized using an Aeroneb® Pro micropump nebulizer (Nektar Inc., San Carlos, CA) for 10 minutes at an air flow rate of 28.3 L/min.

The flow rate was maintained by a vacuum pump (Emerson Electric Co., St. Louis, MO, USA) and calibrated by a TSI mass flow meter (Model 4000, TSI Inc., St. Paul, MN, USA). The mass deposited on each of the stages was collected and analyzed by HPLC as in Section 5.3.3.4. Each experiment was repeated in triplicate.

5.3.4 *In Vivo* Mouse Studies

5.3.4.1 Pulmonary Administration of URF Formulations

Pulmonary dosing of URF formulations was performed in healthy male ICR mice (Harlan Sprague Dawley, Inc., Indianapolis, IN). The study protocol was approved by the Institutional Animal Care and Use Committee (IACUCs) at the University of Texas at Austin, and all animals were maintained in accordance with the American Association for Accreditation of Laboratory Animal Care. Mice were acclimated and pre-conditioned in the restraint tube (Battelle, Inc.,Columbus, OH) for 10–15 min./day for at least 2 days prior to dosing. Proper pre-conditioning is essential for reducing stress to mice, and maintaining a uniform respiration rate for the animals. A small animal dosing apparatus for inhalation was used to dose the mice for this study. The dosing apparatus was designed to hold up to 4 mice as shown schematically in Figure 5.2. The dosing apparatus consists of a small volume hollow tube with dimensions of 20 x 4.5 cm (nominal wall thickness of 0.4 cm) with four 1.75 cm adapter holes drilled at 7 cm

intervals (2 holes along each side). The adapter holes were constructed to accept rodent restraint tubes from the Battelle toxicology testing unit (Figure 5.3).

The URF processed powders were re-dispersed in water (10 mg/mL) followed by sonication for 1 min. prior to dosing. Nebulization of 3 mL of dispersions was conducted using an Aeroneb Pro ultrasonic nebulizer for 10 min. dosing period. After pulmonary dosing, the mice were removed from the dosing apparatus and rested for 15 min. Two mice were sacrificed at each time point by CO_2 narcosis (0.5, 1, 2, 3, 6, 12, 24 and 48 hours). Whole blood (1-mL aliquots) was obtained via cardiac puncture and analyzed according to the standard ELISA procedure outlined in Section 5.3.4.2. In addition, necropsy was performed on each mouse to extract lung tissue. Samples were stored at −20 C until assayed. TAC concentrations in lung tissue were determined using a previously HPLC assay as described in Section 5.3.3.4.

5.3.4.2 Enzyme-Linked Immunosorbent Assay (ELISA) for Analysis of TAC Concentrations in Blood

The determination of TAC in whole blood was performed using the PRO-Trac™ II FK 506 ELISA assay kit (Diasorin Inc., Stillwater, USA) in accordance with the manufacturer's instructions. Specifically, 50 μL of whole blood sample or standards were placed into a conical 1.5 mL polypropylene tube. Digestion reagent was freshly reconstituted, and 300 μL was added to all tubes. The tubes

were vortexed for 30 seconds and incubated at room temperature for 15 min. These tubes was then placed on an aluminum heating block circulated with 75°C water bath for 15 min to stop proteolysis. After vortexing, the tubes were centrifuged at room temperature at 1,800 x*g* for 10 min. The supernatant (100 µL) was transferred to microtiter plate wells in duplicate from each centrifuged tube. Capture monoclonal anti-FK506 (50 µL) was added to the each well, and the plate was shaken at room temperature at 700 rpm for 30 min. TAC horseradish peroxidase conjugate (50µL) was then added to each well, and the plate was shaken at room temperature at 700 rpm for an additional 60 min. The plate was washed, before the addition of 200 µL chromogen. The plate was then shaken at 700 rpm for a further 15 min at room temperature. The subsequent reaction in each plate well was terminated by the addition of 100 µL of stop solution. The absorbance in each well was read at the dual wavelengths of 450 and 630 nm. Data was plotted according to a four-parameter logistic (4PL) curve-fitting program.

5.3.4.3 Solid Phase Extraction and Drug Analysis of Lung Tissues using HPLC

Lung extraction was carried out using solid phase extraction to obtain TAC levels using reverse phase HPLC. The total lung weight was recorded individually from each mouse. Lung tissues were homogenized using a Polytron rotor-stator homogenizer (VWR Scientific Corporation, West Chester, PA) for 40

seconds in 1 mL of normal saline. The homogenized lung samples were then mixed with 0.5 mL solution of 0.4 N zinc sulfate heptahydrate in the mixture of methanol/water (70:30) solution and vortex mixed for 30 seconds. Acetonitrile (1 mL) was added to the homogenized samples before a further vortex mixing for 1.5 minutes, followed by centrifugation at 3000 rpm for 15 minutes to obtain a clear supernatant. Next, the supernatant was collected into a clean vial containing 1 mL purified water. Meanwhile C18 cartridges for solid phase extraction (Supelco Inc., Bellefonte, PA) were preconditioned. First, these columns were pretreated with 2 mL of acetonitrile, followed by 1 mL methanol and then washed with 1 mL of water before loading the supernatant through the column. The sample was transferred and drawn slowly through the column by reducing the vacuum. The column was washed again by passing 1.5 mL mixture of methanol/water (70:30) solution, followed by 0.5 mL of n-hexane and allowed it to dry under vacuum. The sample was finally eluted with 2 mL of acetonitrile (0.5 mL x 4). The eluted material was evaporated under a dry nitrogen stream and then reconstituted with 250 μL of mobile phase using the previously described HPLC assay (Section 5.3.3.4). Data was expressed as μg TAC/gram wet lung tissue analyzed.

5.3.4.4 Pharmacokinetics and Statistical Analysis

The lung tissue concentration vs. time was investigated using a non-compartmental model, while the whole blood concentration vs. time was evaluated using one-compartmental analysis from extravascular administration (via the lung compartment). Pharmacokinetic parameters were calculated using using WinNonlin version 4.1 (Pharsight Corporation, Mountain View, CA). The pharmacokinetic profile of TAC was characterized by maximum concentration (C_{max}), time to C_{max} (T_{max}), half-life ($T_{1/2}$) and area-under-the-curve (AUC) between 0-24 hours. AUC was calculated using the trapezoidal rule; C_{max} and T_{max} were determined from the concentration-time profiles; $T_{1/2}$ was calculated by using the elimination rate constant (K_{el}); K_{el} was obtained from the ln concentration-time profiles.

The data sets were compared using a Student's t-test of the two samples assuming equal variances to evaluate the differences. The significance level ($\alpha = 0.05$) was based on the 95% probability value ($p < 0.05$).

5.4 RESULTS AND DISCUSSION

5.4.1 *In vitro* characterization of URF formulations

The physicochemical properties of TAC powders produced by URF were investigated and compared to the unprocessed TAC. The XRD patterns of the URF formulations and unprocessed TAC are shown in Figure 5.4. The

diffractogram of URF-TAC was similar to that of unprocessed TAC, indicating a high degree of crystallinity. However, the XRD pattern of URF-TAC:LAC confirmed that this composition was amorphous. This suggests that lactose inhibited crystallization of TAC. It is well known that sugars such as lactose can be used to stabilize amorphous drugs, peptides and proteins during drying and subsequent storage [30,31]. The addition of sugars has been shown to extend the shelf life of amorphous systems by preventing crystallization. In addition, lactose is generally regarded as safe (GRAS) for use as an excipient in inhalation systems [32]. This is due to its non-toxic and degradable properties after administration [33].

SEM micrographs of the two URF processed formulations are shown in Figure 5.5 reveal distinct differences in morphology. The morphology of URF-TAC:LAC (Figure 5.5a-5.5b) showed highly porous, nanostructured aggregates. The micrograph at high magnification in Figure 5.5b revealed that the aggregates were composed of branched interconnected nanorods with a diameter of approximately 100-200 nm. URF-TAC (Figure 5.5c-5.5d) appeared as more dense aggregates composed of submicron primary particles. In contrast, the SEM micrograph of unprocessed TAC indicated an irregular, dense and large crystal plate measuring between 50-100 μm in size (Figure 5.5e). Accordingly, the surface areas obtained by the URF processed formulations (URF-TAC:LAC and URF-TAC was 25.9 and 29.3 m^2/g, respectively) were significantly higher than

($p < 0.05$) that of the unprocessed drug (0.53 m^2/g). This result is corroborated by the porous nanostructured aggregates of the URF powders observed by SEM.

The *in vitro* aerosol performance measured by cascade impaction for aqueous dispersions prepared from the URF processed powders are presented in Table 5.1. Comparison of the data suggests similar aerodynamic properties of the drug particles aerosolized from the two URF formulations. The MMAD was 2.86 and 2.57 μm for URF-TAC:LAC and URF-TAC, respectively, and the GSD was less than 2.2 (Table 5.1). It can be concluded that the aerosol droplets contain aggregates of nanoparticles that are in the respirable range by nebulization. Aerodynamic particle size is the most important parameter in determining drug deposition in the lungs and must be considered when developing formulations for pulmonary delivery [34]. Aerosolized particles or droplets with a MMAD ranging from 1 to 5 μm are suitable for deep lung deposition, at the site of the alveoli, where maximum absorption may take place [35]. The optimal aerosolization properties of both URF formulations are also reflected in the high %FPF ranging from 70% to 75%, illustrating efficient lung delivery of drug particles. The TED was only slightly higher for URF-TAC:LAC (5082 μg) compared to that of URF-TAC (4823 μg). These values were not significantly different ($p > 0.05$).

The in vitro dissolution profiles of TAC in SLF media under sink conditions are shown in Figure 5.6. The dissolution rates for both URF processed

powders were significantly increased ($p<0.05$) as compared to the unprocessed TAC. Nanostructured aggregates of the URF processed powders were able to wet and dissolve quickly upon contact in SLF containing 0.02% DPPC, although the formulations contained no surfactant. For URF-TAC:LAC (i.e., amorphous, nanostructured aggregates), the dissolution of TAC was 72% in 30 minutes, compared to 67% for the URF-TAC (i.e., crystalline nanostructured aggregates) and 30% for the unprocessed TAC, respectively. The enhancement is most likely attributed to the high porosity and enhanced surface area of URF processed powders.

Dissolution of TAC at supersaturated conditions was also conducted in the same media. Supersaturated dissolution profiles of the URF processed formulations containing about 15-times the equilibrium solubility of TAC are compared in Figure 5.7. The concentration obtained for the URF-TAC:LAC exceeded the equilibrium solubility of TAC, corresponding to a high degree of supersaturation in the SLF containing DPPC without the presence of surfactants or polymers in the formulation. The level of supersaturation corresponded to about 11-times the equilibrium solubility. This was due to the high-energy phase of the amorphous TAC particles. The maximum concentration occurred at 1 hour, and then decreased to 3-times equilibrium solubility over the next 4 hours. A supersaturation dissolution profile was not observed for URF-TAC because of its crystalline nature.

5.4.2 *In Vivo* Pulmonary Studies

The pharmacokinetic absorption studies were conducted in mice. The murine model has been very effective for small scale inhalation studies [36]. The lung tissue concentration-time profiles following a single inhalation dose are shown in Figure 5.8 while the corresponding pharmacokinetic parameters summarized in Table 5.2. C_{max} for URF-TAC:LAC was significantly higher (14.09 μg/g) compared to URF-TAC (10.86 μg/g) whereas T_{max} was significantly lower ($p< 0.05$) for 2 hours. This could perhaps as a result of a greater dissolved concentration, as seen in the vitro supersaturation results. However, no significant differences in AUC-values (0-24 hr) were observed between the two URF formulations ($p>0.05$). The results indicated that the amorphous nature of the particles affects the rate of drug absorption. TAC in the URF-TAC:LAC was eliminated according to a biphasic pattern with distribution phase and elimination phase. The similar elimination pattern was also found in the URF-TAC The values of K_{el} were not significantly different between the two URF-formulations ($p > 0.05$). The decreasing TAC concentration in the lung for both URF formulations is a consequence of drug distribution and transport into the systemic circulation, as well as particle elimination from the lung. It can be seen clearly that the transfer of nanostructured aggregates (either amorphous or crystalline) from the lung into systemic circulation was likely in a sustained manner after 6 hr.

The measured levels for both URF formulations at 48 hours were below the limit of quantification of the assay (determined to be1 μg/g).

The systemic in vivo pharmacokinetic of drug absorption from the lungs was investigated in mice. Figure 5.9 shows a comparison of mean whole blood concentration-time profiles from each formulation, and the calculated pharmacokinetic parameters following pulmonary administration are presented in Table 5.3. The whole blood concentration profile of each formulation has a similar absorption pattern, for example, T_{max}, compared to the lung concentration profiles (Figure 5.8). However, both URF formulations demonstrated substantially lower TAC concentrations in the blood than was seen in the lung tissue. The whole blood profiles following pulmonary dosing of URF-TAC:LAC and URF-TAC had peak concentrations of 402.11 ng/mL at 2 hr and 300.67 ng/mL at 3 hr, respectively, before concentrations decreased. The $AUC_{(0-24)}$ (1235.66 ng.hr/mL) of the URF-TAC:LAC processed by URF is slightly lower than that of the URF-TAC (1324.35 ng.hr/mL), although there is no statistical difference ($p>0.05$). The levels of TAC decreased rapidly for URF-TAC:LAC with the last time point with a detectable levels occurring at 24 h, while URF-TAC declined in a similar but slower manner (no significant difference in the K_{el} values ($p > 0.05$)). Whole blood concentrations of TAC were below the limit of quantification for both formulations at 48 hours. The systemic and lung concentrations observed after nebulization of both URF formulations in mice

suggest that a substantial lung and systemic exposure to TAC can be achieved in either amorphous nanostructed aggregates or crystalline nanostructed aggregates produced by URF. The observation that either amorphous or crystalline particles produced high systemic concentrations may suggest that high surface area was an important factor. High supersaturation, as a result of delivering amorphous particles in URF-TAC:LAC, correlated with faster absorption rates in both blood and lung tissue as compared to crystalline particles in URF-TAC . Use of supersaturated state in the lungs has not been previously studied yet. However, it has been demonstrated to enhance transdermal and oral absorption of poorly soluble drugs [37-39]. The in vivo data reported by Yamashita et al. [37] showed a high and extended systemic absorption of TAC following oral administration of amorphous solid dispersions with HPMC in beagle dogs. In the Yamashita et al. study, the solid dispersion of TAC with HPMC was prepared by solvent evaporation and was also shown to supersaturate in 0.1N HCl up to 25-times in 2 hours, and this level was maintained for over 24 hours. In our study, supersaturation of TAC from URF-TAC:LAC showed no effect on the extent of drug absorption in both lung tissue and systemic circulation. This can be explained by the fact that supersaturation occurred over a short period of time for the absorption phase and then TAC concentration was rapidly decreased in the elimination phase.

5.5 CONCLUSIONS

High surface area, nanostructured aggregates containing amorphous or crystalline nanoparticles of TAC were produced by the URF process and shown to be effectively aerosolized in an aqueous dispersion by nebulization. Inclusion of lactose prevented crystallization of TAC and resulted in amorphous powder. URF-TAC:LAC (i.e., amorphous nanostructured aggregates) demonstrated the ability to supersaturate in SLF compared to the URF-TAC (i.e., crystalline nanostructured aggregates). Dispersions of nebulized URF formulations exhibited high lung and systemic concentrations. The $AUC_{(0-24)}$ of the URF formulations which reflects the total amount of drug absorbed over the 24 h time period was not significantly different ($p > 0.05$) for either lung or blood profiles. The results indicate that high drug absorption in lung tissue and blood following pulmonary administration was primarily due to high surface area of nanostructured aggregates from both formulations. The ability to achieve high solubility in the lungs translated to higher C_{max} and lower T_{max} values based on results of the *in vivo* studies. We have demonstrated that nanoparticles of TAC can be successfully delivered to the lungs without the use of polymers or surfactants.

5.6 ACKNOWLEDGMENTS

The authors wish to gratefully acknowledge partial financial support from The Dow Chemical Company for its financial support.

5.7 REFERENCES

1. Hooks, M. A. (1994) Tacrolimus, A New Immunosuppressant - A review of the literature. Ann. Pharmacother. . **28**, 501-511.
2. Waldrep, J. C. (1998) New aerosol drug delivery systems for the treatment of immune-mediated pulmonary diseases. Drugs of Today **34**, 549-561.
3. Loser, K., Balkow, S., Higuchi, T., Apelt, J., Kuhn, A., Luger, T. A., and Beissert, S. (2006) FK506 Controls CD40L-Induced Systemic Autoimmunity in Mice**126**, 1307-1315.
4. Tacca, M. D. (2004) Prospects for personalized immunosuppression: pharmacologic tools--a review. Transplant. Proc. **36**, 687-689.
5. Jain, A. B., and Fung, J. J. (1996) Cyclosporin and tacrolimus in clinical transplantation - A comparative review. Clinical Immunotherapeutics **5**, 351-373.
6. Tamura, S., Tokunaga, Y., Ibuki, R., Amidon, G. L., Sezaki, H., and Yamashita, S. (2003) The Site-Specific Transport and Metabolism of Tacrolimus in Rat Small Intestine. J Pharmacol Exp Ther **306**, 310-316.

7. Venkataramanan R, J. A., Warty VW, et al. (1991) Pharmacokinetics of FK506 following oral administration: a comparison of FK506 and cyclosporine. Transplant. Proc. **23**, 931-933.
8. Venkataramanan, R., Swaminathan, A., Prasad, T., Jain, A., Zuckerman, S., Warty, V., McMichael, J., Lever, J., Burckart, G., and Starzl, T. (1995) Clinical pharmacokinetics of tacrolimus. Clin. Pharmacokinet. **29**, 404-430.
9. Kawashima, Y. (2001) Nanoparticulate systems for improved drug delivery. Adv. Drug Deliv. Rev. **47**, 1-2.
10. Grenha, A., Seijo, B., and Remunan-Lopez, C. (2005) Microencapsulated chitosan nanoparticles for lung protein delivery. Eur. J. Pharm. Sci. **25**, 427-437.
11. Taylor, K. M. G., and McCallion, O. N. M. (1997) Ultrasonic nebulisers for pulmonary drug delivery. Int. J Pharm. **153**, 93-104.
12. Martinet, Y., Pinkston, P., Saltini, C., Spurzem, J., Muller-Quernheim, J., and Crystal, R. G. (1988) Evaluation of the in vitro and in vivo effects of cyclosporine on the lung T-lymphocyte alveolitis of active pulmonary sarcoidosis. Am. Rev. Respir. Dis. **138**, 1242-1248.
13. McConville, J. T., Overhoff, K. A., Sinswat, P., Vaughn, J. M., Frei, B. L., Burgess, D. S., Talbert, R. L., Peters, J. I., Johnston, K. P., and Williams, R. O. (2006) Targeted high lung concentrations of itraconazole using

nebulized dispersions in a murine model. Pharmaceutical Research **23**, 901-911.

14. Steckel, H., Eskandar, F., and Witthohn, K. (2003) The effect of formulation variables on the stability of nebulized aviscumine. Int. J Pharm. **257**, 181-194.
15. Fu, J., Fiegel, J., Krauland, E., and Hanes, J. (2002) New polymeric carriers for controlled drug delivery following inhalation or injection. Biomaterials **23**, 4425-4433.
16. Brambilla, G., Ganderton, D., Garzia, R., Lewis, D., Meakin, B., and Ventura, P. (1999) Modulation of aerosol clouds produced by pressurised inhalation aerosols. Int. J Pharm.**186**, 53-61.
17. Keenan, R. J., Zeevi, A., Iacono, A. T., Spichty, K. J., Cai, J. Z., Yousem, S. A., Ohori, P., Paradis, I. L., Kawai, A., and Griffith, B. P. (1995) Efficacy of inhaled cyclosporine in lung transplant patients with refractory rejection: correlation of intragraft cytokine gene expression with pulmonary function and histologic characteristics. Surgery **118**, 385–392.
18. Keenan, R. J., Duncan, A. J., Yousem, S. A., Zenati, M., Schaper, M., Dowling, R. D., Alarie, Y., Burckart, G. J., and Griffith, B. P. (1992) Improved immunosuppression with aerosolized cyclosporine in experimental pulmonary transplantation. Transplantation **53**, 20-25.

19. Blot, F., Tavakoli, R., Sellam, S., Epardeau, B., Faurisson, F., Bernard, N., Becquemin, M.-H., Frachon, I., Stern, M., Pocidalo, J.-J., Carbon, C., Bisson, A., and Caubarrere, I. (1995) Nebulized cyclosporine for prevention of acute pulmonary allograft rejection in the rat: Pharmacokinetic and histologic study. J. Heart Lung Transplant. **14**, 1162-1172.
20. Waldrep, J. C., Arppe, J., Jansa, K. A., and Vidgren, M. (1998) Experimental pulmonary delivery of cyclosporin A by liposome aerosol. Int. J Pharm. **160**, 239-249.
21. Rogers TL, Nelsen AC, Hu J, Johnston KP, Williams III RO. (2002) A novel particle engineering technology to enhance dissolution of poorly water soluble drugs: spray-freezing into liquid. Eur. J. Pharm. Biopharm. **54:** 271-280.
22. Rogers TL, Hu J, Yu Z, Johnston KP, Williams III RO. (2002) A novel particle engineering technology: spray-freezing into liquid. Int. J Pharm. **242:** 93-100.
23. Rogers TL, Nelsen AC, Sarkari M, Young TJ, Johnston KP, Williams III RO. (2003) Enhanced aqueous dissolution of a poorly water soluble drug by novel particle engineering technology: Spray-freezing into liquid with atmospheric freeze-drying. Pharm. Res.**20:** 485-493.

24. Rogers TL, Overhoff KA, Shah P, Johnston KP, Williams III RO. (2003) Micronized powders of a poorly water soluble drug produced by a spray-freezing into liquid-emulsion process. Eur. J. Pharm. Biopharm. **55:** 161-172.

25. Hu, J., Johnston, K. P., Williams III, R. O. (2004) Stable amorphous danazol nanostructured powders with rapid dissolution rates produced by spray freezing into liquid. Drug Dev. Ind. Pharm. **30**: 695-704.

26. Yu Z, Rogers TL, Hu J, Johnston KP, Williams III RO. (2002) Preparation and characterization of microparticles containing peptide produced by a novel process: spray freezing into liquid. Eur. J. Pharm. Biopharm. **54:** 221-228.

27. Evans, J. C., Scherzer, B. D., Tocco, C. D., Kupperblatt, G. B., Becker, J. N., Wilson, D. L., Saghir, S., and Elder, E. J.: Preparation of nanostructured particles of poorly water soluble drugs via a novel ultrarapid freezing technology. *In* Polymeric Drug Delivery Ii: Polymeric Matrices and Drug Particle Engineering, vol. 924, pp. 320-328, 2006.

28. Overhoff, K. A., Engstrom, J. D., Chen, B., Scherzer, B. D., Milner, T. E., Johnston, K. P., and III, R. O. W. Novel Ultra-rapid Freezing Particle Engineering Process for Enhancement of Dissolution Rates of Poorly Water Soluble Drugs. in press. 2006.

29. Davies, N. M., and Feddah, M. R. (2003) A novel method for assessing dissolution of aerosol inhaler products. Int. J Pharm. **255**, 175-187.
30. D.J. Van Drooge, W. L. J. H., H.W. Frijlink,. (2004) Incorporation of lipophilic drugs in sugar glasses by lyophilization using a mixture of water and tertiary butyl alcohol as solvent. J Pharm. Sci. **93**, 713-725.
31. Eriksson, J. H. C., Hinrichs, W. L. J., de Jong, G. J., Somsen, G. W., and Frijlink, H. W. (2003) Investigations into the Stabilization of Drugs by Sugar Glasses: III. The Influence of Various High-pH Buffers. Pharm. Res. **20**, 1437-1443.
32. Bosquillon, C., Lombry, C., Preat, V., and Vanbever, R. (2001) Influence of formulation excipients and physical characteristics of inhalation dry powders on their aerosolization performance. J. Control. Release **70**, 329-339.
33. Wierik, H., and Diepenmaat, P. (2002) Formulation of lactose for inhaled delivery systems. Pharm. Tech. Eur. **11**, 1–5.
34. de Boer, A. H., Gjaltema, D., Hagedoorn, P., and Frijlink, H. W. (2002) Characterization of inhalation aerosols: a critical evaluation of cascade impactor analysis and laser diffraction technique. Int. J Pharm. **249**, 219-231.
35. Zeng, X. M., Martin, G. P., and Marriott, C. (1995) The controlled delivery of drugs to the lung. Int. J Pharm. **124**, 149-164.

36. Miller, F. J., Mercer, R. R., and Crapo, J. D. (1993) Lower Respiratory-Tract Structure of Laboratory-Animals and Humans - Dosimetry Implications. Aerosol Sci. Tech. **18**, 257-271.

37. Yamashita, K., Nakate, T., Okimoto, K., Ohike, A., Tokunaga, Y., Ibuki, R., Higaki, K., and Kimura, T. (2003) Establishment of new preparation method for solid dispersion formulation of tacrolimus. Int. J Pharm. **267**, 79-91.

38. Gao, P., Guyton, M. E., Huang, T., Bauer, J. M., Stefanski, K. J., and Lu, Q. (2004) Enhanced Oral Bioavailability of a Poorly Water Soluble Drug PNU-91325 by Supersaturatable Formulations. Drug Dev. Ind. Pharm. **30**, 221-229.

39. Iervolino, M., Cappello, B., Raghavan, S. L., and Hadgraft, J. (2001) Penetration enhancement of ibuprofen from supersaturated solutions through human skin. Int. J Pharm. **212**, 131-141.

Table 1.1: Potential R&D targets by 2015 for U.S. National Nanotechnology Initiative. Reprinted with permission from G. A. Hughes, Dis. Mon. 51, 342, 2005, Copyright Elsevier (2005).

Nanoscale visualization and simulation of 3-dimensional domains
Transistor beyond/integrated CMOS <10 nm
New catalysts for chemical manufacturing
No suffering and death from cancer when treated
Control of nanoparticles in air, soils, and waters
Advanced materials and manufacturing: one-half from molecular level
Pharmaceuticals synthesis and delivery: one-half on nanoscale level
Converging technologies from nanoscale
Life-cycle biocompatible/sustainable development
Education: nanoscale instead of microscale based

Table 1.2: Examples of different nanoparticles and their applications. Reprinted with permission from G. Orive et al., Trends Pharmacol. Sci. 25, 382, 2004, Copyright Elsevier (2004).

Nanoparticle	Description	Recent applications
Dendrimers	Macromolecular compound that comprises a series of branches around an inner core	Rapid and complete release of paclitaxel (used in the treatment of cancer) from dendrimers; dendrimer degradation products are not cytotoxic
Liposomes	Artificial spherical vesicles produced from natural phospholipids and cholesterol	Liposomal doxorubicin has been employed successfully in the treatment of recurrent uterine adenosarcoma in mice
Ceramic nanoparticles	Nanoparticles made using inorganic compounds such as silica and titania	Ultra-fine silica-based nanoparticles that release water-insoluble anticancer drugs
Nanocapsules	Vesicular systems in which the drug is surrounded by a polymeric membrane	Artificial red blood cell nanocapsules with PEG–PLA membrane; circulation half-life of blood cells is doubled
Micelles	Amphiphilic block copolymers that can self-associate in aqueous solution	PCL–PEO block copolymer micelles that could selectively deliver drugs to specified subcellular targets
Hybrid nanodevices	Hybrid nanoparticles covalently bond to oligonucleotide DNA	TiO_2 nanoparticles with the ability to target, bind and cleave DNA
Nanospheres	Matrix systems in which the drug is physically and uniformly dispersed	Uptake of PLGA nanospheres by human dendritic cells *in vitro*; has implications for the selective activation of the T-cell-mediated immune response

Table 2.1: Adsorption ($W_{surf,ads}$ /$W_{drug,ppt}$) of stabilizers onto ITZ particle surface after EPAS process at 80^{o}C. Drug: organic stabilizer: aqueous stabilizer (0.75:0.1:1) (w/w) at final concentration of 15 mg/ml of ITZ in the aqueous EPAS dispersion.

Aqueous excipients	Organic excipients	$W_{surf,ads}$ /$W_{drug,ppt}$ (w/w, %)
-	-	-
Polysorbate 80	Poloxamer 407	10.72 ± 0.14
PVP K-15	PVP K-15	5.38 ± 0.14
Poloxamer 407	Poloxamer 407	6.46 ± 0.36
Polysorbate 80	PVP K-15	5.86 ± 0.83
PVP K-15	Poloxamer 407	5.70 ± 0.73

Table 2.2: Characterization of ITZ powders. Drug: organic stabilizer: aqueous stabilizer (0.75:0.1:1) (w/w/w) at final concentration of 15 mg/ml of ITZ in the aqueous EPAS dispersion. All dispersions were centrifuged and dried by lyophilization.

Aqueous excipients	Organic excipients	Potency of ITZ (%)	Drug: stabilizer ratio	Surface area (m^2/g)	Contact angle (^{o})
Bulk powder		/	/	4.22 ± 0.10	61.6 ± 0.54
Physical Mixture					
Polysorbate 80	Poloxamer 407			3.09 ± 0.27	52.3 ± 0.85
Polysorbate 80	Poloxamer 407	90.5	9.5	3.25 ± 0.22	30.3 ± 0.66
PVP K-15	PVP K-15	90.3	9.3	5.77 ± 0.33	43.5 ± 0.47
Poloxamer 407	Poloxamer 407	93.8	15.1	6.31 ± 0.61	35.1 ± 0.63
Polysorbate 80	PVP K-15	93.1	13.5	3.33 ± 0.21	32.7 ±0.79
PVP K-15	Poloxamer 407	91.4	10.6	5.87 ± 0.38	42.8 ± 0.84

/ not measured; * provided by manufacturer

Table 3.1: Different EPAS formulations of ITZ and their compositions.

Formulation no.	Aqueous stabilizer (%w/v)	organic stabilizer (%w/v)	Drug: stabilizer Raio (w/w)
E1	Poloxamer 407	Poloxamer 407	0.62 [a]
E2	Poloxamer 188	Poloxamer 188	0.60 [a]
E3	PVP K15	PVP K15	0.64 [a]
E4	Poloxamer 407	Poloxamer 407	10.76 [b]
E5	Poloxamer 407	Poloxamer 407	5.36 [b]
E6	Poloxamer 407	Poloxamer 407	3.57 [b]

Dispersion concentration: 15 mg/ml

[a] Without centrifugation

[b] After centrifugation and remove some free stabilizer

Table 3.2: Physicochemical characteristics of EPAS powders in various compositions.

Formulation no.	**Particle Size (μm)**	**Polydispersity Index**	**Potency of ITZ (%)**	**Surface area (m^2/g)**	**Contact angle (^{o})**	**Drug-to-Stabilizer Ratio**
Bulk ITZ	1.43*	n/a	100	2.02 ± 0.10	61.6 ± 0.54	n/a
E1	5.63 ± 0.91	1.81 ± 0.02	38.2	8.79 ± 0.42	30.2 ± 0.62	0.62
E2	9.75 ± 1.43	1.22 ± 0.02	37.7	5.82 ± 0.62	36.8 ± 0.41	0.60
E3	15.5 ± 1.84	1.43 ± 0.05	38.9	4.16 ± 0.37	39.5 ± 0.39	0.64
E4	5.94 ± 0.83	1.81± 0.02	91.5	7.25 ± 0.58	35.7 ±0.58	10.76
E5	5.87 ± 1.15	1.45 ± 0.01	84.3	8.44 ± 0.81	32.5 ±0.52	5.36
E6	6.12 ± 1.22	1.66 ± 0.04	78.1	8.51 ± 0.69	30.6 ±0.36	3.57

* provided by manufacturer

Table 3.3: Different tablet formulations of ITZ and their composition (%).

Formulation no.	Itraconazole EPAS Powders (%)*	Avicel (PH101) (%)	Lactose Monohydrate (%)	Sodium starch glycolate (%)	Cab-o-sil (%)	Magnesium Stearate (%)
Tablet E1	40.0	34.0	20.0	5.0	0.5	0.5
Tablet E2	40.0	34.0	20.0	5.0	0.5	0.5
Tablet E3	40.0	34.0	20.0	5.0	0.5	0.5

* equivalent to 30 mg ITZ per 200 mg Tablet

Table 3.4: Physical characteristics of ITZ EPAS tablets.

Formulation no.	MeanWeight (mg)	Hardness (kg/cm^2)	Disintegration Time (sec)	Friability (%)
Tablet E1	199.75	11.4	20	0.11
Tablet E2	200.28	11.2	21	0.09
Tablet E3	199.47	10.6	22	0.16

Table 4.1: Molecular structures of drug and polymers used in this study.

Compounds	Chemical structure
Bulk REP	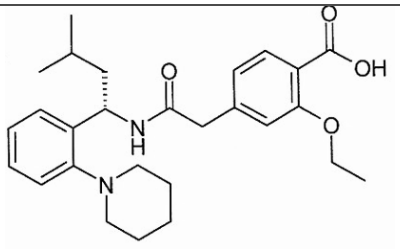
HPMC	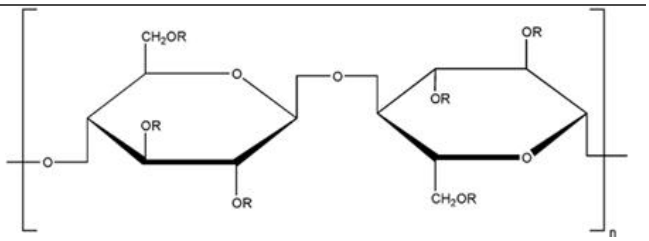
PVP	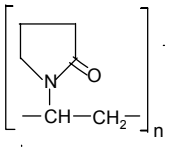
PEG	(-CH2–CH2–O-)n
PVA	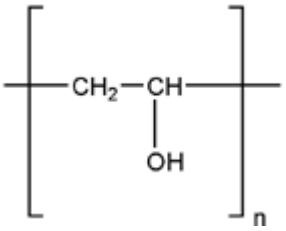

Table 4.2: Calculated and experimental dissolution rates of REP powders made by CP.

Sample	BET surface area (m^2/g)	Total surface area, A (cm^2)	Diameter (nm)	Exp. initial rate	Calculated initial rate
REP/HPMC E5	9.35	374	642	2.38	6.85
REP/PVPK15	5.08	203.2	1180	1.66	2.02
REP/PEG8000	4.97	198.8	1210	1.66	1.94
REP/PVA	3.57	142.8	1680	1.0	1.00

*Experimental rates were based on the 2 min. concentration value from Figure 6, all rates are reported relative to the 1:1 REP/PVA case.

Table 5.1: Physicochemical properties of TAC powder compositions prepared by the URF process and aerosol characteristics of aqueous dispersions of URF powder compositions delivery by nebulization.

.

Formulations	Physical State of Drug	Surface Area (m^2/g)	TED (μg)	%FPF	MMAD (μm)	GSD
URF-TAC:LAC	Amorphous	29.3	5082	74.6	2.57	2.24
URF-TAC	Crystalline	25.9	4823	70.2	2.86	1.97

TED: total emitted dose.
MMAD: mass median aerodynamic diameters.
GSD: geometric standard deviation.
FPF: fine particle fraction, as percentage of total loaded dose < 5 μm.

Table 5.2: In vivo pharmacokinetic parameters for the lung tissue concentrations of the URF formulations.

Formulations	C_{max} (μg/g)	T_{max} (hrs)	K_{el} (hrs^{-1})	$T_{1/2}$ (hrs)	$AUC_{(0-24)}$ (μg.hr/g)
URF-TAC	10.86 ±1.07	3	0.0346	20.02	111.19 ± 20.16
URF-TAC:LAC	14.09±1.50	2	0.0334	20.75	122.42 ± 6.19

C_{max} : maximum concentration
T_{max} : time to C_{max}
K_{el} : elimination rate constant
$T_{1/2}$: half-life
$AUC_{(0-24)}$: area-under-the-curve between 0-24 hours

Table 5.3: In vivo pharmacokinetic parameters for the whole-blood concentrations of the URF formulations following the pulmonary administration.

Formulation	C_{max} (ng/mL)	T_{max} (hrs)	K_{el} (hrs^{-1})	$T_{1/2}$ (hrs)	$AUC_{(0-24)}$ (ng.hr/mL)
URF-TAC	300.67 $\pm$ 27.04	3	0.123	5.63	1324.35 $\pm$ 318.07
URF-TAC:LAC	402.11 $\pm$ 35.99	2	0.115	6.02	1235.66 $\pm$ 65.86

C_{max} : maximum concentration
T_{max} : time to C_{max}
K_{el} : elimination rate constant
$T_{1/2}$: half-life
$AUC_{(0-24)}$: area-under-the-curve between 0-24 hours

Table C.1: Specific surface area of processed TAC compositions.

Composition	**Surface Area (m^2/g)**
URF-TAC:Inulin	32.5
URF-TAC:Lactose	29.3
URF-TAC: Mannitol	21.8
URF-TAC: Glucose	15.6
Unprocessed TAC	0.53

Table D.1: Experimental Conditions.

Temperature of organic (MeCl2) and aqueous solution	80^{o} C
Flow rate Q (ml/min)/pressure drop ΔP (MPa)	1.0/~20
Crimp Nozzle: stainless steel tube	1/16 in. o.d.
Drug concentration in feed solution	15% w/v
Conc. of Pluronic F127 in aqueous and organic phases	2% w/v
Conc. of Ammonium Carbonate (add in organic solution and sonicate for 40 sec.)	0, 0.5 and 1% w/v
Volume of receiving aqueous solution Vrec	50 ml
Spraying time	5 min
Drug/surfactant ratio (w/w) in dispersion	0.68
Drying technique: lyophilization	

Table D.2: Properties of EPAS ITZ powders.

Formulation	Surface area (m^2/g)	Contact angle (^{o})
E1 (0%$(NH_4)_2CO_3$)	8.19 $\pm$ 0.42	30.4 $\pm$ 0.52
E2 (0.5%$(NH_4)_2CO_3$)	9.65 $\pm$ 0.51	31.5 $\pm$ 0.58
E3 (1.0%$(NH_4)_2CO_3$)	14.89 $\pm$ 0.73	30.9 $\pm$ 0.67

Organic phase: 15% w/v ITZ + 2% w/v Poloxamer 407 in $MeCl_2$
Aqueous phase: 2% w/v Poloxamer 407
Drug :Surfactant Ratio : 1:1.47 by weight
All dispersions were dried by rapid freezing into liquid nitrogen and lyophilization
Contact angle was measured against dissolution media.(0.1N HCl, 0.5% SLS)

Figure 1.1: Schematic representation of different nanotechnology-based drug delivery systems. Reprinted with permission from S. K. Sahoo and V. Labhasetwar, 8, 1112, 2003, Copyright Elsevier (2003).

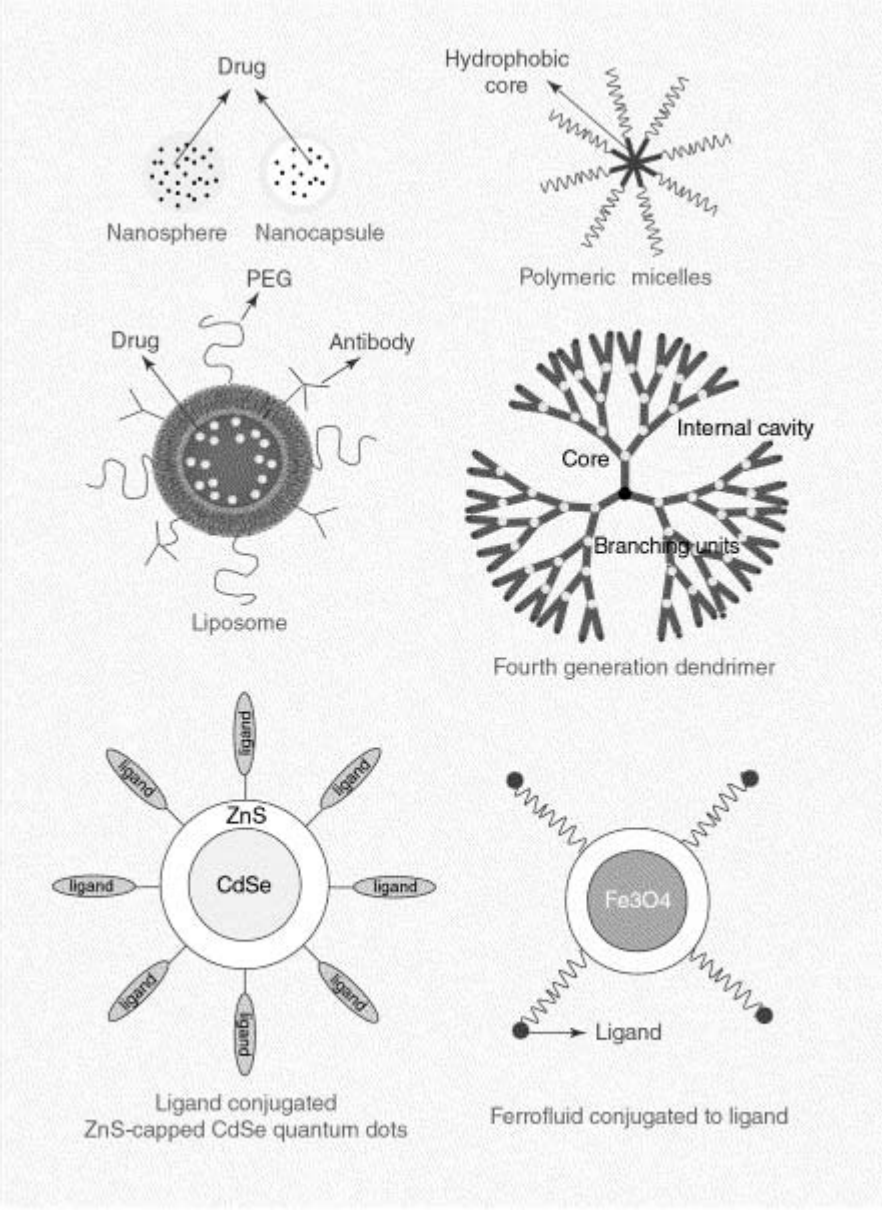

Figure 1.2: Targeting of intracellular bacteria with antibiotic colloidal carriers, liposomes or nanoparticles. P, Phagosome, L, Lysosome, PL, Phagolysosome. Reprinted with permission from H. Pinto-Alphandary et al. Int. J. Antimicrob. Agents, 13, 155, 2000, Copyright Elsevier (2000).

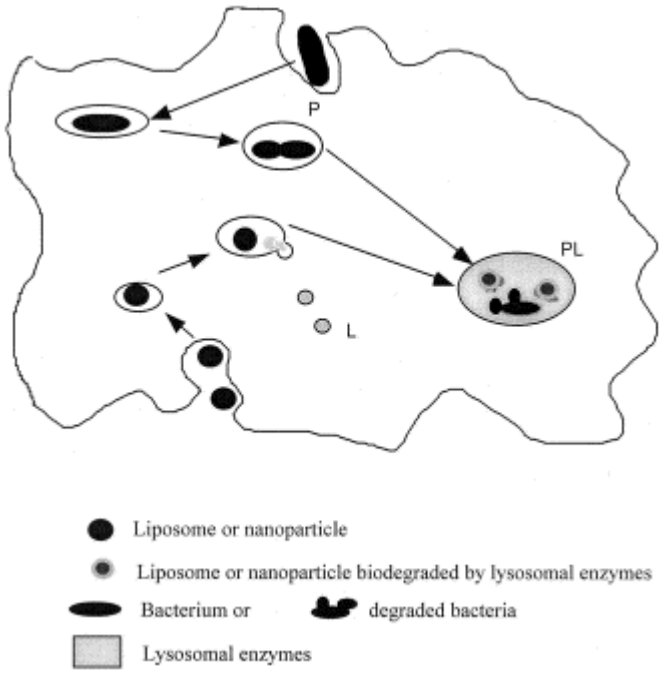

Figure 1.3: Schematic diagrams of the (a) RESS, (b) GAS, and (c) PCA/SAS/ASES processes. Reprinted with permission from B. Subramaniam et al., J. Pharm. Sci., 86, 885, 1997, Copyright American Scientific Publishers (1997).

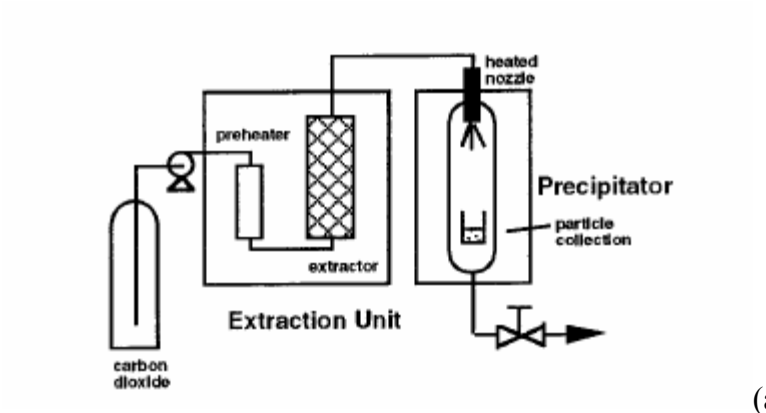

(a.)

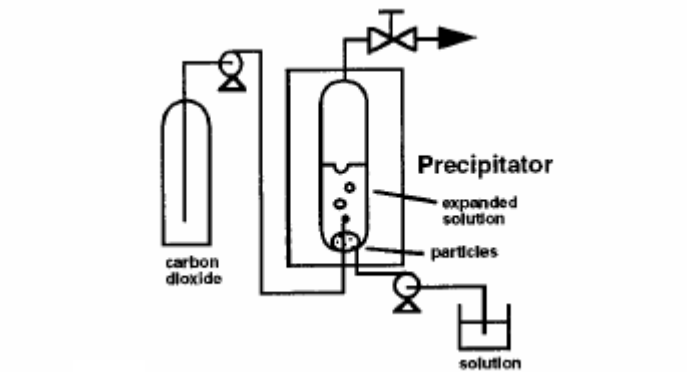

(b.)

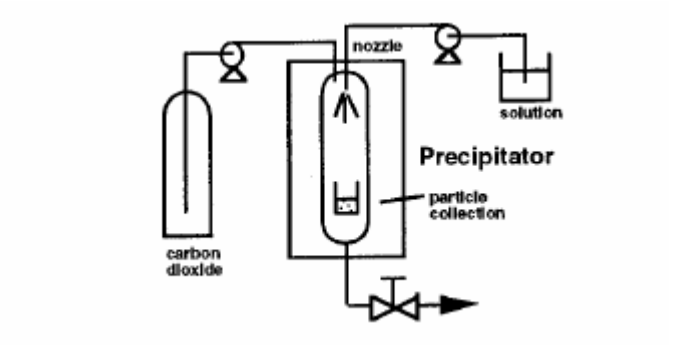

(c.)

Figure 1.4: Schematic flow diagram of the SEDS process along with the cross-section of the co- and tri-axial fluid nozzles. Reprinted with permission from J. Jung and M. Perrut, J. Supercrit. Fluids, 20, 179, 2001, Copyright Elsevier (2001).

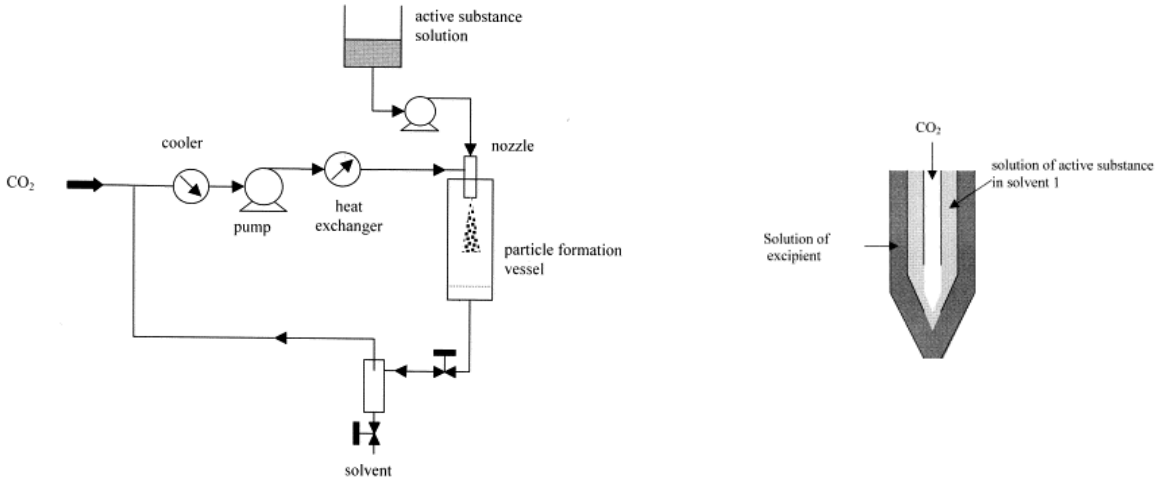

Figure 1.5: Adsorption isotherms and corresponding adsorption models, (A) particles <1 μm, (B) particles>1 μm. Reprinted with permission from G. Ponchel et al., Eur. J. Pharm. Biopharm., 44, 25, 1997, Copyright Elsevier (1997).

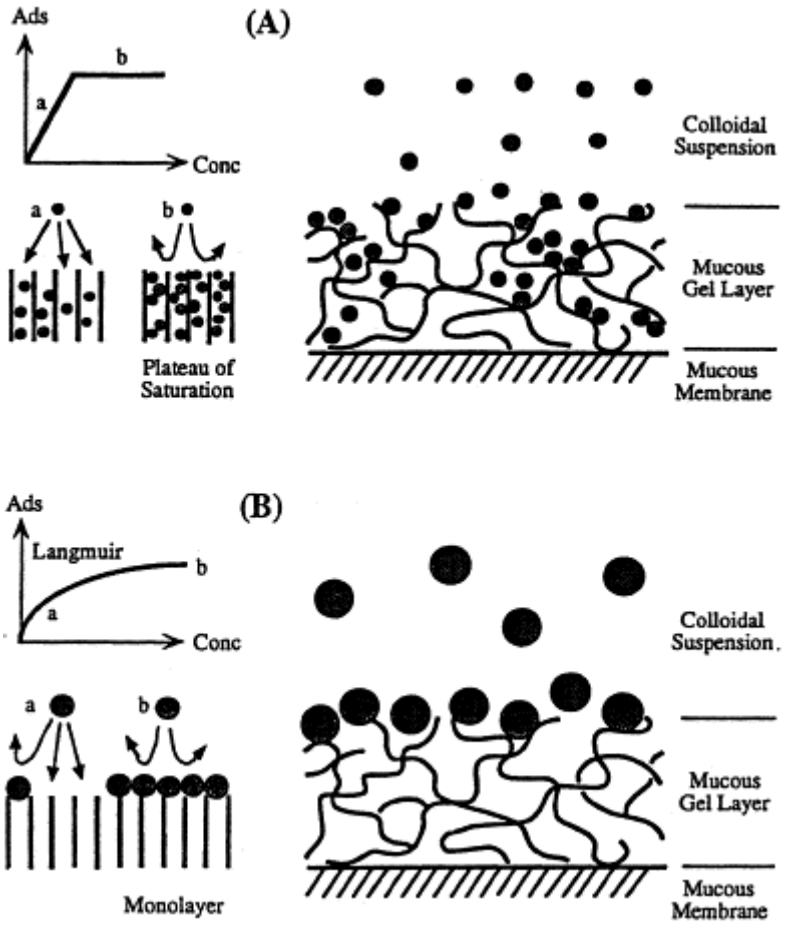

Figure 2.1: Schematic representation of EPAS process and the photograph showing intense atomization of the spray.

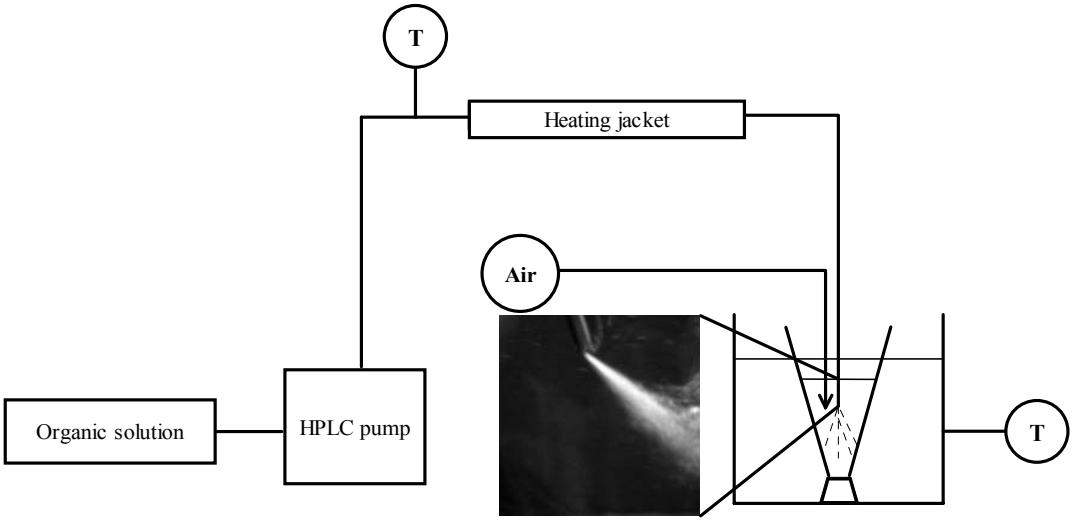

Figure 2.2: The adsorption isotherms of various stabilizers onto ITZ particles.

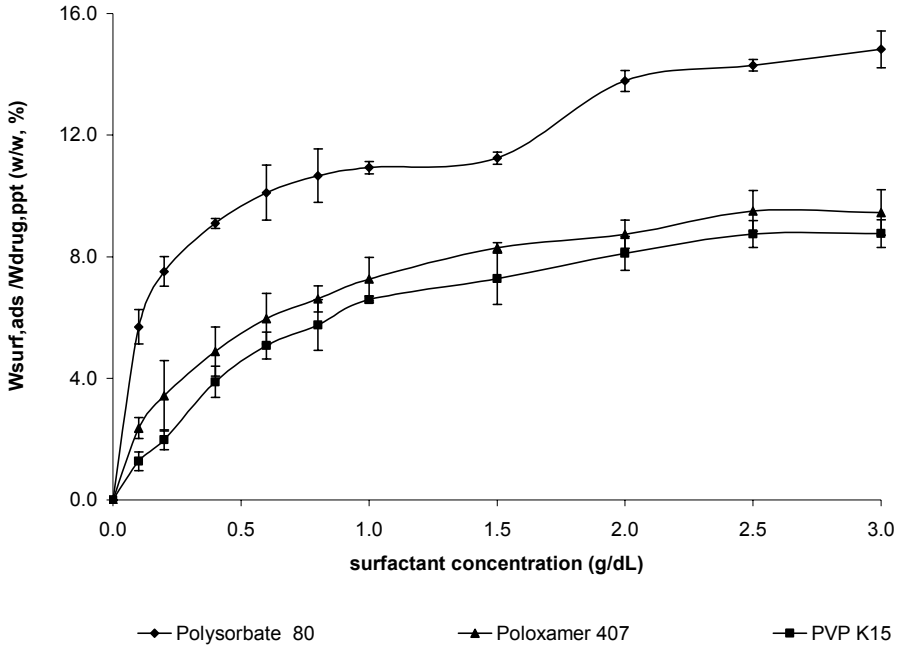

Figure 2.3: Dissolution profile of itraconazole with different surfactant systems. The weight ratios shown are ITZ:organic stabilizer: aqueous stabilizer. All dispersions were centrifuged and dried by lyophilization. The final drug concentration was 15 mg/ml. The dissolution media was enzyme-free simulated gastric fluid containing 0.5% SLS (pH 1.2) and dissolution profiles were determined in replicates of 6.

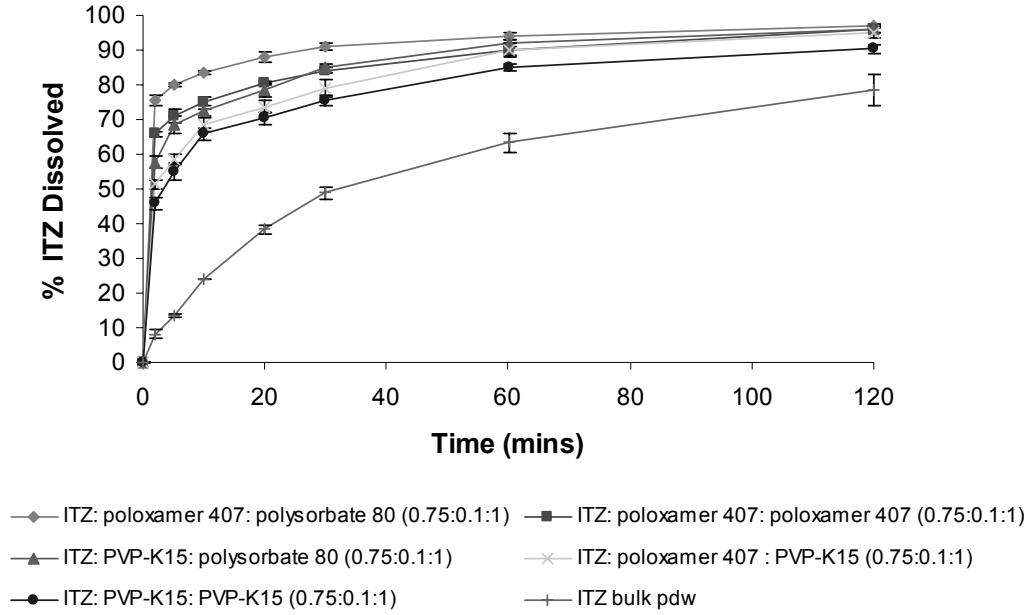

Figure 2.4: TEM micrograph of of itraconazole EPAS particles with poloxamer 407 as organic stabilizer and polysorbate 80 as aqueous stabilizer. The ratios of ITZ:organic stabilizer:aqueous stabilizer were 0.75:0.1:1. The dispersion was centrifuged and dried by lyophilization. The final drug concentration was 15 mg/ml.

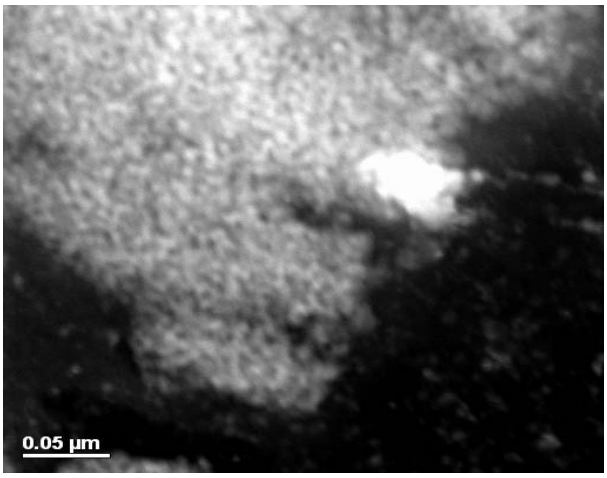

Figure 2.5: EDS Spectrum of itraconazole EPAS particles with poloxamer 407 as organic stabilizer and polysorbate 80 as aqueous stabilizer. The ratios of ITZ:organic stabilizer:aqueous stabilizer were 0.75:0.1:1. The dispersion was centrifuged, frozen and dried by lyophilization. The final drug concentration was 15 mg/ml. Presence of N and Cl confirms ITZ.

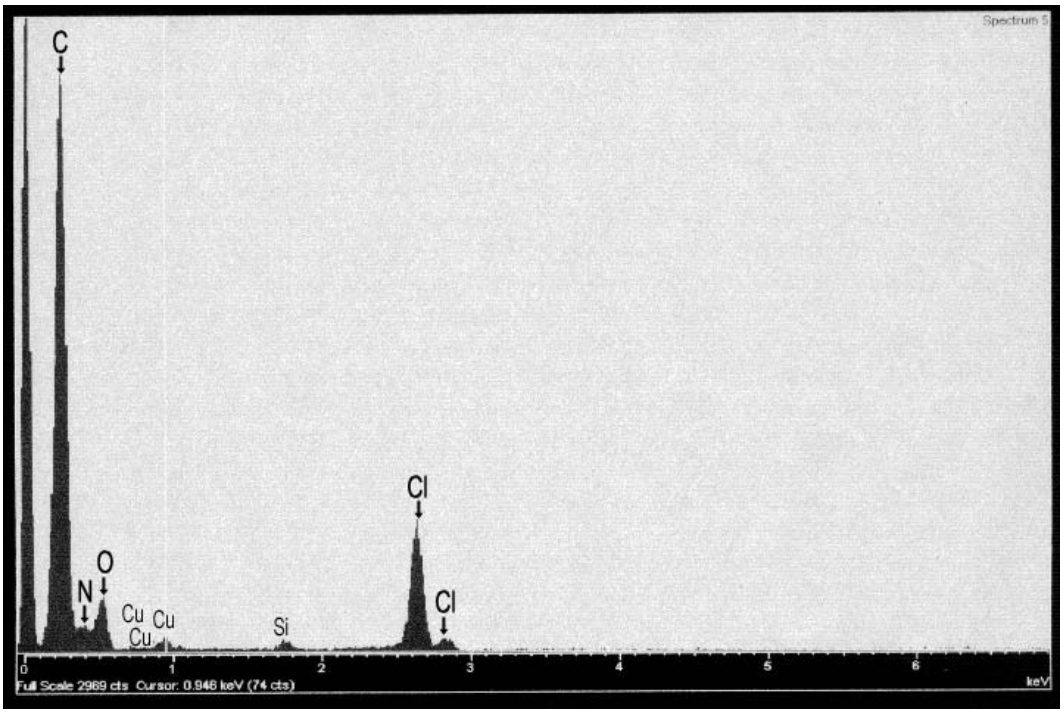

Figure 2.6: X-ray diffraction patterns of ITZ formed by EPAS (a) control: bulk ITZ, (b) ITZ: PVP K15: PVP K15, (c) ITZ:PVP K15:poloxamer 407, (d) ITZ:poloxamer 407:poloxamer 407, (e) ITZ:poloxamer 407:polysorbate 80 and ITZ:poloxamer 407:PVP K15. The ratios of ITZ:organic stabilizer:aqueous stabilizer were 0.75:0.1:1. All dispersions were centrifuged and dried by lyophilization. The final drug concentration was 15 mg/ml. The patterns clearly demonstrate the crystallinity of the processed ITZ.

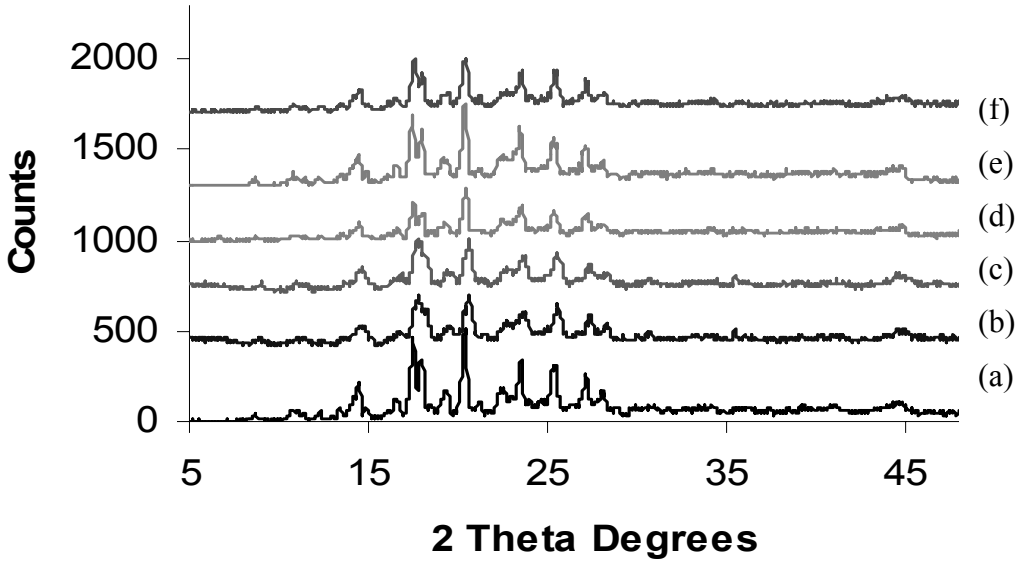

Figure 3.1: Schematic representation of EPAS process and the photograph showing intense atomization of the spray.

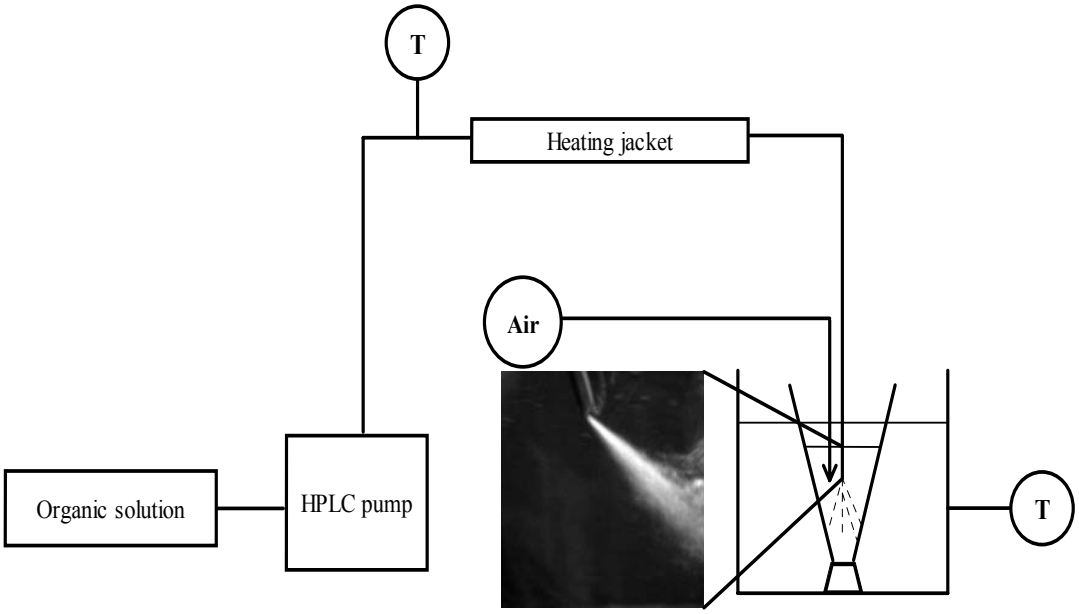

Figure 3.2: SEM micrographs of (a) Bulk ITZ; (b) EPAS with poloxamer 407 (E1 powders); (c) EPAS with poloxamer 188 (E2 powders); (d) EPAS with PVPK15 (E3 powders).

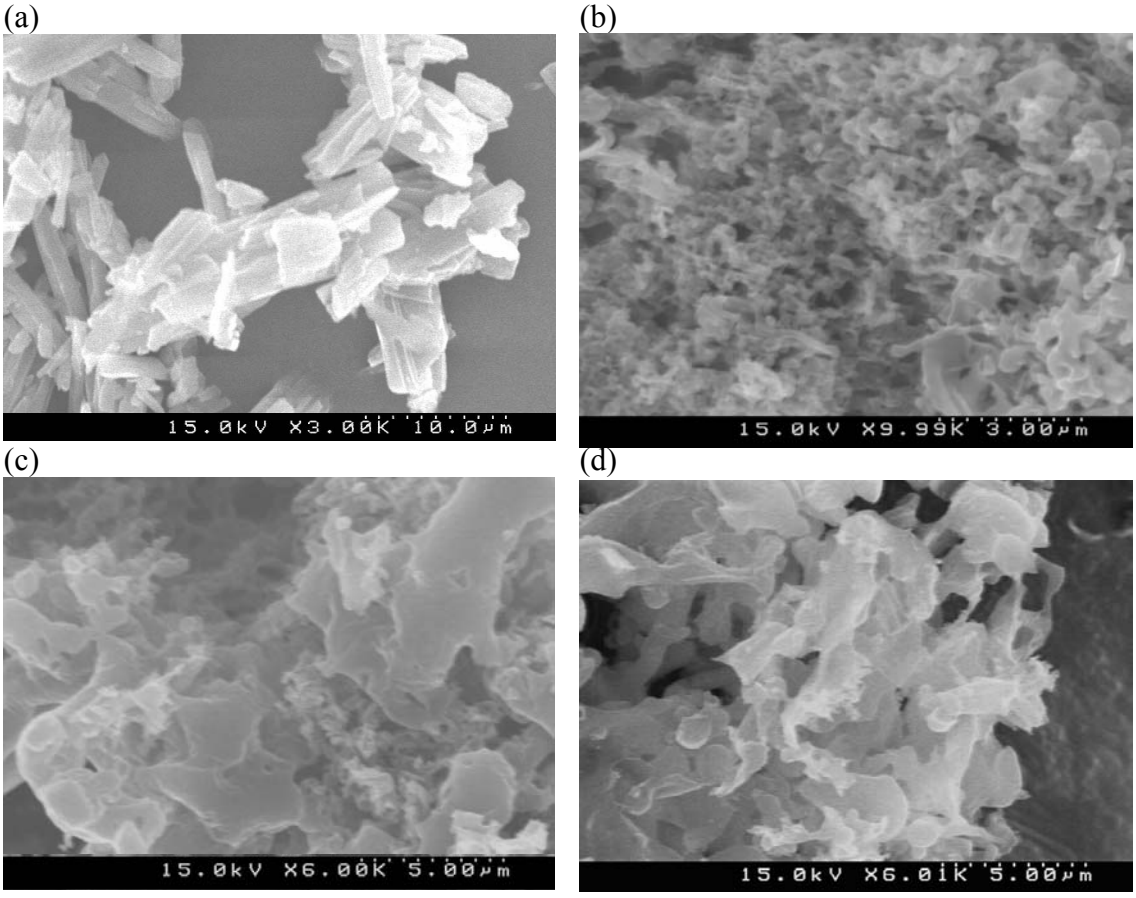

Figure 3.3: (a) Dissolution profile of EPAS processed powders with different stabilizer systems. (●, E1 powders) EPAS with poloxamer 407, (▲, E2 powders) EPAS with poloxamer 188, (■, E3 powders) EPAS with PVPK15 and (○) Bulk ITZ.

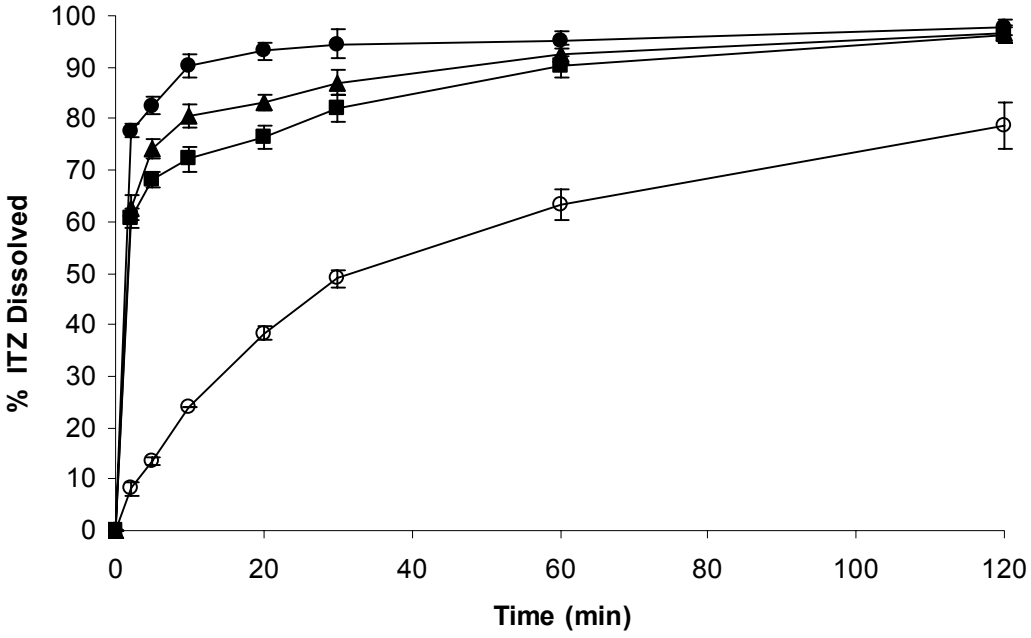

(b) Dissolution profiles of ITZ EPAS powders with poloxamer 407 at different drug-to-stabilizer ratios. (●, E1 powders) 0.62, (♦, E4 powders) 10.76, (x, E5 powders) 5.36, (Δ, E6 powders) 3.57 and (○) Bulk ITZ. Each result shows the mean ± S.D. (n = 6) and error bars are in the symbols.

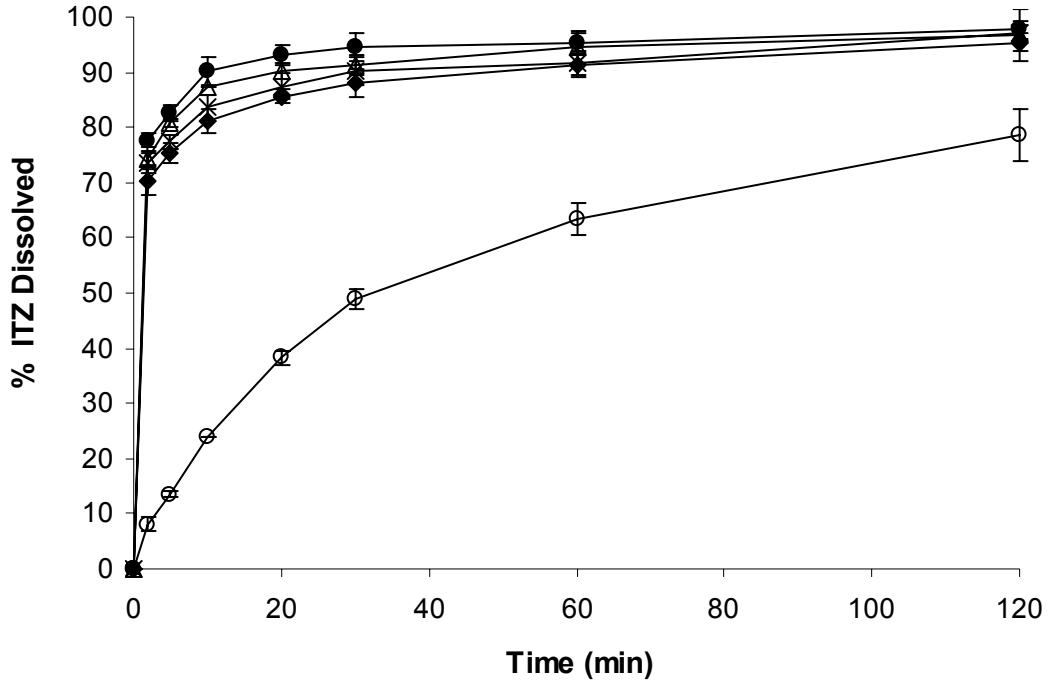

Figure 3.4: X-ray diffraction profiles of ITZ systems (a) bulk ITZ (b) E1 powders (c) E2 powders (d) E3 powders (e) E4 powders (f) E5 powders (g) E6 powders.

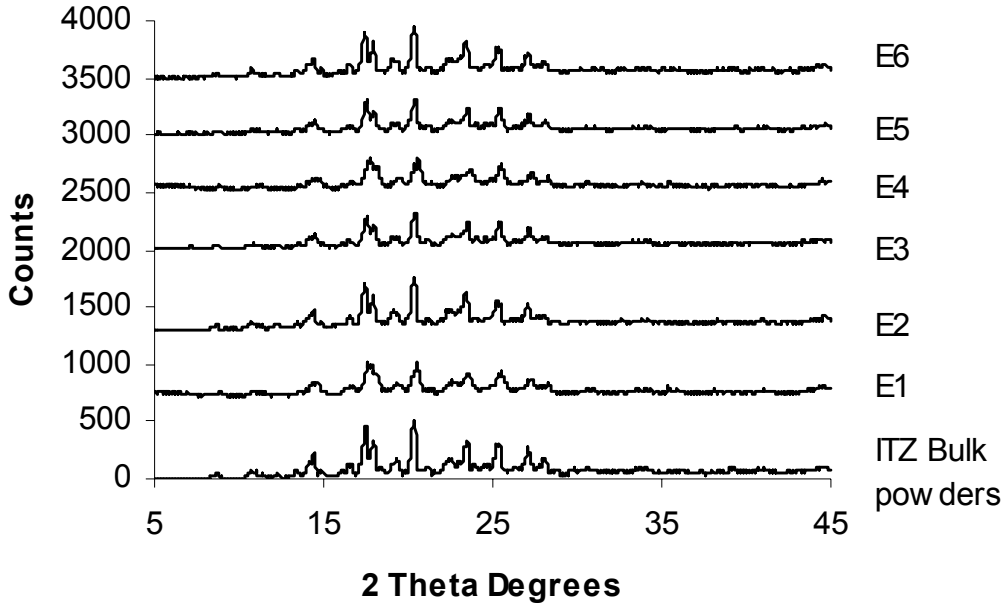

Figure 3.5: Dissolution profile of EPAS tablets with various stabilizer systems. (●,Tablet E1) Tablet prepared from EPAS processed powders of ITZ with poloxamer 407, (▲,Tablet E2) Tablet prepared from EPAS processed powders of ITZ with poloxamer 188 and (■,Tablet E3) Tablet prepared from EPAS processed powders of ITZ with PVPK15.

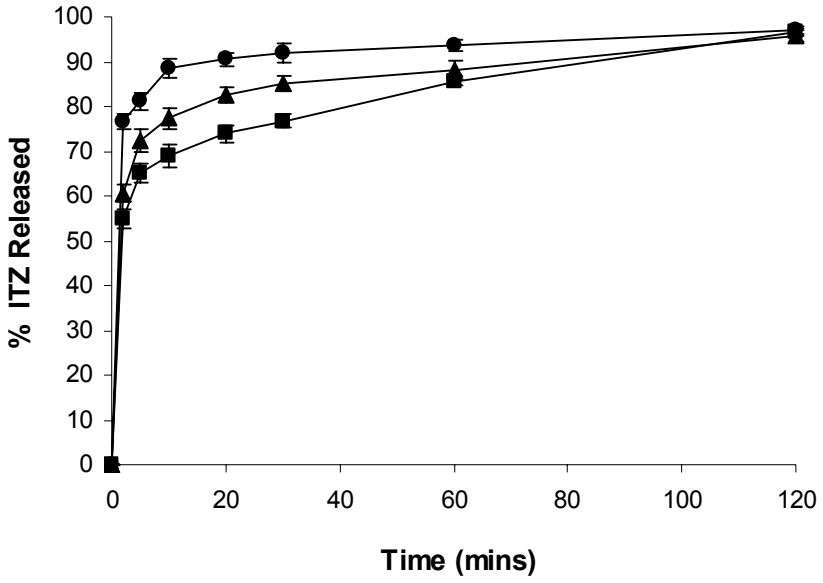

Figure 4.1: Schematic representation of controlled precipitation technology.

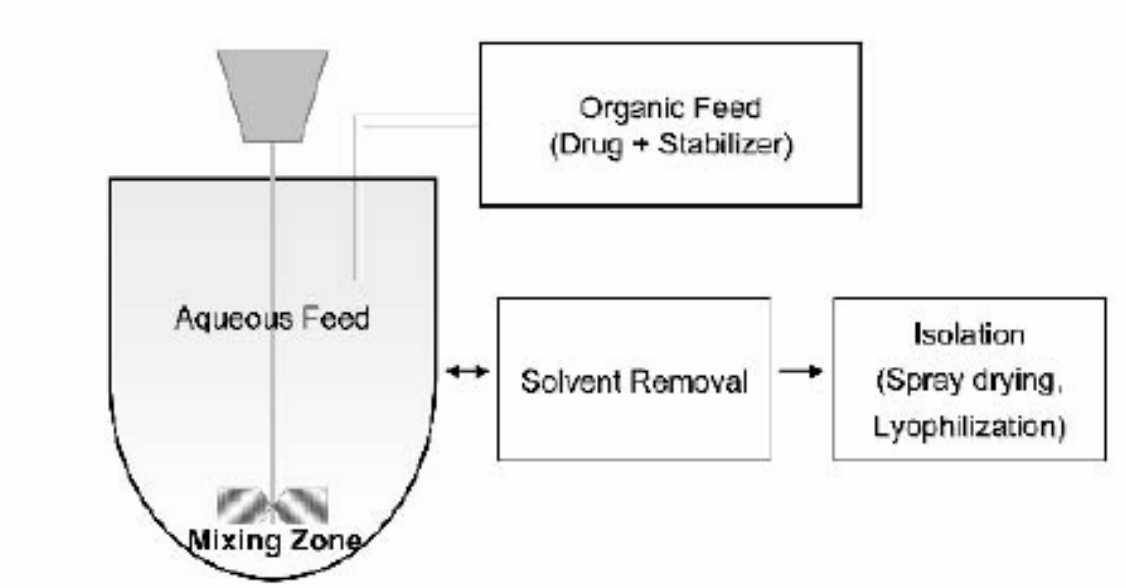

Figure 4.2: SEM images of REP particles with different stabilizing polymer systems (1:1). The dispersion was frozen dropwise into liquid nitrogen and lyophilized. (a) Bulk REP (b) REP: HPMC E5, (c) REP: PVP K 15, (d) REP: PEG 8000, (e) REP: PVA.

(a)

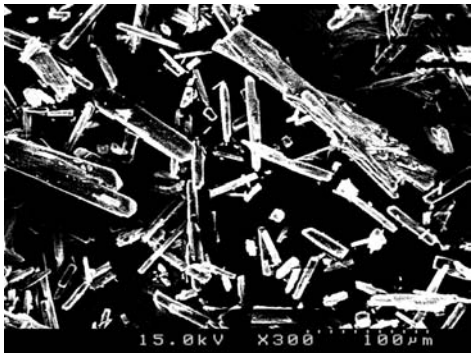

(b)

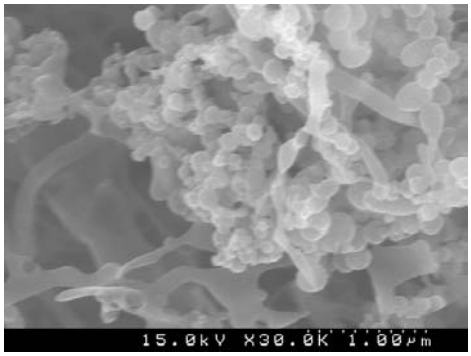

(c)

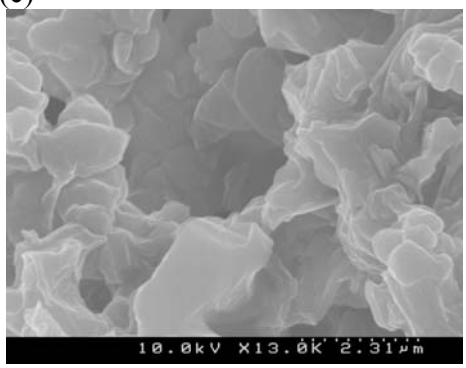

(d)

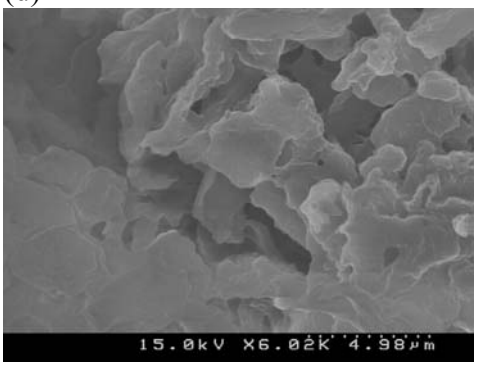

(e)

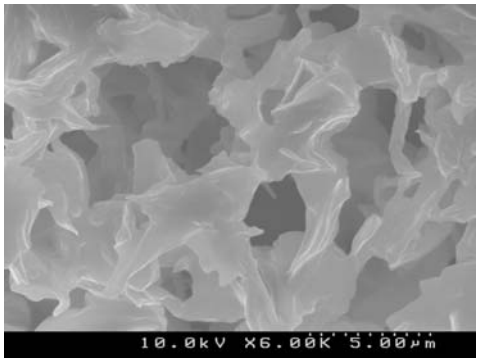
10.0kV X6.00K 5.00µm

Figure 4.3A: X-ray diffraction patterns of REP powders formed by controlled precipitation technology. (a) control: Bulk REP, (b) Physical mixture of components REP: HPMC E5 (1:1), (c) REP: HPMC E5 (1:1), (d) REP: PEG 8000 (1:1), (e) REP: PVP K 15 (1:1), (f) REP: PVA (1:1).

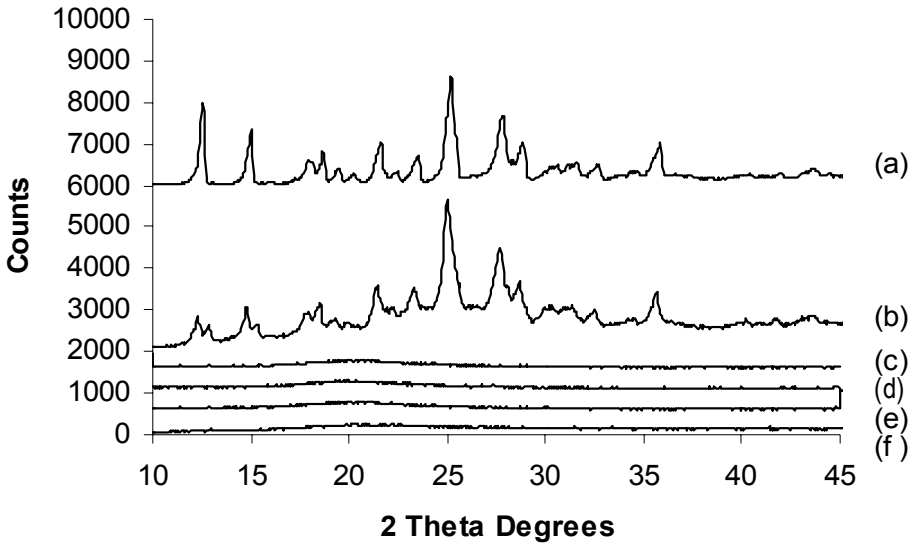

Figure 4.3B: X-ray diffraction patterns.(a) control: Bulk REP, (b) Physical mixture of REP: HPMC E5 (1:1), (c) REP: HPMC E5 (1:1)-initial, (d) REP: HPMC E5 (1:1)- during 3 month storage.

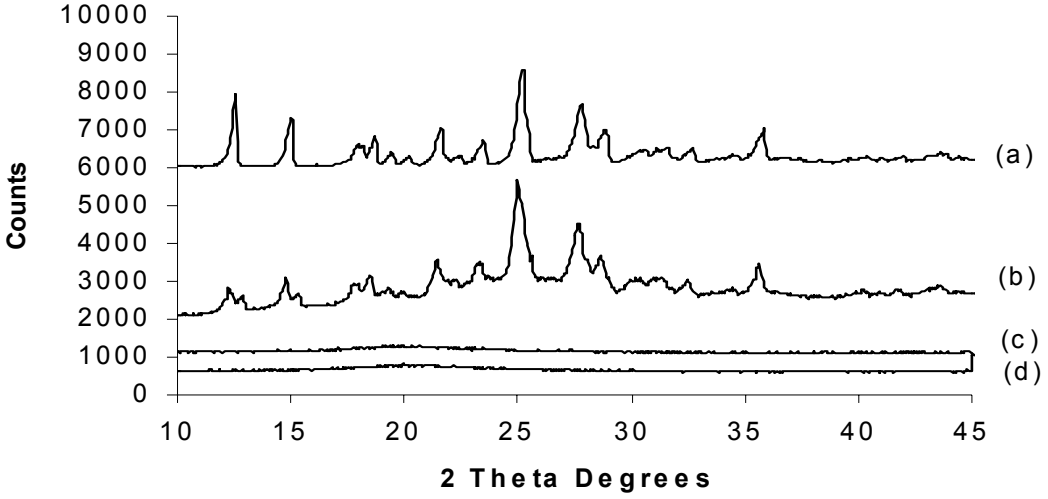

Figure 4.4: The reversing heat flow curves of REP with different stabilizing polymer systems in which the ratio of polymer towards drug is 1:1.

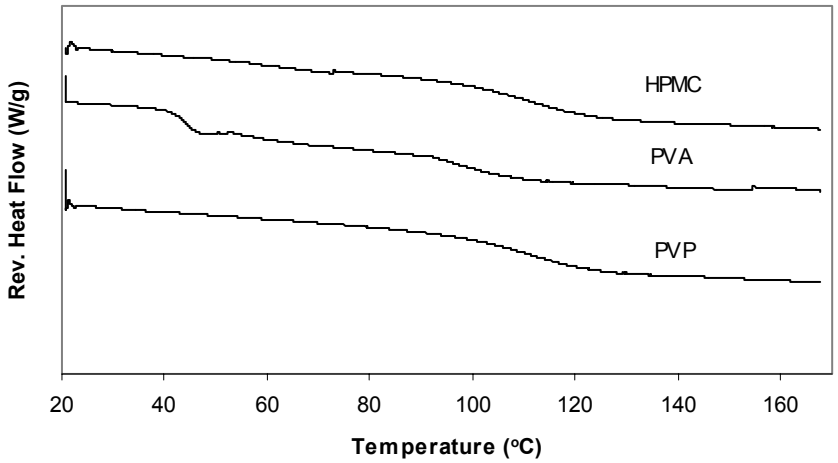

Figure 4.5: Glass transition temperatures of REP containing PVP K15 and HPMC E5 at initial period and 3 months.

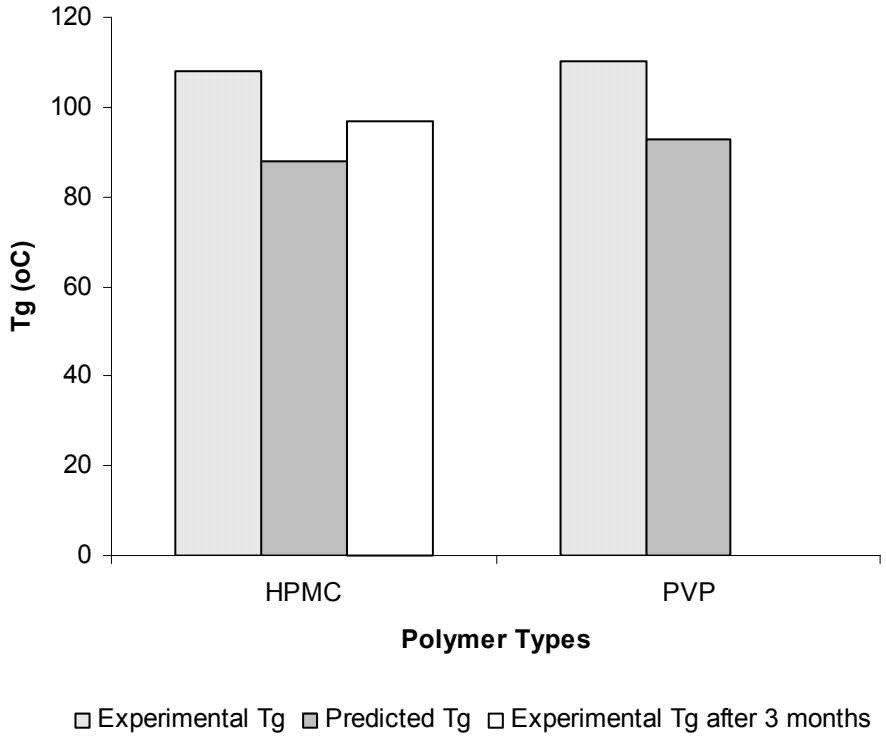

Figure 4.6: Dissolution profiles of REP with different stabilizing polymer systems. (x) REP: HPMC E5 (1:1), (●)REP: PVP K 15 (1:1), (■)REP: PEG 8000 (1:1), (▲)REP: PVA (1:1), (□) Bulk REP . The dissolution media was citric acid/sodium phosphate dibasic buffer with a pH of 4.5 and dissolution profiles were determined in replicates of 6.

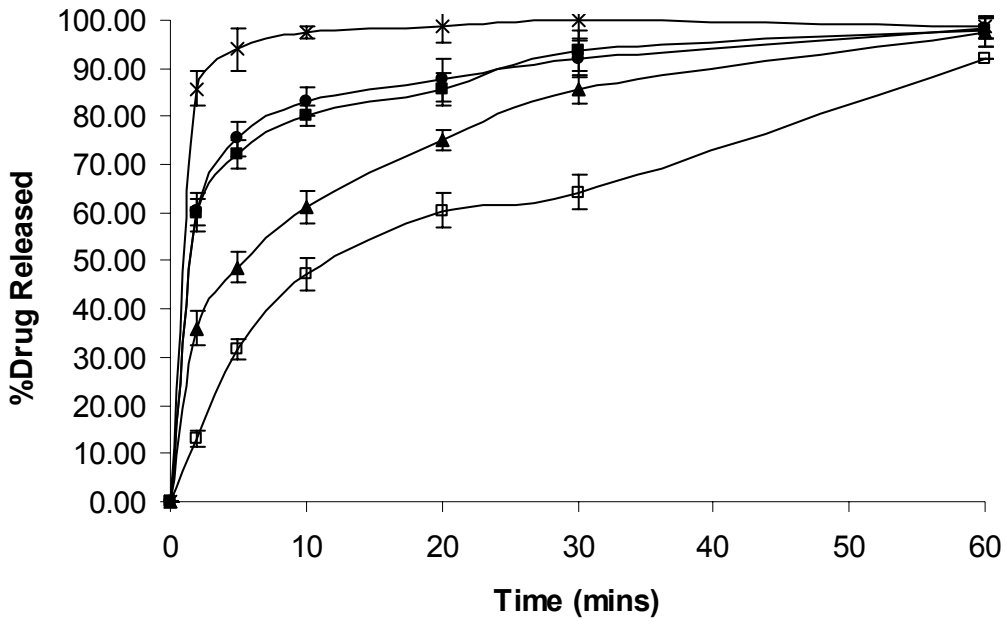

Figure 4.7: Supersaturated dissolution of REP with various compositions at drug loading (10x). (▲)HPMC E5 ; (x) PVP K15 (■) PEG 8000 ; (●)PVA. The dissolution media was citric acid/sodium phosphate dibasic buffer with a pH of 4.5, 50 rpm, 37^{o}C, small volume paddle method. The dissolution profiles were determined in replicates of 3.

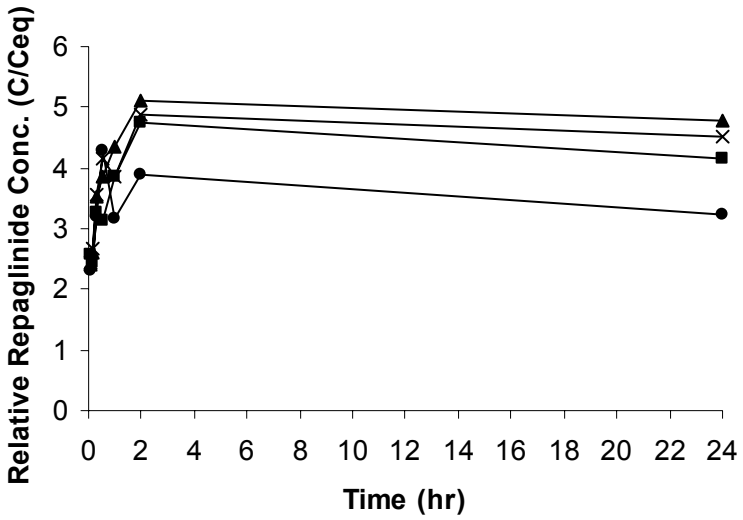

Figure 4.8: Supersaturated dissolution of REP: HPMC E5. (▲)Drug loading (25x) at initial time point ; (■) Drug loading (10x) at initial time point ; (●)Drug loading (10x) after 3 months at 25°C /60% RH. The dissolution media was citric acid/sodium phosphate dibasic buffer with a pH of 4.5, 50 rpm, 37°C, small volume paddle method. Dissolution profiles were determined in replicates of 3.

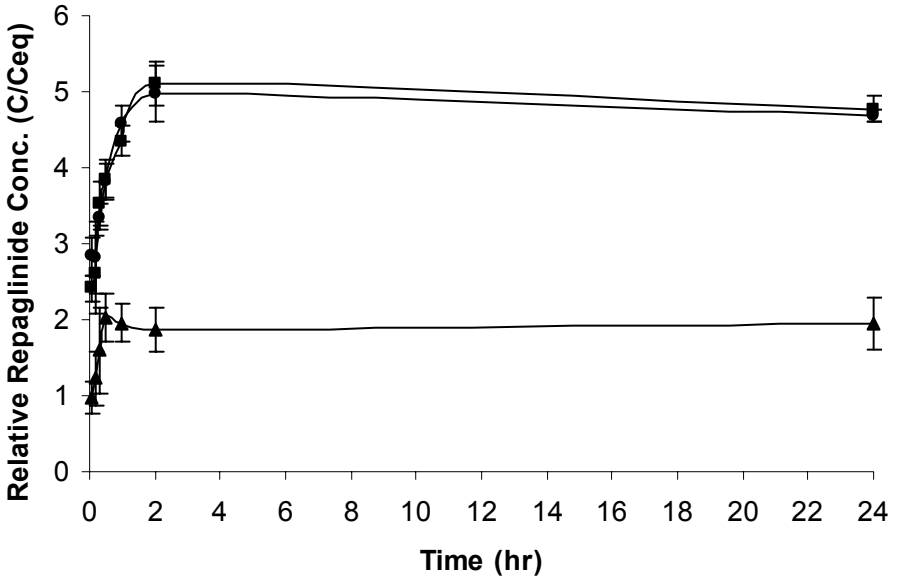

Figure 5.1: Schematic representation of URF technology.

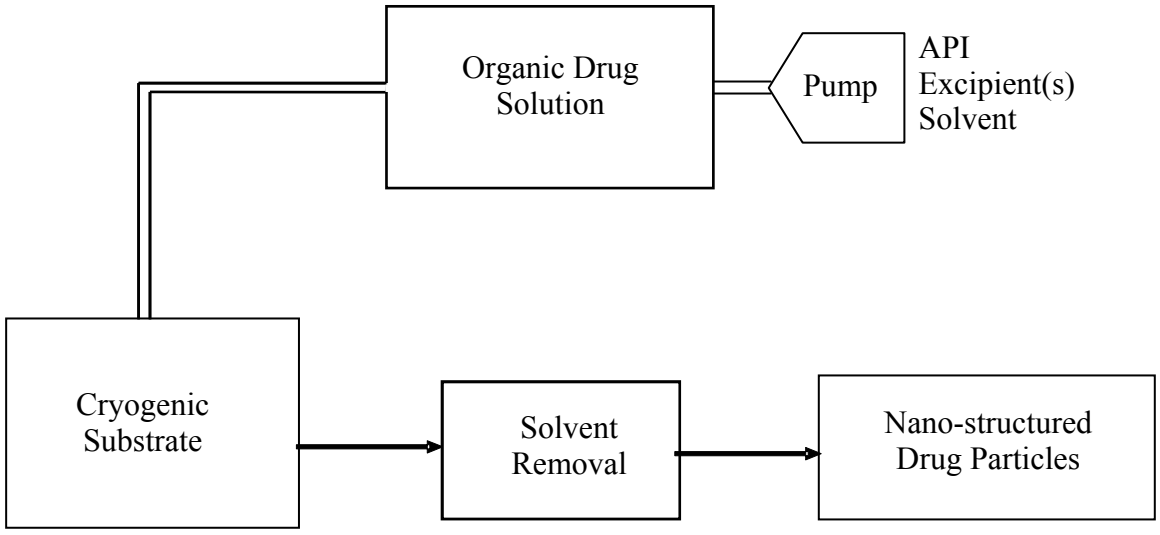

Figure 5.2: Schematic diagram of small animal nose-only dosing apparatus.

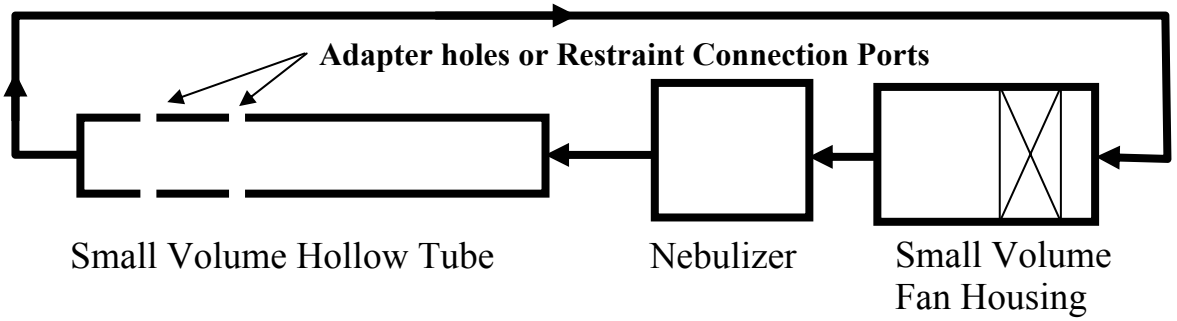

Figure 5.3: Restraint tubes from the Battelle® toxicology testing unit.

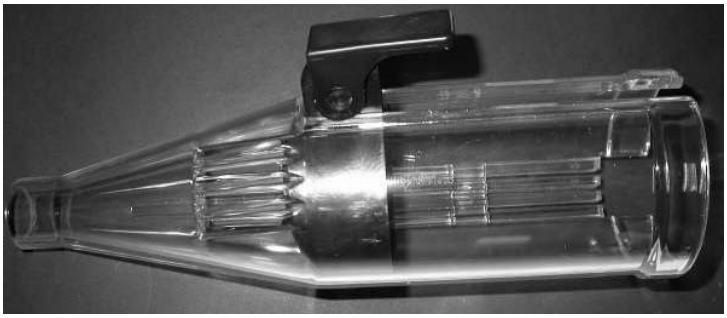

Figure 5.4: X-ray diffraction profiles of TAC URF formulations compared to unprocessed TAC.

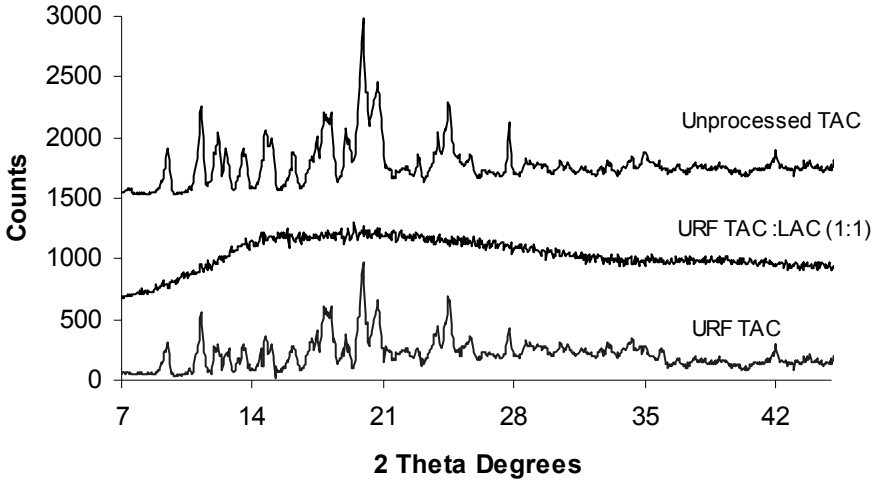

Figure 5.5: SEM micrographs of (a) URF-TAC:LAC (1:1) at low magnification, (b) URF-TAC:LAC (1:1) at high magnification, (c) URF-TAC at low magnification, (d) URF-TAC at high magnification t, (e) Unprocessed TAC at low magnification.

(a)

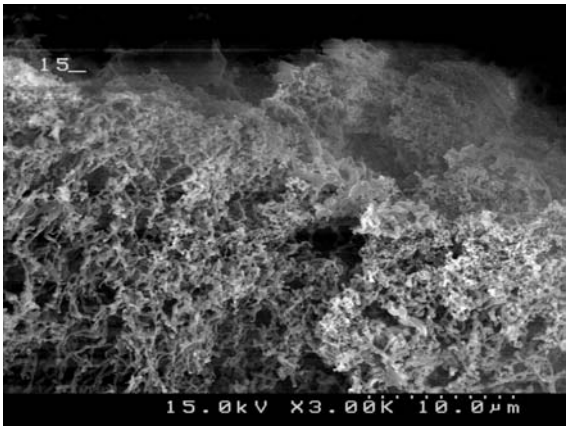

(b)

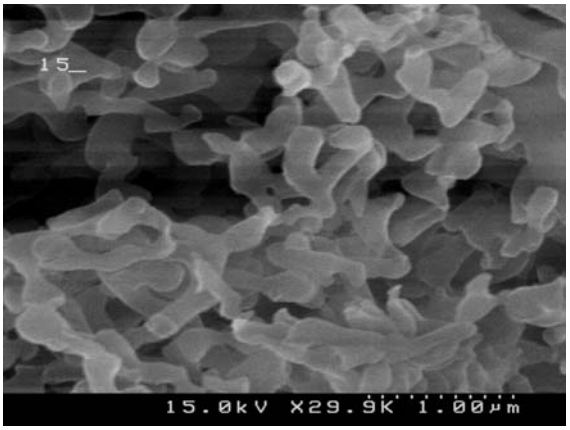

(c)

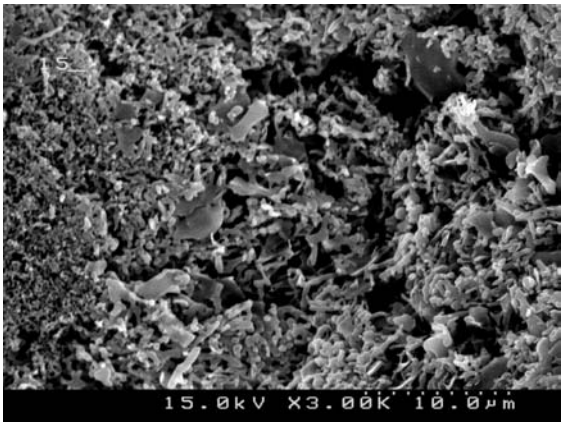

(d)

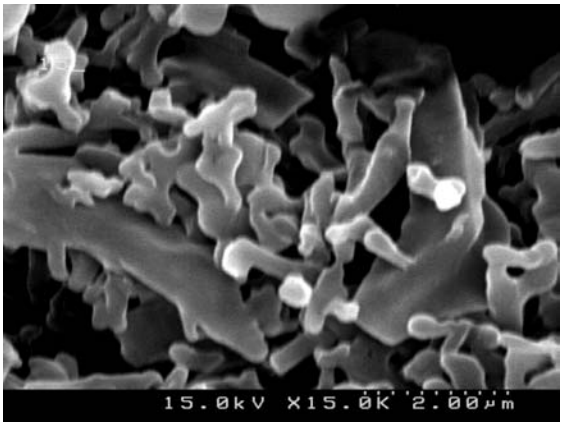

(e)

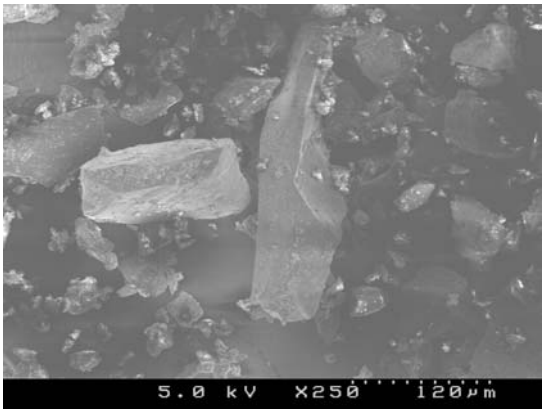
5.0 kV X250 120µm

Figure 5.6: Sink dissolution profiles for (■) Amorphous URF composition TAC: lactose (1:1), (▲) Crystalline URF composition TAC alone and (●)Unprocessed TAC. The dissolution media was modified simulated lung fluids (SLF) containing 0.02 % DPPC at 100 rpm and 37^{o}C (equilibrium solubility of TAC in this media ~ 6.8 μg/mL). Dissolution profiles were determined in replicates of 3.

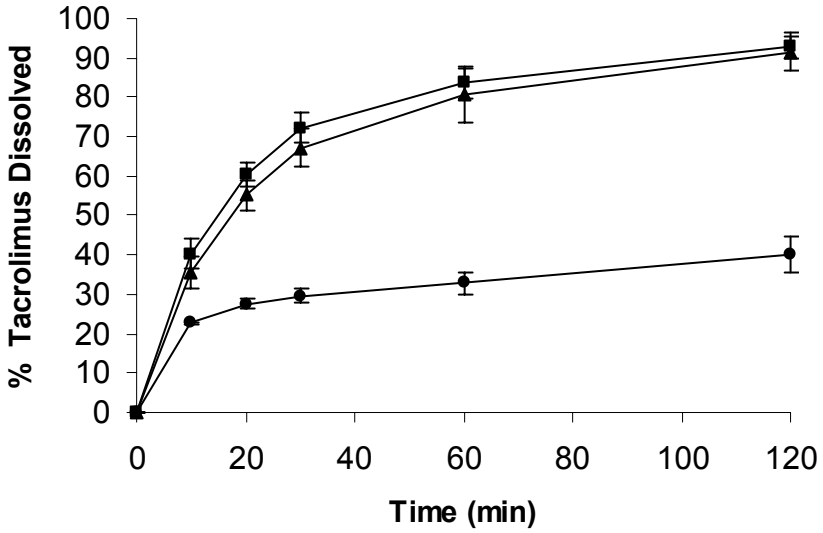

Figure 5.7. Supersaturated dissolution profiles. for (●) Amorphous URF composition TAC: lactose (1:1); (■) Crystalline URF composition TAC alone and (---) Equilibrium solubility of TAC in the dissolution media (6.8 μg/mL). The dissolution media was modified simulated lung fluids (SLF) containing 0.02 % DPPC at 100 rpm and 37^{o}C. Dissolution profiles were determined in replicates of 3.

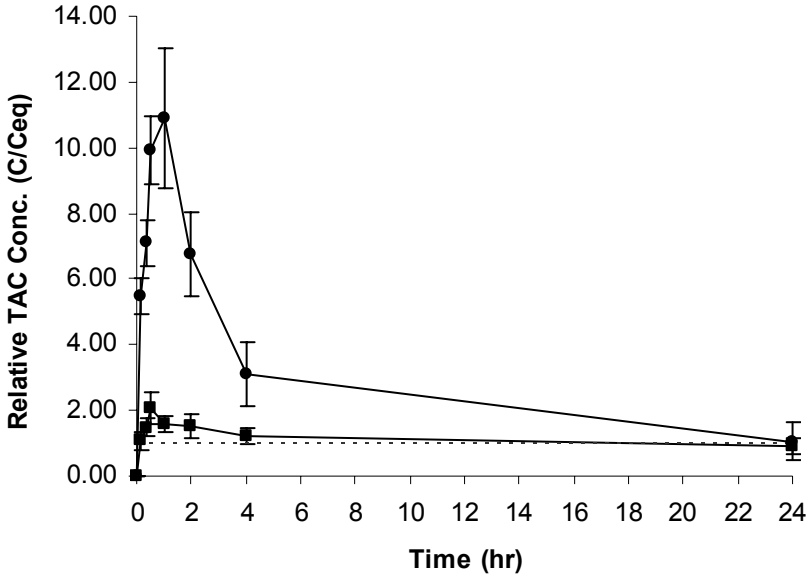

Figure 5.8: Comparison of mean lung concentration (µg TAC/g tissue) versus time profiles of the URF formulations. (●) Amorphous URF composition TAC: lactose (1:1) and (■) Crystalline URF composition TAC alone.

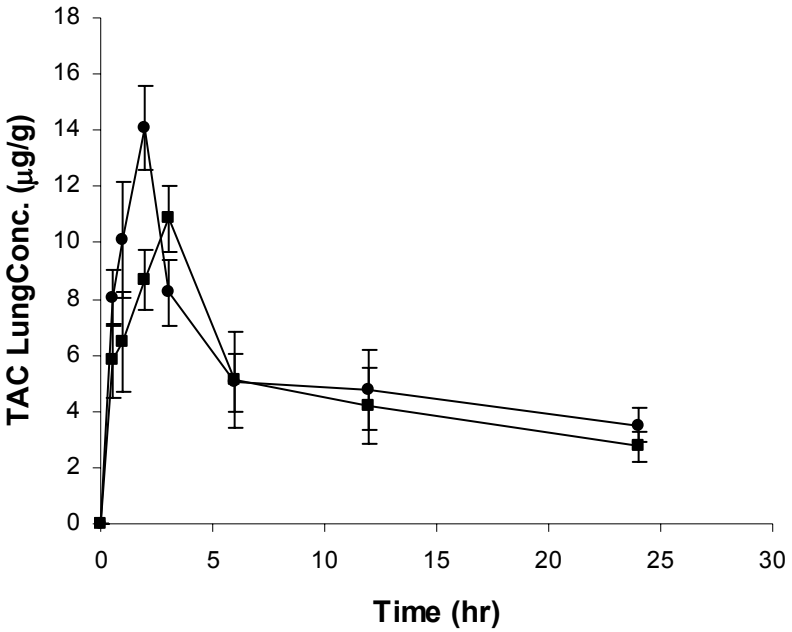

Figure 5.9: Comparison of mean whole-blood TAC concentration profiles of the URF formulations after a single inhalation administration. (●) Amorphous URF composition TAC: lactose (1:1) and (■) Crystalline URF composition TAC alone.

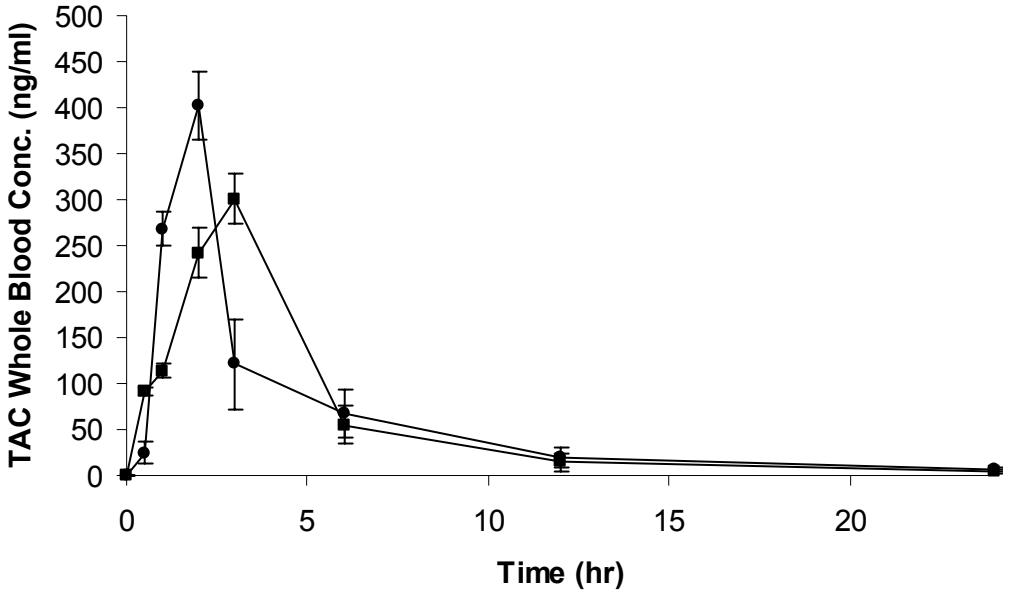

Figure B.1: In vitro dosing uniformity using nose-only dosing apparatus.

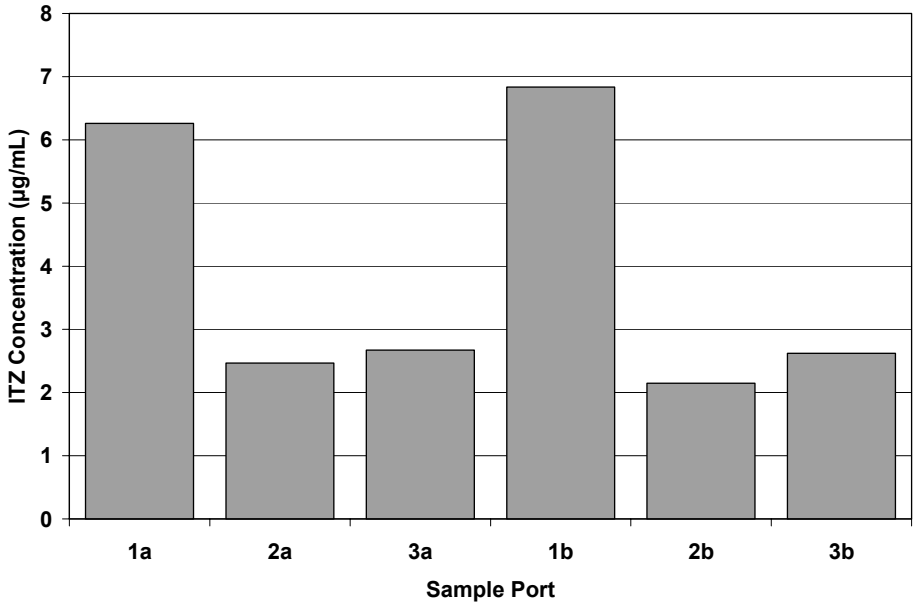

Figure B.2: In vivo dosing based on individual wet lung weights for mice dosed with an amorphous ITZ pulmonary composition using nose-only dosing apparatus.

.

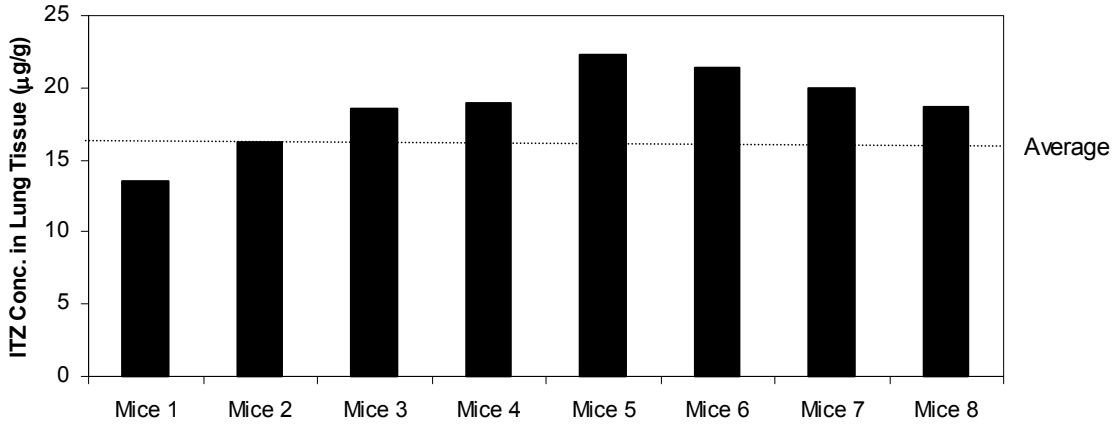

Figure C.1: SEM micrographs of TAC particles processed by URF with (a) lactose; (b) mannitol; (c) glucose; (d) inulin.

(a)

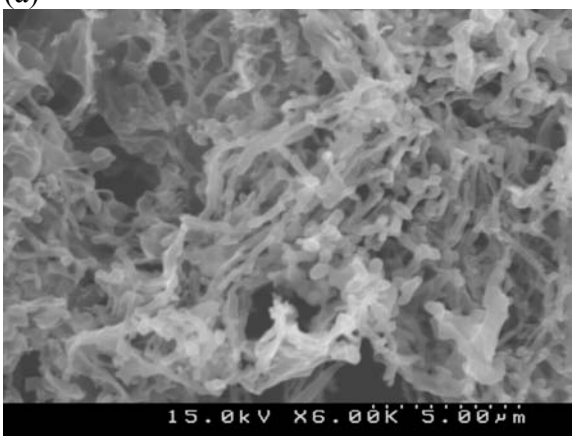

(b)

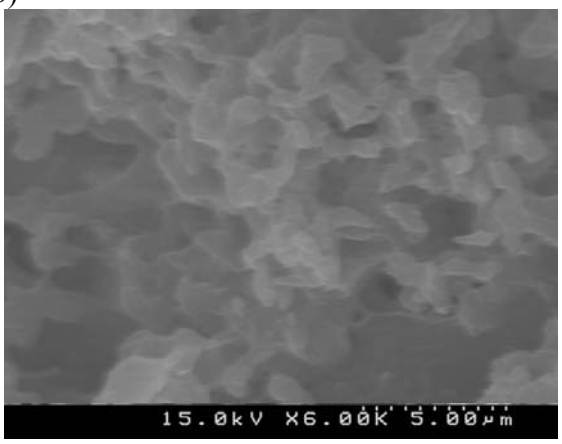

(c)

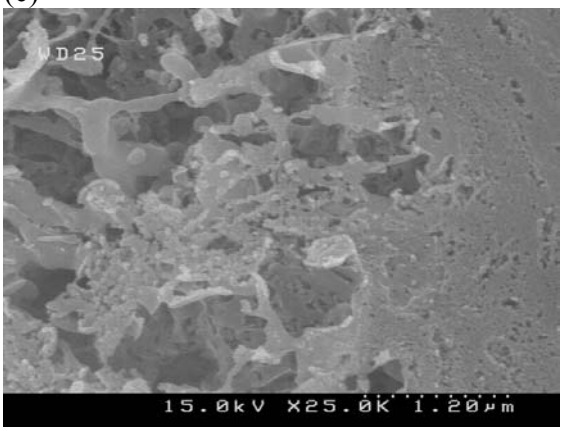

(d)

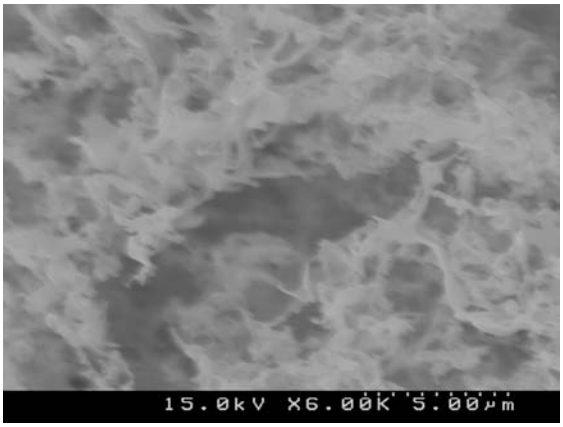

Figure C.2: X-ray diffraction patterns of processed TAC compositions compared to unprocessed TAC.

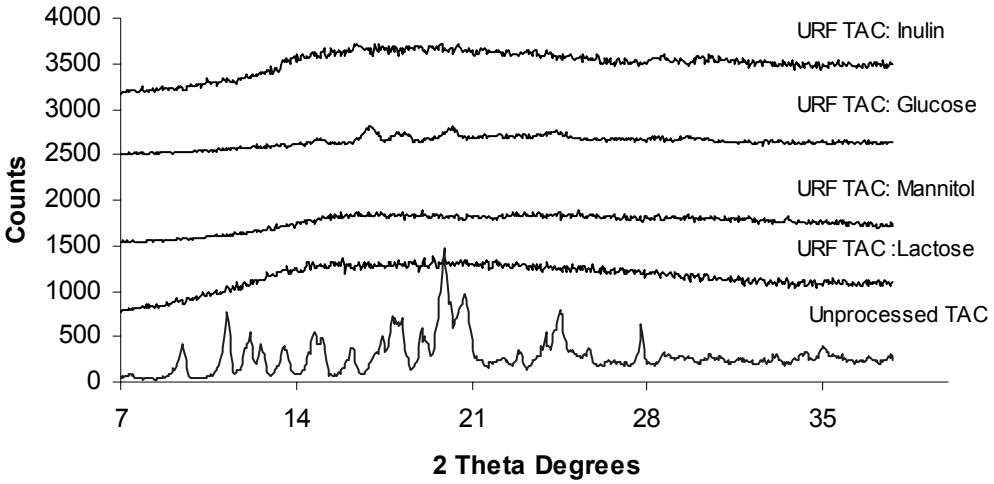

Figure C.3: Dissolution profiles of processed TAC compositions compared to unprocessed TAC (●) URF-TAC:Inulin ;(■) URF-TAC:Lactose ;(▲)URF-TAC: Mannitol ;(x) URF-TAC: Glucose ;(○) Unprocessed TAC. The dissolution media was modified simulated lung fluids (SLF) containing 0.02 % DPPC at 100 rpm and 37^{o}C (equilibrium solubility of TAC in this media ~ 6.8 µg/mL). Dissolution profiles were determined in replicates of 3.

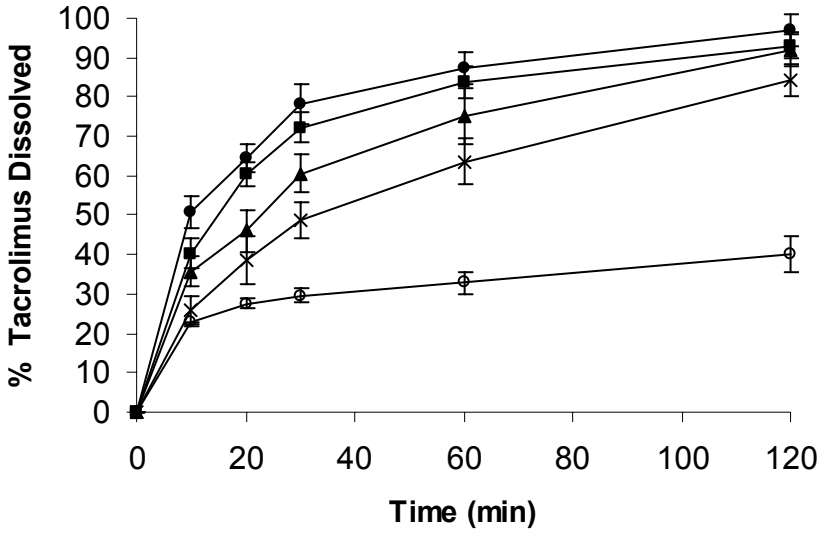

Figure D.1: X-ray diffraction patterns of processed ITZ compositions compared to bulk ITZ.

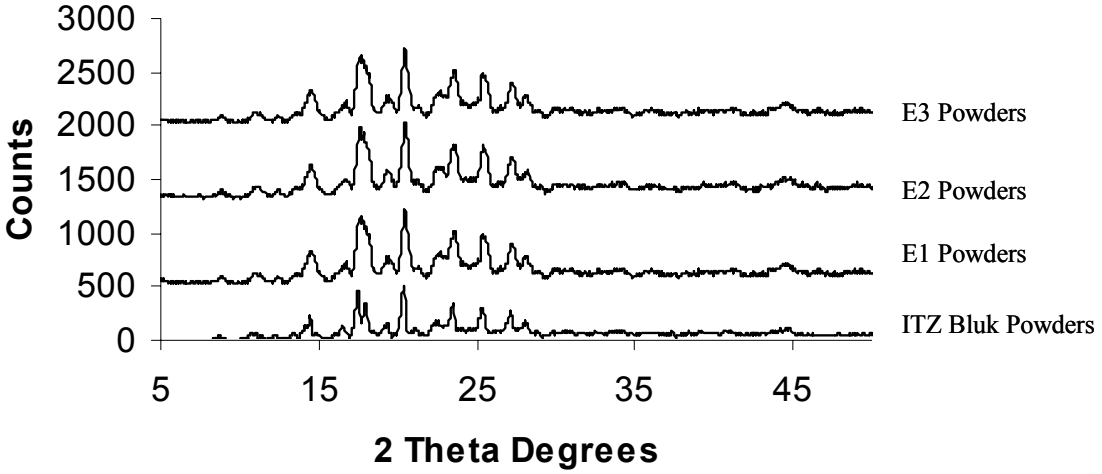

Figure D.2: SEM micrographs of EPAS powders containing 0%$(NH_4)_2CO_3$, E1 powders (a); 0.5%$(NH_4)_2CO_3$, E2 powders (b); 1.0%$(NH_4)_2CO_3$, E3 powders (c).

(a)

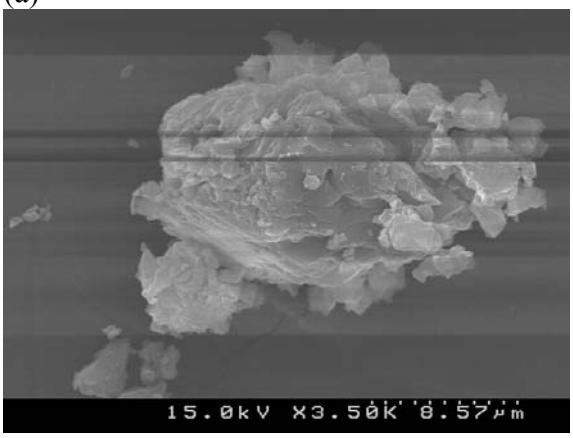

(b)

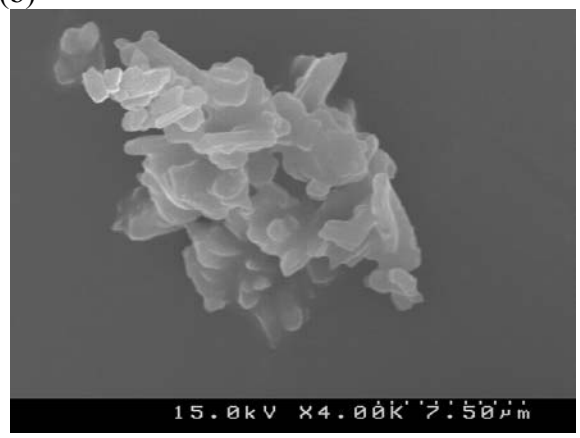

(c)

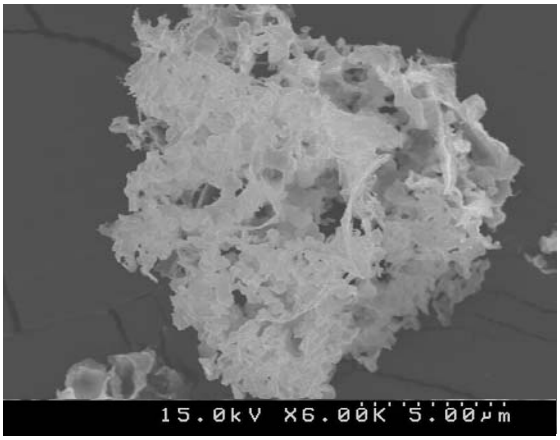

Figure D.3: Dissolution profiles of EPAS powders in 0.1N HCl, 0.5% SLS at 37°C and paddle speed of 50 rpm.

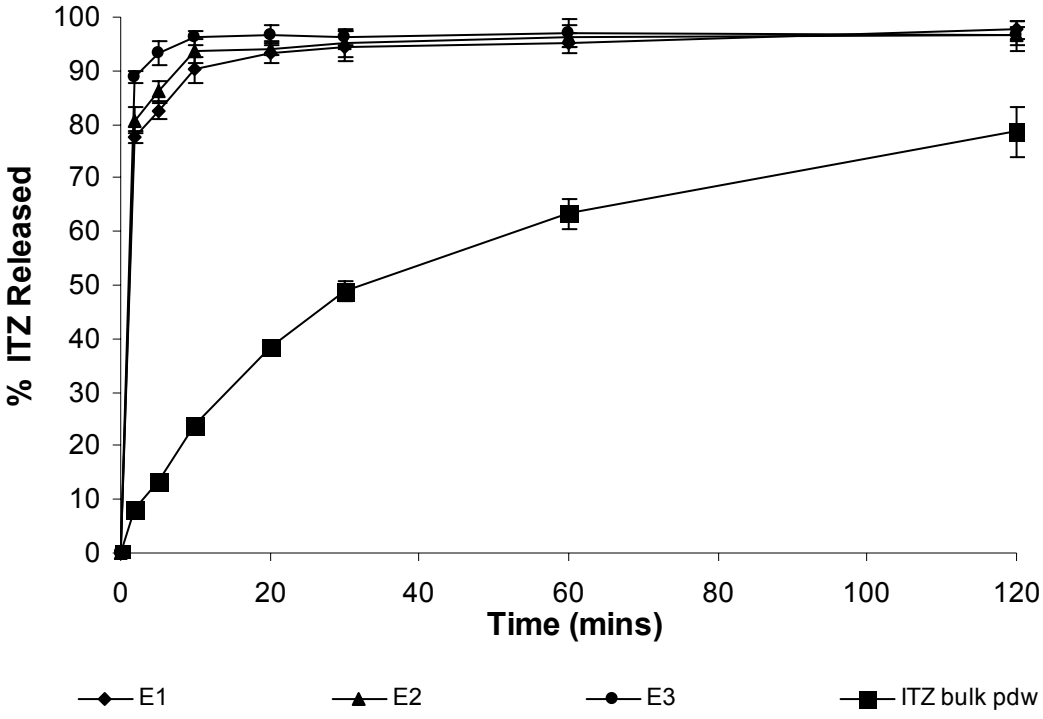

Appendix A: Lyophilization Recipes used in Chapter 5

Lyophilization Recipe A1 (long recipe) used in for URF-TAC: LAC (1:1)

Step	Temperature (°C)	Time (min)	Vac (mT)	R/H
1	-60	500	200	H
2	-40	500	200	H
3	-30	1440	100	R
4	-20	180	100	R
5	-10	180	100	R
6	0	180	100	R
7	10	180	100	R
8	25	180	100	R
9	25	500	100	H

Lyophilization Recipe A2 (short recipe) used in for URF-TAC

Step	Temperature (°C)	Time (min)	Vac (mT)	R/H
1	-40	180	400	H
2	-30	180	200	R
3	-20	180	200	R
4	-10	180	200	R
5	0	180	300	R
6	10	180	400	R
7	20	180	500	R
8	30	240	600	H

Appendix B: In Vitro and In Vivo Evaluation of a Nose-Only Aerosol Dosing Apparatus for Rodents

B.1 PURPOSE

Appendix B is a supplement to Chapter 5. In Appendix B, the dosing uniformity and variability of itraconazole (ITZ) was investigated both in vitro and in vivo using the nose-only aerosol dosing apparatus described in Chapter 5. This dosing apparatus was designed to deliver the aerosol directly to the nose. Such design is required a small amount of test material thereby it is useful for delivering 'expensive' drugs.

B.2 MATERIALS AND METHODS

B.2.1 Materials

The following materials were purchased: ITZ (ITZ; Hawkins Chemical, Minneapolis, MN); poloxamer 407, polysorbate 80, potassium phosphate monobasic, sodium hydroxide (NaOH) and sodium chloride (NaCl) (Spectrum Chemicals, Gardena, CA); high performance liquid chromatography (HPLC) grade acetonitrile and dichloromethane (EM Industries Inc., Gibbstown, NJ). Liquid nitrogen was obtained from Boc Gases (Murray Hill, NJ).

B.2.2 Production of an Amorphous ITZ Pulmonary Composition

Amorphous nanoparticles of ITZ were produced using the particle engineering process spray freezing into liquid (SFL). A solution of ITZ,

polysorbate 80 and poloxamer 407 was prepared at a 1:0.75:0.75 ratio in acetonitrile with 4% w/w dichloromethane as a cosolvent. This solution was atomized through a 63 μm poly-etherether-ketone (PEEK) nozzle (Upchurch Scientific, Oak Harbor, WA) via an HPLC pump (Jasco PU-2086plus, Jasco Inc., Easton, MD) at 20 mL/min below the surface of liquid nitrogen. The frozen microparticles were then separated from the liquid nitrogen and the solvent was removed by lyophilization (VirTis Advantage, VirTis, Gardiner, NY). The dried powders were stored under vacuum until dispersion and administration.

B.2.3 *In Vitro* Aerosol Exposure

An aliquot sample of the aerosol was taken from each exposure port following nebulization. ITZ concentration was determined using a Shimadzu LC-10 liquid chromatograph. The mobile phase for in vitro assay consisted of acetonitrile: water (70:30 v/v) containing 0.02% diethylamine. The flow rate was 1.0 mL/min and the absorption wavelength (λmax) was 263 nm. ITZ was eluted from an Inertsil 5um ODS-2 column (4.6 mm i.d. x 150 mm; Alltech Associates, Inc., Deerfield, IL) at 5 min using an injection volume of 50 μl.

B.2.4 *In Vivo* Aerosol Exposure in a Mouse Model

Eight male ICR mice were placed in the chamber and dosed with an amorphous ITZ formulation for 10 minutes using the nose-only dosing apparatus described in Chapter 5.2.4.1 A schematic diagram of this dosing apparatus is shown in Figure. 5.2. The processed powders were redispersed in water (20

mg/mL) followed by sonication for 1 min prior to dosing. Nebulization of 4 mL dispersions was conducted using an Aeroneb® ultrasonic nebulizer for 10 minutes. Following dosing, the mice were removed from the chamber and allowed to equilibrate for 15 minutes. The mice were sacrificed and lungs (all lobes) were harvested from each animal.

B.2.5 Lung Extraction Analysis Using HPLC

Homogenized lung samples were analyzed using HPLC. Briefly, normal saline (1mL) was added to each harvested lung sample, this was then homogenized using tip ultrasonication. Aliquots of homogenate (250 μL) were transferred to 4 separate vials and drug was extracted similarly to the serum samples. Barium hydroxide 0.3 N (50μL) and 0.4 N zinc sulfate heptahydrate solution (50 μL) was then added to each to precipitate out water-soluble proteins. The samples were then vortex mixed (30 seconds). Acetonitrile (1 mL) containing 100 ng/mL ketoconazole as an internal standard was added before a further vortex mixing (1.5 minute), followed by centrifugation at 3000 rpm (15 minutes). The supernatant was transferred to 1.5 mL centrifuge tubes and seated in an aluminum heating block (60°C), under a stream of nitrogen to dryness over 1 hour. Samples were then reconstituted with 250 μL mobile phase (62% acetonitrile:38% 0.05M potassium phosphate monobasic buffer adjusted to pH 6.7 with NaOH) and vortex mixed (1 minute) before filtering (0.45 μm) into HPLC glass injection vials with low volume inserts (150 μL). The sample was then analyzed using a Shimadzu

LC-10 liquid chromatograph (Shimadzu Corporation, Columbia, Maryland) equipped with a heated (37°C) C-18 base-deactivated column (5 μm, 250 x 4.6 mm) protected by a C-18 guard column (5 μm, 7.5 x 4.6 mm) (Alltech Associates, Inc., Deerfield, IL).

B.3 RESULTS

The variability of ITZ concentrations was measured in vitro at the 4 adapter ports, and in vivo from the lungs of 8 outbred-ICR mice in the appropriate mice restraining tubes at the adapter ports. For in vitro study, ITZ concentrations were determined to be 3.35 $\pm$ 0.75 μg/mL at the adapter ports following 5 minutes nebulization (Figure B.1). For in vivo study, the lung concentrations of ITZ were found to be 18.71 $\pm$ 2.77 μg/g wet lung weight (n=8). This result was found to be two times higher than had previously been determined using a restraint-free whole body exposure unit in the same strain of mouse and double the exposure period. The variation in the exposures received is shown in Figure B.2. Each mouse showed a similar lung concentration with relative standard deviation (RSD) of only 15%. The low variability of ITZ concentrations obtained in lung demonstrated the effectiveness of the nose-only dosing apparatus to generate a uniform dosing. Therefore, high concentrations of ITZ can be achieved in the mouse lung with low variability using nose-only aerosol dosing apparatus. In addition, the simplicity and inexpensive design of this aerosol dosing apparatus makes it very useful to study any kind of aerosol delivery.

Appendix C: Formulation Development of TAC for Aerosol Delivery to the Lung

C.1 PURPOSE

The objective of the study in the Appendix C was to investigate the effect of various excipients on physicochemical properties of nanostructured aggregates of TAC produced by URF intended for pulmonary delivery. Four types of excipient used in this study, including glucose, lactose, mannitol and inulin. The samples were characterized by x-ray diffraction (XRD), scanning electron microscopy (SEM), specific surface area, contact angle and dissolution testing.

C.2 MATERIALS AND METHODS

C.2.1 Materials

The four excipients used in this study, including glucose, lactose, mannitol and inulin were purchased from Spectrum Chemicals (Gardena, CA). All other materials used were analytical grade and described in Chapter 5.3.1.

C.2.2 Production of URF formulations

The method for manufacture of URF formulations was described in Chapter 5.3.2.

C.2.3 X-Ray Powder Diffraction

The method for measurement of crystallinity using X-ray powder diffraction is outlined in Chapter 5.3.3.1.

C.2.4 BET Specific Surface Area

The method for measurement of surface area is outlined in Chapter 5.3.3.2.

C.2.5 Scanning Electron Microscopy

The method for scanning electron microscopy is outlined in Chapter 5.3.3.3.

C.2.6 Dissolution Testing at Below Equilibrium Solubility

The procedure utilized for determination of dissolution rate is outlined in Chapter 5.3.3.4.

C.3 RESULTS

The morphological characteristics of TAC particles processed by URF with different compositions have been observed by SEM, showing the presence of porous nanostructed aggregates comprised of small particle domains (Figure C.1). The XRD patterns of the various samples investigated are shown in Figure C.2. X-ray diffraction of the unprocessed TAC yielded the intense characteristic crystalline peaks at 19.10, 19.95 and 23.45 2θ degrees. The XRD patterns for TAC processed powders with lactose, mannitol and inulin at drug-to-excipient ratio of 1:1 demonstrated the lack of crystalline peaks, indicating an amorphous

morphology. In contrast, the TAC composition with glucose displayed a slight peak at the location of the major peak for TAC, indicating a small degree of crystallinity. The BET method was used to measure the surface area of the sample powders. Specific surface areas of the various samples investigated are shown in Table C.1. Unprocessed TAC had a surface area of 0.53 m^2/g. The surface areas of TAC processed powders with inulin, lactose, mannitol and glucose ranged from 15-33m^2/g, which were much larger than that of the unprocessed TAC. The high surface area was evident in the nanostrutured aggregates shown in the SEM micrographs. The dissolution profiles of the TAC processed powders and unprocessed TAC are shown in Figure C.3. In 30 min, 78, 72, 60 and 48% of TAC dissolved from the URF formulations with inulin, lactose, mannitol and glucose, respectively. Unprocessed TAC dissolved much more slowly, achieving only 29% in the first 30 min of the dissolution testing period. The enhanced dissolution rates of TAC processed powders prepared with glucose, lactose, mannitol, and inulin may be due to many factors such as the hydrophilic character of these excipients and increased surface area of the drug.

Appendix D: Investigation of the Effect of evaporating the volatile salt on the physicochemical properties of EPAS powders

D.1 PURPOSE

The objective of the study in the Appendix D was to investigate the effect of evaporating the volatile salt on the physicochemical properties of EPAS powders. It was hypothesized that the surface area of EPAS powders can be increased by adding ammonium carbonate ($(NH_4)_2CO_3$) as pore forming agent. The powders were characterized by x-ray diffraction (XRD), scanning electron microscopy (SEM), specific surface area, contact angle and dissolution testing

D.2 MATERIALS AND METHODS

D.2.1 Materials

The materials used for this study were described in Chapter 3.3.1.

D.2.2 Production of EPAS powders

The method for manufacture of EPAS powders was described in Chapter 3.3.2 and the experimental conditions are summarized in Table D.1.

D.2.3 Scanning Electron Microscopy

The method for scanning electron microscopy is outlined in Chapter 3.3.3.1.

D.2.4 Contact Angle

The procedure utilized for determination of contact angle is outlined in Chapter 3.3.3.4.

D.2.5 BET Specific Surface Area

The method for measurement of surface area is outlined in Chapter 3.3.3.5.

D2.6 X-Ray Powder Diffraction

The method for measurement of crystallinity using X-ray powder diffraction is outlined in Chapter 3.3.3.6.

D.2.7 Dissolution Testing

The procedure utilized for determination of dissolution rate is outlined in Chapter 3.3.6.

D.3 RESULTS

In all case, EPAS powder showed the major peaks for ITZ, indicating a high degree of crystallinity (Figure D.1). Similar contact angles were also observed for all formulations (E1-E3) as shown in Table D.2. The contact angles for water on the E2 and E3 compacted pellets were 31.5° and 30.9°, respectively, compared to 30.4° for E1 formulation. This result showed that the addition of ammonium carbonate has no effect on wettability of formulation. SEM micrographs of ITZ processed by EPAS are shown in Figure D.2. EPAS powders

generally show non-porous particles composed of submicron sizes which are aggregated to form larger particles. However, SEM micrograph of the E3 powder displays a higher porous structure compared to E1 and E2. The specific surface area shown in Table D.2 also illustrates the differences in porosity and primary particle sizes seen in the E1, E2 and E3 particles, with surface areas of 8.79 m^2/g, 9.65 m^2/g and 14.89 m^2/g, respectively. Surface area of ITZ EPAS powders containing 1% $(NH_4)_2CO_3$ is almost 2 folds higher than EPAS powders without $(NH_4)_2CO_3$. The dissolution profiles shown in Figure D.3 illustrates the enhanced dissolution rate achieved through E1-E3 formulations compared to bulk ITZ. Dissolution rate of 77, 80 and 89% ITZ in only 2 minutes from EPAS powders containing 0, 0.5 and 1%$(NH_4)_2CO_3$ respectively. This finding was further established through BET specific surface area measurements, where E3 particles showed higher specific surface area, due to a high porosity and nanostructured network of polymer and drug. Within 10 minutes, the E1-E3 dissolution rates were similar and were much higher than for the bulk ITZ. A possible explanation for the high initial drug release might be the evolution of NH_3 and CO_2 gases leads to pore formation and consequently, both increase surface area and dissolution of ITZ EPAS powders.

BIBLIOGRAPHY

Ahlin P, Kristl J, Kristl A, Vrecer F. (2002) Investigation of polymeric nanoparticles as carriers of enalaprilat for oral administration. Int. J Pharm.**239:** 113-120.

Ahsan F, Rivas IP, Khan MA, Torres Suarez AI. (2002) Targeting to macrophages: role of physicochemical properties of particulate carriers--liposomes and microspheres--on the phagocytosis by macrophages. J. Control. Release **79:** 29-40.25.

Akers M.M. (2002) Excipient-drug interactions in parenteral formulations. J Pharm. Sci. **91**: 2283-2300.

Amidon GL, Lennernas H, Shah VP, Crison JRA. (1995) Theoretical basis for biopharmaceutical drug classification: The correlation of in vitro drug product dissolution and in vivo bioavailability. Pharm. Res. **12:** 413-420.

Bilati U, Allemann E, Doelker E. (2005) Development of a nanoprecipitation method intended for the entrapment of hydrophilic drugs into nanoparticles. Eur. J. Pharm. Sci. **24:** 67-75.

Bivas-Benita M, Zwier R, Junginger HE, Borchard G. (2005) Non-invasive pulmonary aerosol delivery in mice by the endotracheal route. Eur. J. Pharm. Biopharm. **61:** 214-218.

Blot F, Tavakoli R, Sellam S, et al. (1995) Nebulized cyclosporine for prevention of acute pulmonary allograft rejection in the rat: Pharmacokinetic and histologic study. J. Heart Lung Transplant. **14:** 1162-1172.

Borm, P., Klaessig, F. C., Landry, T. D., Moudgil, B., Pauluhn, J., Thomas, K., Trottier, R., and Wood, S. (2006) Research Strategies for Safety Evaluation of Nanomaterials, Part V: Role of Dissolution in Biological Fate and Effects of Nanoscale Particles. Toxicol. Sci. **90**, 23-32.

Bowers VD, Locker S, Ames S, Jennings W, Corry RJ. (1991) The Hemodynamic-Effects of Cremophor-El. Transplantation **51:** 847-850.

Brannon-Peppas L. (1995) Recent advances on the use of biodegradable microparticles and nanoparticles in controlled drug delivery. Int. J Pharm. **116:** 1-9.

Brannon-Peppas L, Blanchette JO. (2004) Nanoparticle and targeted systems for cancer therapy. Adv. Drug Deliv. Rev. **56:** 1649-1659.

Calvo P, Gouritin B, Chacun H, et al. (2001) Long-circulating pegylated polycyanoacrylate nanoparticles as new drug carrier for brain delivery. Pharm. Res. **18:** 1157-1166.

Canadas, O., R. Guerrero, R. Garcia-Canero, G. Orellana, M. Menendez, and C. Casals, (2004) Characterization of liposomal tacrolimus in lung surfactant-like phospholipids and evaluation of its immunosuppressive activity. Biochemistry, **43**(30): 9926-9938.

Carlotti ME, Pattarino F, Gasco MR, Cavalli R. (1995) Use of polymeric and non-polymeric surfactants in o/w emulsion formulation. Int. J. Cosmetic Sci. **17:** 13-25.

Carroll, C.L. and A.B. Fleischer, (2004) Tacrolimus ointment: the treatment of atopic dermatitis and other inflammatory cutaneous disease. Expert Opin. Pharmacother., **5**(10): 2127-2137.

Carstensen JT, Van Scooik K. (1990) Amorphous-to-crystalline transformation of sucrose. Pharm. Res. **12:** 1278-1281.

Cassella R, Williams DA, Jambhekar SS. (1998) Solid-state-cyclodextrin complexes containing indomethacin, ammonia and water. II. Solubility studies. Int. J. Pharm. **165:** 15-22.

Chakinala, M.N., Kollef, M.H. and Trulock E.P. (2002) Critical care aspects of lung transplant patients. J. Intensive Care Med., **17**(1): 8-33.

Chellat F, Merhi Y, Moreau A, Yahia LH. (2005) Therapeutic potential of nanoparticulate systems for macrophage targeting. Biomaterials **26:** 7260-7275.

Chen X, Benhayoune Z, Williams III RO, Johnston KP. (2004) Rapid dissolution of high potency itraconazole particles produced by evaporative precipitation into aqueous solution. J. Drug Del. Sci. Technol. **14:** 299-304.

Chen X, Vaughn JM, Yacaman MJ, Williams III RO, Johnston KP. (2004) Rapid dissolution of high-potency danazol particles produced by evaporative precipitation into aqueous solution. J. Pharm. Sci. **93:** 1867-1878.

Chen X, Young TJ, Sarkari M, Williams I, Robert O., Johnston KP. (2002) Preparation of cyclosporine A nanoparticles by evaporative precipitation into aqueous solution. Int. J Pharm. **242:** 3-14.

Chiba, Y., Kohri N, Iseki K, and K., M. (1991) Improvement of dissolution and bioavailability for mebendazole, an agent for human echinococcosis, by preparing solid dispersion with polyethylenen-glycol. Chem. Pharm. Bull.**39**: 2158-2160.

Commercial Insight: Transplantation, Data Monitor, www.researchandmarkets.com, 2006.

Couderc S, Li Y, Bloor DM, Holzwarth JF, Wyn-Jones E. (2001) Interaction between the nonionic surfactant hexaethylene glycol mono-n-dodecyl ether (C12EO6) and the surface active nonionic ABA block copolymer pluronic F127 (EO97PO69EO97)-formation of mixed micelles studied using isothermal titration calorimetry and differential scanning calorimetry. Langmuir **17:** 4818-4824.Gennes DP. (1987) Polymers at an interface: a simplified view. Adv Colloid Interface Sci. **27:** 189-209.

Couvreur P, Puisieux F. (1993) Nano- and microparticles for the delivery of polypeptides and proteins. Adv. Drug Deliv. Rev. **10:** 141-162.

Culy, C., Jarvis, B. (2001) Repaglinide, a review of its therapeutic use in Type 2 diabetes mellitus. Drugs **61**, 1625-1660.

Curran, M.P. and C.M. Perry, (2005) Tacrolimus - In patients with rheumatoid arthritis. Drugs, **65**(7): 993-1001.

Dailey LA, Schmehl T, Gessler T, et al. (2003) Nebulization of biodegradable nanoparticles: impact of nebulizer technology and nanoparticle characteristics on aerosol features. J. Control. Release **86:** 131-144.

Dong Y, Feng S-S. (2005) Poly(d,l-lactide-co-glycolide)/montmorillonite nanoparticles for oral delivery of anticancer drugs. Biomaterials **26:** 6068-6076.

Dowling RD ZM, Burckart GJ, et al. (1990) Aerosolized cyclosporine as single-agent immunotherapy in canine lung allografts. Surgery, pp. 198-204.

Eerikainen H, Kauppinen EI. (2003) Preparation of polymeric nanoparticles containing corticosteroid by a novel aerosol flow reactor method. Int. J Pharm. **263:** 69-83.

Elamin AA, Sebhatu T, Ahlneck C. (1995) The use of amorphous model substances to study mechanically activated materials in the solid state. Int. J. Pharm. **119:** 25-36.

Evans, R.T., C.J. Arnold, E.T. Moss, J. Yeh, and A.M. Hotz, Less Growth, More Risk, Lower Multiple. Black Book - Pharmaceutical Quarterly, **2002**: p. 201-210.

Evora C, Soriano I, Rogers RA, Shakesheff KM, Hanes J, Langer R. (1998) Relating the phagocytosis of microparticles by alveolar macrophages to surface chemistry: the effect of 1,2-dipalmitoylphosphatidylcholine. J. Control. Release **51:** 143-152.

Fahr A. (1993) Cyclosporin clinical pharmacokinetics. Clin. Pharmacokinet. **24:** 472-495.

Fang C, Shi B, Pei Y-Y, Hong M-H, Wu J, Chen H-Z. (2006) In vivo tumor targeting of tumor necrosis factor-[alpha]-loaded stealth nanoparticles: Effect of MePEG molecular weight and particle size. Eur. J. Pharm. Sci. **27:** 27-36.

Fawaz F, Bonini F, Maugein J, Lagueny AM. (1998) Ciprofloxacin-loaded polyisobutylcyanoacrylate nanoparticles: pharmacokinetics and in vitro antimicrobial activity. Int. J Pharm. **168:** 255-259.

Ferrari M. (2005) Cancer nanotechnology: Opportunities and challenges. Nat. Rev. Cancer **5:** 161-171.

Fessi HC, Devissaguet JP. (1992) Process for the preparation of dispersible colloidal systems of a substance in the form of nanoparticles. US Patent 5,118,528.

Fessi H, Puisieux F, Devissaguet JP, Ammoury N, Benita S. (1989) Nanocapsule formation by interfacial polymer deposition following solvent displacement. Int. J Pharm. **55:** R1-R4.

Fishbein I, Chorny M, Rabinovich L, Banai S, Gati I, Golomb G. (2000) Nanoparticulate delivery system of a tyrphostin for the treatment of restenosis. J. Control. Release **65:** 221-229.

Fleisher D, Bong R, Stewart BH. (1996) Improved oral drug delivery: solubility limitations overcome by the use of prodrugs. Adv. Drug Deliv. Rev. **19:** 115-130.

Forestier F, Gerrier P, Chaumard C, Quero AM, Couvreur P, Labarre C. (1992) Effect of Nanoparticle-Bound Ampicillin on the Survival of Listeria Monocytogenes in Mouse Peritoneal Macrophages. J. Antimicrob. Chemother. **30:** 173-179.

Fox JL. (2000) Researchers discuss NIH's nanotechnology initiative **18:** 821.

Gao P, Guyton ME, Huang T, Bauer JM, Stefanski KJ, Lu Q. (2004) Enhanced Oral Bioavailability of a Poorly Water Soluble Drug PNU-91325 by Supersaturatable Formulations. Drug Dev. Ind. Pharm.**30:** 221-229.

Gao P, Rush BD, Pfund WP, et al. (2003) Development of a supersaturable SEDDS (S-SEDDS) formulation of paclitaxel with improved oral bioavailability. J. Pharm. Sci. **92:** 2386-2398.

Garcia-Garcia E, Andrieux K, Gil S, Couvreur P. (2005) Colloidal carriers and blood-brain barrier (BBB) translocation: A way to deliver drugs to the brain? Int. J Pharm. **298:** 274-292.

Gautier JC, Grangier JL, Barbier A, et al. (1992) Biodegradable nanoparticles for subcutaneous administration of growth hormone releasing factor (hGRF). J. Control. Release **20:** 67-77.

Geys J, Coenegrachts L, Vercammen J, et al. (2006) In vitro study of the pulmonary translocation of nanoparticles: A preliminary study. Toxicol. Lett. **160:** 218-226.

Gordon, M., and Taylor, J. S. (1952) Ideal copolymers and the second order transition of synthetic rubbers 1. Non-crystalline co-polymers. J. Appl. Chem. **2**, 493-500.

Grenha A, Seijo B, Remunan-Lopez C. (2005) Microencapsulated chitosan nanoparticles for lung protein delivery. Eur. J. Pharm. Sci. **25:** 427-437.

Griffies, J.D., C.L. Mendelsohn, W.S. Rosenkrantz, R. Muse, M.J. Boord, and C.E. Griffin, (2004) Topical 0.1% tacrolimus for the treatment of discoid lupus erythematosus and pemphigus erythematosus in dogs. J. Am. Anim. Hosp. Assoc., **40**(1): 29-41.

Gupta, A.K., A. Adamiak, and M. Chow, (2002)Tacrolimus: a review of its use for the management of dermatoses. J. Eur. Acad. Dermatol. Venereol., **16**(2): 100-114.

Guzman M, Molpeceres J, Garcia F, Aberturas MR, Rodriguez M. (1993) Formation and Characterization of Cyclosporine-Loaded Nanoparticles. J. Pharm. Sci. **82:** 498-502.

Hancock BC, Zografi G. (1997) Characteristics and significance of the amorphous state in pharmaceutical systems. J. Pharm. Sci. **86:** 1-12.

Harries M, Ellis P, Harper P. (2005) Nanoparticle albumin-bound paclitaxel for metastatic breast cancer. J. Clin. Oncol. **23:** 7768-7771.

Hata, T., Y. Tokunaga, S. Fumio, S. Kimura, T. Hirose, and S. Ueda, Medicinal composition, US Patent #6,346,537. **2002**

Hatorp, V., Oliver, S., and Su, C.-A. P. F. Bioavailabitity of repaglinide, a novel antidiabetic agent, administered orally in tablet or solution form or intravenously in healthy male volunteers. Int. J Clin. Pharmacol. Ther. 36, 636-641 (1998).

Hecq J, Deleers M, Fanara D, Vranckx H, Amighi K. (2005) Preparation and characterization of nanocrystals for solubility and dissolution rate enhancement of nifedipine. Int. J Pharm. **299:** 167-177.

Henrymichelland S, Alonso MJ, Andremont A, Maincen P, Sauzieres J, Couvreur P. (1987) Attachment of Antibiotics to Nanoparticles - Preparation, Drug-Release and Antimicrobial Activity Invitro. Int. J Pharm. **35:** 121-127.

Hersperger, R., K.H. Buchheit, S. Cammisuli, A. Enz, O. Lohse, M. Ponelle, W. Schuler, A. Schweitzer, C. Walker, H. Zehender, G. Zenke, A.G. Zimmerlin, M. Zollinger, L. Mazzoni, and J.R. Fozard, (2004) A locally active antiinflammatory macrolide (MLD987) for inhalation therapy of asthma. J. Med. Chem., **47**(20): 4950-4957.

Hilt JZ. (2004) Nanotechnology and biomimetic methods in therapeutics: molecular scale control with some help from nature. Adv. Drug Deliv. Rev. **56:** 1533-1536.

Hoeben B. J., McConville J. T., Najvar L. K., Talbert R. L., Peters J. I., Wiederhold N. P., Frei B. L., Graybill J. R., Bocanegra R., Sinswat P., Johnston K. P., and Williams R. O. (2006) In Vivo Efficacy of Aerosolized Nanostructured Itraconazole Formulations for the Prevention of Invasive Pulmonary Aspergilliosis. Antimicrob. Agents Chemother.-submitted.

Honbo, T., H. Seno, and M. Nishiyama, Medicament for treating idiopathic thrombocytopenic purpura, US Patent #5,643,901. **1997**

Horter D, Dressman JB. (2001) Influence of physicochemical properties on dissolution of drugs in the gastrointestinal tract. Adv. Drug Deliv. Rev. **46:** 75-87.

Hoover JL, Rush BD, Wilkinson KF, et al. (1992) Peptides are better absorbed from the lung than the gut in the rat. Pharm. Res. **9:** 1103-1106.

Hu J, Johnston KP, Williams III RO. (2004) Nanoparticle Engineering Processes for Enhancing the Dissolution Rates of Poorly Water Soluble Drugs. Drug Dev. Ind. Pharm. **30:** 233-245.

Hu, J., Johnston, K. P., Williams III, R. O. (2004) Stable amorphous danazol nanostructured powders with rapid dissolution rates produced by spray freezing into liquid. Drug Dev. Ind. Pharm. **30**: 695-704.

Hu J, Johnston KP, Williams III, R. O. (2004) Rapid dissolving high potency danazol powders produced by spray freezing into liquid process. Int. J Pharm. **271:** 145-154.

Huang Z, Chen HC, Yan LJ, Roco MC. (2005) Longitudinal nanotechnology development (1991-2002): National Science Foundation funding and its impact on patents. J. Nanopart. Res. **7:** 343-376.

Hughes GA. (2005) Nanostructure-Mediated Drug Delivery. Dis. Mon. **51:** 342-361.

Hussain, N., Jaitley, V., and Florence, A. T. (2001) Recent advances in the understanding of uptake of microparticulates across the gastrointestinal lymphatics. Adv. Drug Deliv. Rev. **50**, 107-142.

Huynh GH, Deen DF, Szoka J, Francis C. (2006) Barriers to carrier mediated drug and gene delivery to brain tumors. J. Control. Release **110:** 236-259.

Hyvonen S, Peltonen L, Karjalainen M, Hirvonen J. (2005) Effect of nanoprecipitation on the physicochemical properties of low molecular weight poly(l-lactic acid) nanoparticles loaded with salbutamol sulphate and beclomethasone dipropionate. Int. J Pharm. **295:** 269-281.

Iacono AT, Keenan RJ, Duncan SR, et al. (1996) Aerosolized cyclosporine in lung recipients with refractory chronic rejection Am. J. Respir. Crit. Care Med., pp. 1451-1455.

Iervolino, M., Cappello, B., Raghavan, S. L., and Hadgraft, J. (2001). Penetration enhancement of ibuprofen from supersaturated solutions through human skin. Int. J Pharm. **212**, 131-141.

Iervolino, M., Raghavan, S. L., and Hadgraft, J. (2000). Membrane penetration enhancement of ibuprofen using supersaturation. Int. J Pharm. **198**, 229-238.

Ingu A, Komatsu K, Ichimiya S, et al. (2005) Effects of Inhaled FK 506 on the Suppression of Acute Rejection After Lung Transplantation: Use of a Rat Orthotopic Lung Transplantation Model. J. Heart Lung Transplant. **24:** 538-543.

Ivanova R, Alexandridis P, Lindman B. (2001) Interaction of poloxamer block copolymers with cosolvents and surfactants. Colloids and Surfaces A-Physicochem. Eng. Aspects. **183:** 41-53.

Jacobson, P.A., C.E. Johnson, N.J. West, and J.A. Foster, (1997) Stability of tacrolimus in an extemporaneously compounded oral liquid. Am. J. Health-Syst. Pharm., **54**(2): 178-180.

Jaiswal J, Kumar Gupta S, Kreuter J. (2004) Preparation of biodegradable cyclosporine nanoparticles by high-pressure emulsification-solvent evaporation process. J. Control. Release **96:** 169-178.

Jasti BR, Berner B, Zhou S-L, Li X. (2004) A Novel Method for Determination of Drug Solubility in Polymeric Matrices J. Pharm. Sci. pp. 2135-2141.

Jiao Y, Ubrich N, Marchand-Arvier M, et al. (2002) In vitro and in vivo evaluation of oral heparin-loaded polymeric nanoparticles in rabbits. Circulation **105:** 230-235.

Jung J, Perrut M. (2001) Particle design using supercritical fluids: Literature and patent survey J. Supercrit. Fluid, pp. 179-219.

Jusko, W.J. and R. Dambrosio, (1991) Monitoring Fk-506 Concentrations in Plasma and Whole-Blood. Transplant. Proc., **23**(6): 2732-2735.

Jusko, W.J., W. Piekoszewski, G.B. Klintmalm, M.S. Shaefer, M.F. Hebert, A.A. Piergies, C.C. Lee, P. Schechter, and Q.A. Mekki, (1995) Pharmacokinetics of Tacrolimus in Liver-Transplant Patients. Clin. Pharmacol. Ther., **57**(3): 281-290.

Kagayama, A., S. Tanimoto, S. Murata, and T. Hata, Lotion for FK 506, US Patent #5,939,427. **1999**

Kawashima Y. (2001) Nanoparticulate systems for improved drug delivery. Adv. Drug Deliv. Rev. **47:** 1-2.

Kawashima Y, Yamamoto H, Takeuchi H, Fujioka S, Hino T. (1999) Pulmonary delivery of insulin with nebulized -lactide/glycolide copolymer (PLGA) nanospheres to prolong hypoglycemic effect. J. Control. Release **62:** 279-287.

Kayser O, Olbrich C, Yardley V, Kiderlen AF, Croft SL. (2003) Formulation of amphotericin B as nanosuspension for oral administration. Int. J Pharm.**254:** 73-75.

Keenan RJ, Duncan AJ, Yousem SA, et al. (1992) Improved immunosuppression with aerosolized cyclosporine in experimental pulmonary transplantation. Transplantation **53:** 20-25.

Kelly, J.S., S.P. Butcher, and J. Sharkey, Use of macrolides for the treatment of cerebral ischemia, US Patent #5,648,351. **1997**

Kim YI, Fluckiger L, Hoffman M, Lartaud-Idjouadiene I, Atkinson J, Maincent P. (1997) The antihypertensive effect of orally administered nifedipine-loaded nanoparticles in spontaneously hypertensive rats. Br. J. Pharmacol. **120:** 399-404.

Kim DW, Shin S, Oh S-G. (2000) Preparation and stabilization of silver colloids in aqueous sufactant solutions. In: (Eds) KLMaDOS (ed.) in:Adsorption and aggregation of surfactants in solution. Surfactant Science Series. New York: Marcel Dekker, pp. 255-268.

Kind M. (2002) Colloidal aspects of precipitation processes. Chem. Eng. Sci. **57:** 4287-4293.

Kipp JE. (2004) The role of solid nanoparticle technology in the parenteral delivery of poorly water-soluble drugs. Int. J Pharm. **284:** 109-122.

Knez Z, Weidner E. (2003) Particles formation and particle design using supercritical fluids. Curr. Opin. Solid State Mater. Sci. **7:** 353-361.

Kondo N, Iwao T, Masuda H, et al. (1993) Improved oral absorption of a poorly water-soluble drug, HO-221, by wet-bead milling producing particles in submicron region. Chem. Pharm. Bull. **41:** 737-740.

Koshika, T., Use of macrolide compounds for the treatment of ARDS US Patent #6,333,334. **2001**

Koshkina NV, Golunski E, Roberts LE, Gilbert BE, Knight V. (2004) Cyclosporin A aerosol improves the anticancer effect of paclitaxel aerosol in mice. J. Aerosol Sci. **17:** 7-14.

Koziara JM, Lockman PR, Allen DD, Mumper RJ. (2004) Paclitaxel nanoparticles for the potential treatment of brain tumors. J. Control. Release **99:** 259-269.

Kreuter J. (2001) Nanoparticulate systems for brain delivery of drugs. Adv. Drug Deliv. Rev. **47:** 65-81.

Kreuter, J. (1991)Peroral administration of nanoparticles. Adv. Drug Deliv. Rev. **7**, 71-86.

Kreuter J, Alyautdin RN, Kharkevich DA, Ivanov AA. (1995) Passage of peptides through the blood-brain barrier with colloidal polymer particles (nanoparticles). Brain Research **674:** 171-174.

Kriwet B, Walter E, Kissel T. (1998) Synthesis of bioadhesive poly(acrylic acid) nano- and microparticles using an inverse emulsion polymerization method for the entrapment of hydrophilic drug candidates. J. Control. Release **56:** 149-158.

Kubik T, Bogunia-Kubik K, Sugisaka M. (2005) Nanotechnology on duty in medical applications. Curr. Pharm. Biotechnol. **6:** 17-33.

Kubo H, Osawa T, Takashima K, Mizobe M. (1996) Enhancement of oral bioavailability and pharmacological effect of 1-(3,4-dimethoxyphenyl)-2,3 bis(methoxycarbonyl)-4-hydroxy-6,7,8-trimethoxynapthalene (TA-7552), a new hypocholesterolemic agent by micronization in co-ground mixture with D-mannitol. Biol. Pharm. Bull. **19:** 741-747.

Kushida I, Ichikawa M, Asakawa N. (2002) Improvement of dissolution and oral absorption of ER-34122, a poorly water-soluble dual 5-lipoxygenase/cyclooxygenase inhibitor with anti-inflammaory activity by preparing solid dispersion. J. Pharm. Sci. **91:** 258-266.

Lake, J.R., K.J. Gorman, C.O. Esquivel, R.H. Wiesner, G.B. Klintmalm, C.M. Miller, B.W. Shaw, and J.A. Gordon, (1995) The Impact of Immunosuppressive Regimens on the Cost of Liver-Transplantation -

Results from the Us Fk506 Multicenter Trial. Transplantation, **60**(10): 1089-1095.

Lampen, A., U. Christians, F.P. Guengerich, P.B. Watkins, J.C. Kolars, A. Bader, A.K. Gonschior, H. Dralle, I. Hackbarth, and K.F. Sewing, (1995) Metabolism of the immunosuppressant tacrolimus in the small intestine: Cytochrome P450, drug interactions, and interindividual variability. Drug Metab. Dispos., **23**(12): 315-1324.

Lamprecht A, Ubrich N, Hombreiro Perez M, Lehr C-M, Hoffman M, Maincent P. (1999) Biodegradable monodispersed nanoparticles prepared by pressure homogenization-emulsification. Int. J Pharm. **184:** 97-105.

Lamprecht, A., H. Yamamoto, H. Takeuchi, and Y. Kawashima, (2004) Design of pH-sensitive microspheres for the colonic delivery of the immunosuppressive drug tacrolimus. Eur. J. Pharm. Biopharm., **58**(1): 37-43.

Lamprecht, A., H. Yamamoto, N. Ubrich, H. Takeuchi, P. Maincent, and Y. Kawashima, (2005) FK506 microparticles mitigate experimental colitis with minor renal calcineurin suppression. Pharm. Res., **22**(2): 193-199.

Lawrence MJ, Rees GD. (2000) Microemulsion-based media as novel drug delivery systems. Adv. Drug Deliv. Rev. **45:** 89-121.

Layre A-M, Gref R, Richard J, et al. (2005) Nanoencapsulation of a crystalline drug. Int. J Pharm.**298:** 323-327.

Lee, M.J., R.M. Straubinger, and W.J. Jusko, (1995) Physicochemical, Pharmacokinetic and Pharmacodynamic Evaluation of Liposomal Tacrolimus (Fk-506) in Rats. Pharm. Res., **12**(7): 1055-1059.

Lee VHL. (2004) Nanotechnology: challenging the limit of creativity in targeted drug delivery. Adv. Drug Deliv. Rev. **56:** 1527-1528.

Letsou GV, Safi HJ, Reardon MJ, et al. (1999) Pharmacokinetics of liposomal aerosolized cyclosporine A for pulmonary immunosuppression. Ann. Thorac. Surg. **68:** 2044-2048.Leuner C, Dressman J. (2000) Improving drug solubility for oral delivery using solid dispersions. Eur. J. Pharm. Biopharm. **50:** 47-60.

Leuner, C., and Dressman, J. (2000) Improving drug solubility for oral delivery using solid dispersions. Eur. J Pharm. Biopharm. **50**: 47-60.

Li Y-P, Pei Y-Y, Zhang X-Y, et al. (2001) PEGylated PLGA nanoparticles as protein carriers: synthesis, preparation and biodistribution in rats. J. Control. Release **71:** 203-211.

Lipinski, C. A. (2002) Poor aqueous solubility--an industry wide problem in drug discovery. Am. Pharm. Rev. **5**: 82-85 .

Lipinski CA, Lombardo F, Dominy BW, Feeney PJ. (1997) Experimental and computational approaches to estimate solubility and permeability in drug discovery and development settings. Adv. Drug Deliv. Rev. **23:** 3-25.

Liversidge GG, Cundy KC. (1995) Particle size reduction for improvement of oral bioavailability of hydrophobic drugs: I. Absolute oral bioavailability of nanocrystalline danazol in beagle dogs. Int. J Pharm.**125:** 91-97.

Liversidge GG, Cundy KC, Bishop J, Czekai D. (1991) Surface modified drug nanoparticles. US Patent No. 5145684.

Lockman PR, Mumper RJ, Khan MA, Allen DD. (2002) Nanoparticle technology for drug delivery across the blood-brain barrier. Drug Dev. Ind. Pharm. **28:** 1-13.

Loftsson T, Brewster ME. (1996) Pharmaceutical applications of cyclodextrins. 1. Drug solubilization and stabilization. J. Pharm. Sci. **85:** 1017-1025.

Lu Y, Chen SC. (2004) Micro and nano-fabrication of biodegradable polymers for drug delivery. Adv. Drug Deliv. Rev. **56:** 1621-1633.

Luckham PF, Bailey AI, Miano F, Tadros TF. (1995) Effectiveness of surfactants as steric stabilizers. In: (Eds) RS (ed.) in: Surfactant adsorption and surface solubilization ACS symposium series 615. American Chemical Society, Washington, DC, pp. 166-182.

Mancinelli, L.M., L. Frassetto, L.C. Floren, D. Dressler, S. Carrier, I. Bekersky, L.Z. Benet, and U. Christians, (2001)The pharmacokinetics and metabolic disposition of tacrolimus: A comparison across ethnic groups. Clin. Pharmacol. Ther., **69**(1): 24-31.

Mandal S, Phadtare S, Sastry M. (2005) Interfacing biology with nanoparticles. Curr. Appl. Phys. **5:** 118-127.

Marr R, Gamse T. (2000) Use of supercritical fluids for different processes including new developments--a review. Chem. Eng. Process. **39:** 19-28.

Martinet, Y., Pinkston, P., Saltini, C., Spurzem, J., Muller-Quernheim, J., and Crystal, R. G. (1988) Evaluation of the in vitro and in vivo effects of cyclosporine on the lung T-lymphocyte alveolitis of active pulmonary sarcoidosis. Am. Rev. Respir. Dis., **138:** 1242-1248.

Martis L, Hall NA, Thakkar AL. (1972) Micelle formation and testerone solubilization by sodium glycocholate. J. Pharm. Sci. **61:** 1757-1761.

Marbury, T., Huang, W.-C., Strange, P., and Lebovitz, H. (1999). Repaglinide versus glyburide: a one-year comparison trial. Diabetes Res. Clin. Prac. **43**: 155-166.

Marbury, T. C., Ruckle, J. L., Hatorp, V., Andersen, M. P., Nielsen, K. K., Huang, W. C., and Strange, P. (2000) Pharmacokinetics of repaglinide in subjects with renal impairment. Clin. Pharmacol.Ther. 67, 7-15.

McAlister, V.C., K. Peltekian, H. Bitter-Suermann, A.S. MacDonald, and L. Beaudry, (1998) Cost of liver transplantation using tacrolimus. Transplant. Proc., **30**(4): 1502-1502.

McCabe, W. L., Smith, J. C., and Harriott, P. (2001): Unit Operations of Chemical Engineering, McGraw-Hill, New York.

Mentzer, R.M., M.S. Jahania, and R.D. Lasley, (1998) Tacrolimus as a rescue immunosuppressant after heart and lung transplantation. Transplantation, **65**(1): 109-113.

Merisko-Liversidge E, Liversidge GG, Cooper ER. (2003) Nanosizing: a formulation approach for poorly-water-soluble compounds. Eur. J. Pharm. Sci. **18:** 113-120.

Mitruka SN, Pham SM, Zeevi A, et al. (1998) Aerosol cyclosporine prevents acute allograft rejection in experimental lung transplantation. J. Thorac. Cardiovasc. Surg. **115:** 28-37.

Miyazaki S, Yamahira T, Morimoto Y, Nadai T. (1981) Micellar interaction of indomethacin and phenylbutazone with bile-salts. Int. J. Pharm. **8:** 303-310.

Mochizuki, M. and Y. Iwaki, Use of macrolide compounds for eye diseases, US Patent #5,514,686. **1996**

Moffatt, S.D., V. McAlister, R.Y. Calne, and S.M. Metcalfe, (1999) Potential for improved therapeutic index of FK506 in liposomal formulation demonstrated in a mouse cardiac allograft model. Transplantation, **67**(9): 1205-1208.

Moghimi SM, Hunter AC, Murray JC. (2001) Long-Circulating and Target-Specific Nanoparticles: Theory to Practice. Pharmacol Rev **53:** 283-318.

Mok, C.C., K.H. Tong, C.H. To, Y.P. Siu, and T.C. Au, (2005) Tacrolimus for induction therapy of diffuse proliferative lupus nephritis: An open-labeled pilot study. Kidney Int., **68**(2): 813-817.

Moore, J.W. and Flanner, H.H. (1996) Mathematical comparison of dissolution profiles. Pharm. Technol. **20**:64–74.

Morris-Stiff, G., T. Richards, J. Singh, K. Baboolal, V. Balaji, K. Ostrowski, R. Moore, C. Darby, R. Lord, and W.A. Jurewicz, (1998) Pharmaco-economic study of FK 506 (Prograf) and cyclosporine A neoral in cadaveric renal transplantation. Transplant. Proc., **30**(4): 1285-1286.

Mroso PN, Li Wan Po A, Irwin WJ. (1982) Solid state stability of aspirin in the presence of exciplents: kinetic interpretation, modelling and prediction. J. Pharm. Sci. **71:** 1096-1101.

Mukherji G, Murthy RSR, Miglani BD. (1989) Preparation and evaluation of polyglutaraldehyde nanoparticles containing 5-fluorouracil. Int. J Pharm. **50:** 15-19.

Müller RH, Becker R, Kruss B, Peters K. (1998) Pharmaceutical nanosuspensions for medicament administration as system of increased saturation solubility and rate of solution. US Patent No. 5858410.

Muller, R. H., Jacobs, C., and Kayser, O. (2001) Nanosuspensions as particulate drug formulations in therapy: Rationale for development and what we can expect for the future. Adv. Drug Deliv. Rev. 47, 3-19.

Muller RH, Mader K, Gohla S. (2000) Solid lipid nanoparticles (SLN) for controlled drug delivery - a review of the state of the art. Eur. J. Pharm. Biopharm. **50:** 161-177.

Murata, S., F. Shiomojo, Y. Tokunaga, and T. Hata, Aerosol Compositions, US Patent #6,524,556. **2003**

Mykhaylyk O, Dudchenko N, Dudchenko A. (2005) Doxorubicin magnetic conjugate targeting upon intravenous injection into mice: High gradient magnetic field inhibits the clearance of nanoparticles from the blood. J. Magn. Magn. Mater. **293:** 473-482.

Na GC, Yuan BO, Stevens HJ, Weekley BS, Rajagopalan N. (1999) Cloud point of nonionic surfactants: Modulation with pharmaceutical excipients. Pharm. Res. **16:** 562-568.

Nakanishi, S. and Yamanaka, Pharmaceutical solution containing FK-506 US Patent #5,260,301. **1993**

Nakano M. (2000) Places of emulsions in drug delivery. Adv. Drug Del. Rev. **45**, 1-4.

Neylan, J.F., E.M. Sullivan, B. Steinwald, and T.F. Goss, (1998) Assessment of the frequency and costs of posttransplantation hospitalizations in patients receiving tacrolimus versus cyclosporine. Am. J. Kidney Dis., **32**(5): 770-777.

Noskov BA, Akentiev AV, Miller R. (2002) Dynamic surface properties of poly(vinylpyrrolidone) solutions. J. Colloid Interface Sci. **255:** 417-424.

Okimoto, K., Miyake, M., Ibuki, R., Yasumura, M., Ohnishi, N., and Nakai, T. (1997) Dissolution mechanism and rate of solid dispersion particles of nilvadipine with hydroxypropylmethylcellulose. Int. J Pharm. **159**, 85-93.

Okuhara, M., H. Tanaka, T. Goto, T. Kino, and H. Hatanaka, Tricyclo compounds, a process for their production and a pharmaceutical composition containing the same US Patent #4,894,366. **1990**

Oppenheim RC. (1981) Solid Colloidal Drug Delivery Systems - Nanoparticles. Int. J Pharm.**8:** 217-234.

Orive G, Gascon AR, Hernandez RM, Dominguez-Gil A, Pedraz JL. (2004) Techniques: New approaches to the delivery of biopharmaceuticals. Trends Pharmacol. Sci. **25:** 382-387.

Pandey R, Sharma A, Zahoor A, Sharma S, Khuller GK, Prasad B. (2003) Poly (DL-lactide-co-glycolide) nanoparticle-based inhalable sustained drug delivery system for experimental tuberculosis. J. Antimicrob. Chemother. **52:** 981-986.

Pandey R, Zahoor A, Sharma S, Khuller GK. (2003) Nanoparticle encapsulated antitubercular drugs as a potential oral drug delivery system against murine tuberculosis. Tuberculosis **83:** 373-378.

Panyam J, Labhasetwar V. (2003) Biodegradable nanoparticles for drug and gene delivery to cells and tissue. Adv. Drug Deliv. Rev. **55:** 329-347.

Peyman, G., Ocular solutions, US Patent #7,087,237. **2006**

Pattanaik M, Bhaumik S. (2000) Adsorption behaviour of polyvinyl pyrrolidone on oxide surfaces. Materials Letters **44:** 352-360.

Pedersen M. (1997) The bioavailability difference between genuine cyclodextrin inclusion complexes and freeze-dried or ground drug cyclodextrin samples may be due to supersaturation differences. Drug Dev. Ind. Pharm.**23:** 331-335.

Peeters J, Neeskens P, Tollenaere JP, Van Remoortere P, Brewster ME. (2002) Characterization of the interaction of 2-hydroxypropyl- -cyclodextrin with itraconazole at pH 2, 4, and 7. J. Pharm. Sci. **91:** 1414-1422.

Peppas NA, Huang Y. (2004) Nanoscale technology of mucoadhesive interactions. Adv. Drug Deliv. Rev. **56:** 1675-1687.

Peters K, Leitzke S, Diederichs JE, et al. (2000) Preparation of a clofazimine nanosuspension for intravenous use and evaluation of its therapeutic efficacy in murine Mycobacterium avium infection. J. Antimicrob. Chemother. **45:** 77-83.

Palakodaty S, York P. (1999) Phase behavioral effects on particle formation processes using supercritical fluids. Pharm. Res. **16:** 976-985.

Peracchia MT, Fattal E, Desmaele D, et al. (1999) Stealth(R) PEGylated polycyanoacrylate nanoparticles for intravenous administration and splenic targeting. J. Control. Release **60:** 121-128.

Peters, D.H., A. Fitton, G.L. Plosker, and D. Faulds, (1993) Tacrolimus - a Review of Its Pharmacology, and Therapeutic Potential in Hepatic and Renal-Transplantation. Drugs, **46**(4): 746-794.

Pikal MJ, Dellerman KM, Roy ML, Riggin RM. (1991) The effects of formulation variables on the stability of freeze-dried human growth hormone. Pharm. Res. **8:** 427-436.

Pinto-Alphandary H, Andremont A, Couvreur P. (2000) Targeted delivery of antibiotics using liposomes and nanoparticles: research and applications. Int. J. Antimicrob. Agents **13:** 155-168.

Pirsch, J.D., J. Miller, M.H. Deierhoi, F. Vincenti, and R.S. Filo, (1997)A comparison of tacrolimus (FK506) and cyclosporine for immunosuppression after cadaveric renal transplantation. Transplantation, **63**(7): 977-983.

Pohlmann AR, Weiss V, Mertins O, Da Silveira NP, Guterres SS. (2002) Spray-dried indomethacin-loaded polyester nanocapsules and nanospheres: Development, stability evaluation and nanostructure models. Eur. J. Pharm. Sci. **16:** 305-312.

Ponchel G, Montisci M-J, Dembri A, Durrer C, Duchene D. (1997) Mucoadhesion of colloidal particulate systems in the gastro-intestinal tract. Eur. J. Pharm. Biopharm. **44:** 25-31.

Quintanar-Guerrero D, Allemann E, Fessi H, Doelker E. (1999) Pseudolatex preparation using a novel emulsion-diffusion process involving direct displacement of partially water-miscible solvents by distillation. Int. J Pharm. **188:** 155-164.

Rabinow B. E. (2004) Nanosuspensions in drug delivery. Nat. Rev. Drug Discov. **3**: 785-796.

Raghavan SL, Trividic A, Davis AF, Hadgraft J. (2000) Effect of cellulose polymers on supersaturation and in vitro membrane transport of hydrocortisone acetate Int. J Pharm., **193**: 231-237.

Raghavan, S. L., Trividic, A., Davis, A. F., and Hadgraft, J. (2001)Crystallization of hydrocortisone acetate: influence of polymers. Int. J Pharm. **212**: 213-221.

Randolph, T. W., and M.A. Larson: Theory of Particulate Processes, Academic Press, San Diego, 1998.

Rees A, Collett JH. (1974) The dissolution of salicylic acid in micellar solutions of polysorbate-20. J. Pharm. Pharmacol. **26:** 956-960.

Reverchon E. (1999) Supercritical antisolvent precipitation of micro- and nano-particles. J. Supercrit. Fluid **15:** 1-21.

Roco MC. (2001) International strategy for nanotechnology research and development. J. Nanopart. Res. **3:** 353-360.

Roco MC. (2005) International perspective on government nanotechnology funding in 2005. J. Nanopart. Res. **7:** 707-712.

Rogers TL, Gillespie IB, Hitt JE, et al. (2004) Development and characterization of a scalable controlled precipitation process to enhance the dissolution of poorly water-soluble drugs. Pharm. Res. **21:** 2048-2057.

Rogers TL, Nelsen AC, Hu J, Johnston KP, Williams III RO. (2002) A novel particle engineering technology to enhance dissolution of poorly water soluble drugs: spray-freezing into liquid. Eur. J. Pharm. Biopharm. **54:** 271-280.

Rogers TL, Hu J, Yu Z, Johnston KP, Williams III RO. (2002) A novel particle engineering technology: spray-freezing into liquid. Int. J Pharm. **242:** 93-100.

Rogers TL, Nelsen AC, Sarkari M, Young TJ, Johnston KP, Williams III RO. (2003) Enhanced aqueous dissolution of a poorly water soluble drug by novel particle engineering technology: Spray-freezing into liquid with atmospheric freeze-drying. Pharm. Res.**20:** 485-493.

Rogers TL, Overhoff KA, Shah P, Johnston KP, Williams III RO. (2003) Micronized powders of a poorly water soluble drug produced by a spray-

freezing into liquid-emulsion process. Eur. J. Pharm. Biopharm. **55:** 161-172.

Roney C, Kulkarni P, Arora V, et al. (2005) Targeted nanoparticles for drug delivery through the blood-brain barrier for Alzheimer's disease. J. Control. Release **108:** 193-214.

Sahoo SK, Labhasetwar V. (2003) Nanotech approaches to drug delivery and imaging. Drug Discov. Today **8:** 1112-1120.

Sakuma, S., Use of macrolide compounds for treating glaucoma, US Patent #6,384,073. **2002**

Saleki-Gerhardt A, Zografi G. (1994) Non-isothermal and isothermal crystallization of sucrose from the amorphous state. Pharm. Res. **11:** 1166-1173.

Sarkari M, Brown J, Chen X, Swinnea S, Johnston KP, Williams III RO. (2002) Enhanced drug dissolution using evaporative precipitation into aqueous solution. Int. J Pharm. **243:** 17-31.

Sato T, Kohnosu S. (1994) Effect of polyvinylpyrrolidone on the physical properties of titanium dioxide suspensions. Colloids and Surfaces A-Physicochem. Eng. Aspects. **88:** 197-205.

Scherrmann J-M. (2002) Drug delivery to brain via the blood-brain barrier. Vascular Pharmacology **38:** 349-354.

Sengoku, T., S. Sakuma, S. Satoh, S. Kishi, T. Ogawa, Y. Ohkubo, and S. Mutoh, (2003) Effect of FK506 eye drops on late and delayed-type responses in ocular allergy models. Clin. Exp. Allergy, **33**(11): 1555-1560.

Sham JO-H, Zhang Y, Finlay WH, Roa WH, Lobenberg R. (2004) Formulation and characterization of spray-dried powders containing nanoparticles for aerosol delivery to the lung. Int. J Pharm. **269:** 457-467.

Shoji, J., T. Sakimoto, K. Muromoto, N. Inada, M. Sawa, and C.S. Ra, (2005) Comparison of topical dexamethasone and topical FK506 treatment for the experimental allergic conjunctivitis model in Balb/c mice. Jpn. J. Ophthalmol., **49**(3): 205-210.

Simha, R., and Boyer, R. F. General relation involving the glass transition temperature and coefficient of expansion of polymers. J. Chem. Phys. 37, 1003-1007 (1962).

Sinswat P, Gao X, Yacaman MJ, Williams III RO, Johnston KP. (2005) Stabilizer choice for rapid dissolving high potency itraconazole particles formed by evaporative precipitation into aqueous solution. Int. J Pharm. **302:** 113-124.

Six, K., Berghmans, H., Leuner, C., Cressman, J., Werde, K. V., Mullens, J., Benoist, L., Thimon, M., Meublat, L., Verreck, G., Peeters, J., Brewster, M. E., and G. Van den Mooter Characterization of Solid Dispersions of

Itraconazole and Hydroxypropylmethylcellulose Prepared by Melt Extrusion-Part II. Pharm. Res. 20, 1047-1054.

Sohnel O, Garside J. (1992) Precipitation: Basic Principles and Industrial Applications. Butterworth Heinemann.

Solans C, Izquierdo P, Nolla J, Azemar N, Garcia-Celma MJ. (2005) Nano-emulsions. Curr. Opin. Colloid Interface Sci. **10:** 102-110.

Starzl, T.E., S. Todo, J. Fung, A.J. Demetris, R. Venkataramman, and A. Jain, (1989) Fk-506 for Liver, Kidney, and Pancreas Transplantation. Lancet, **2**(8670): 1000-1004.

Stella V. J. and Rajewski R. A. (1997) Cyclodextrins: their future in drug formulation and delivery. Pharm. Res. **14**: 556-567.

Stylios GK, Giannoudis PV, Wan T. (2005) Applications of nanotechnologies in medical practice. Injury **36:** S6-S13.

Subramaniam B, Rajewski RA, Snavely K. (1997) Pharmaceutical processing with supercritical carbon dioxide. J. Pharm. Sci. **86:** 885-890.

Suzuki, H., and Sunada, H. (1998) Influence of water-soluble polymers on the dissolution of nifedipine solid dispersions with combined carriers. Chem. Pharm. Bull. **46**: 482-487.

Takeuchi H, Yamamoto H, Kawashima Y. (2001) Mucoadhesive nanoparticulate systems for peptide drug delivery Adv. Drug Deliv. Rev., pp. 39-54.

Tanabe, K., (2003) Calcineurin inhibitors in renal transplantation - What is the best option? Drugs, **63**(15): 1535-1548.

Tanaka, K., Kitamura, S., and Kitagawa, T. (2005) Effect of structural relaxation on the physical and aerosol properties of amorphous form of FK888 (NK1 antagonist). Chem. Pharm. Bull. **53**: 498-502.

The Top 200 Prescriptions for 2004 by U.S. Sales, RxList, I., http://www.rxlist.com/top200_sales_2004.htm, **2006**.

Torchilin VP. (2001) Structure and design of polymeric surfactant-based drug delivery systems. J. Control. Release **73:** 137-172.

Tripp CP, Hair ML. (1996) Kinetics of the adsorption of a polystyrene-poly(ethylene oxide) block copolymer on silica: a study of the time dependence in surface/segment interactions. Langmuir. **12:** 3952-3956.

Trotta M, Gallarate M, Carlotti ME, Morel S. (2003) Preparation of griseofulvin nanoparticles from water-dilutable microemulsions. Int. J Pharm. **254:** 235-242.

Tsapis N, Bennett D, Jackson B, Weitz DA, Edwards DA. (2002) Trojan particles: Large porous carriers of nanoparticles for drug delivery. Proceedings of the National Academy of Sciences of the United States of America **99:** 12001-12005.

Turk M, Hils P, Helfgen B, Schaber K, Martin H-J, Wahl MA. (2002) Micronization of pharmaceutical substances by the Rapid Expansion of

Supercritical Solutions (RESS): a promising method to improve bioavailability of poorly soluble pharmaceutical agents. J. Supercrit. Fluid **22:** 75-84.

Ueda, K., K. Shimojo, T. Shimazaki, I. Kado, and K. Honbo, Solid Dispersion of FR-900506 substance, US Patent #US4,916,138. **1990**

Vaughn J M, Gao X, Yacaman M-J, Johnston K P, Williams III R O. (2005) Comparison of powder produced by evaporative precipitation into aqueous solution (EPAS) and spray freezing into liquid (SFL) technologies using novel Z-contrast STEM and complimentary techniques. Eur. J. Pharm. Biopharm. **60:** 81-89.

Vaughn, J. M., McConville, J. T., Burgess, D., Peters, J. I., Johnston, K. P., Talbert, R. L., and Williams III, R. O. (2006) Single dose and multiple dose studies of itraconazole nanoparticles. European Journal of Pharmaceutics and Biopharmaceutics **63**, 95-102.

Venkatesh S, Lipper RA. (2000) Role of the development scientist in compound lead selection and optimization. J. Pharm. Sci. **89:** 145-154.

Verreck, G., Six, K., Mooter, G. V. d., L. Baert, J. P., and Brewster, M. E. Characterization of solid dispersions of itraconazole and hydroxypropylmethylcellulose prepared by melt extrusion - part I. Int. J Pharm. 251, 165-174 (2003).

Vonderscher J, Meinzer A. (1994) Rationale for the Development of Sandimmune-Neoral. Transplant. Proc. **26:** 2925-2927.

Webb SD, Golledge SL, Cleland JL, Carpenter JF, Randolph TW. (2002) Surface adsorption of recombinant human interferon-[Gamma] in lyophilized and spray-lyophilized formulations. J. Pharm. Sci. **91:** 1474-1487.

Wissing SA, Kayser O, Muller RH. (2004) Solid lipid nanoparticles for parenteral drug delivery. Adv. Drug Deliv. Rev. **56:** 1257-1272.

Woestsnborghs R, Heykants J, Gasparini R, Gauwenbergh G. (1989) The effects of food and dose on the oral systemic availability of itraconazole in healthy subjects. Eur. J. Clin. Pharmacol. **36:** 423-426.

Wong, S. M., Kellaway, I. W., and Murdan, S. (2006). Enhancement of the dissolution rate and oral absorption of a poorly water soluble drug by formation of surfactant-containing microparticles. Int. J. Pharm. **317**: 61-68.

Yamada T, Iwasaki Y, Tada H, et al. (2003) Nanoparticles for the delivery of genes and drugs to human hepatocytes. Nat Biotech.**21:** 885-890.

Yamashita, K., E. Hashimoto, Y. Nomura, F. Shimojo, S. Tamura, T. Hirose, S. Ueda, T. Saitoh, R. Ibuki, and T. Ideno, Sustained release preparations US Patent #6,440,458. **2002**

Yamashita, K., Nakate, T., Okimoto, K., Ohike, A., Tokunaga, Y., Ibuki, R., Higaki, K., and Kimura, T. Establishment of new preparation method for

solid dispersion formulation of tacrolimus. Int. J Pharm. 267, 79-91 (2003).

Yeo S-D, Kiran E. (2005) Formation of polymer particles with supercritical fluids: A review. J. Supercrit. Fluid **34:** 287-308.

Young TJ, Mawson S, Johnston KP, Henriksen IB, Pace GW, Mishra AK. (2000) Rapid Expansion from Supercritical to Aqueous Solution to Produce Submicron Suspensions of Water-Insoluble Drugs. Biotechnol. Prog. **16:** 402-407.

Yu JW, Chien YW. (1997) Pulmonary drug delivery: Physiologic and mechanistic aspects. Crit Rev Ther Drug Carrier Syst **14:** 395-453.

Yu Z, Garcia AS, Johnston KP, Williams I, Robert O. (2004) Spray freezing into liquid nitrogen for highly stable protein nanostructured microparticles. Eur. J. Pharm. Biopharm. **58:** 529-537.

Yu Z, Rogers TL, Hu J, Johnston KP, Williams III RO. (2002) Preparation and characterization of microparticles containing peptide produced by a novel process: spray freezing into liquid. Eur. J. Pharm. Biopharm. **54:** 221-228.

Vita

Prapasri Sinswat was born in Bangkok, Thailand, on March 21, 1972, the daughter of Mr. Saiya and Mrs. Boonsom Sinswat. She graduated from Nongkhaem High School, Bangkok, Thailand, in 1990 and entered the Faculty of Pharmaceutical Sciences at Chulalongkorn University, Bangkok, Thailand. She received the degree of Bachelor of Science (Pharmacy) in 1995 with a second class honors. After receiving the B.S. degree, I was awarded scholarship by the Ministry of University Affairs (MUA) to pursue a Master of Science degree in Pharmacy from the same institute. She received her M.S. in 1997 and decided to join as a faculty member at the Department of Pharmacy of Chulalongkorn University thereafter. In January 2002, she entered the University of Texas at Austin to pursue a doctoral degree in Pharmaceutics in the College of Pharmacy and worked under the supervision of Robert O. Williams III. As a graduate student, Prapasri has served as a teaching and research assistant, presented her research at many pharmaceutical conferences and completed a summer internship position at Abbott Laboratories (GPRD), Waukegan, IL in 2004. She was awarded a Bruton Fellowship and a University of Texas Fellowship from 2003-2005. She graduated and earned her Ph.D. degree in August 2006.

Permanent address: 48/7, Kratumlom, Samphran, Nakornpathom, Thailand

This dissertation was typed by Prapasri Sinswat.